Studies on Adsorption of Protective Agents on the Surface of Silver Nanoparticle Synthesized by the Improved Vacuum Evaporation on Running Oil Substrate Method

March 2018

Graduate School of Systems Engineering

Wakayama University

Takashi IENAGA

改良型流動油面上真空蒸着法を用いて
合成した銀ナノ粒子表面における
保護剤吸着に関する研究

2018 年 3 月

和歌山大学大学院システム工学研究科

家永　隆史

Preface

The studies of this thesis were carried out under the guidance of Professor Setsuko Yajima at Graduate School of Systems Engineering, Wakayama University.

The objective of these studies is to investigate the adsorption of protective agents on the surface of silver nanoparticle with the improved vacuum evaporation on running oil substrate method.

Takashi IENAGA

Graduate School of Systems Engineering,
Wakayama University
Sakae-dani 930, Wakayama 640-8510, Japan

March 2018

Abstract

For the efficient synthesis of metal nanoparticles, the selection of the protective agent is highly important. However, such investigation has been strictly limited by the complex experimental conditions in the synthetic process. In this research, the improved vacuum evaporation on running oil substrate (VEROS) method was employed for understanding the adsorption of protective agents on the surface of silver nanoparticle. This method provides the extremely simple environment for molecular adsorption of protective agents in the synthesis of metal nanoparticles.

In this study, the author mainly disclosed the following three points.

1. Effects of protective agents in the synthesis of silver nanoparticles by the improved VEROS method were investigated. Among five protective agents, sorbitan monoolate and oleic acid showed the better protection performance than oleylamine, oleyl alcohol, and methyl oleate (Chapter 2).
2. The oleic-acid-capped silver nanoparticles synthesized by physical and chemical synthetic methods were compared. The adsorption states of oleic acid on the surface of silver nanoparticles were almost the same regardless of the ionization of oleic acid in the synthetic process (Chapter 3).
3. Physical adsorption strength of protective agents on the surface of silver nanoparticle were compared through ligand exchange. Oleic acid was exchanged by octanoic acid but it was not exchanged by *n*-octylamine. These results were in good agreement with those of the improved VEROS method for the synthesis of silver nanoparticles (Chapter 4).

Based on these results, the author concludes that the improved VEROS method may be highly useful for determining a suitable protective agent for the protection of metal nanoparticles with physical adsorption.

概要

金属ナノ粒子を効果的に合成するには、保護剤の選定が極めて重要である。しかし、保護剤の選定に関する調査は、合成過程における複雑な実験条件により厳しい制約を受け困難とされている。この研究では、銀ナノ粒子表面への保護剤の吸着を理解するために改良型流動油面上真空蒸着（VEROS）法を採用した。この手法は、金属ナノ粒子の合成において、保護剤が分子吸着する上で極めて単純な環境が提供される特徴を持つ。

この研究においては主に以下の三点を明らかにした。

1. 改良型 VEROS 法による銀ナノ粒子合成における保護剤の効果を調査した。5 種類の保護剤を試した結果、ソルビタンモノオレートとオレイン酸は、オレイルアミンやオレイルアルコールおよびオレイン酸メチルエステルより良い保護性能を示した（第二章)。

2. 物理法および化学法によって合成されたオレイン酸保護銀ナノ粒子の比較を行った。合成過程におけるオレイン酸のイオン化の有無によらず、銀ナノ粒子上のオレイン酸の吸着状態はほとんど変わらなかった（第三章)。

3. 銀ナノ粒子表面への保護剤の物理的な吸着力を、配位子交換を用いることで比較した。オレイン酸はオクタン酸によって置き換えが可能であったが、オクチルアミンへ置き換えることはできなかった。この結果は改良型 VEROS 法における銀ナノ粒子の合成結果と良く一致した（第四章)。

これらの結果を基にして、改良型 VEROS 法は物理的な吸着力による金属ナノ粒子保護に適した保護剤を選定するのに非常に有望であると結論づけた。

INDEX

Chapter 1: General Introduction

Section 1-1: Background

Metal nanoparticles have been attracting much attention as new materials in the industrial field. The miniaturization with a nanosize level befits the trend of resource saving in recent years. General synthetic methods for metal nanoparticles consist of supply of raw materials and protection of unstable surfaces. In a typical synthetic method, a metal complex is used as a source of metal supply and the growth of particle by the supply of metal is restricted by adsorption of organic molecules which are called protective agents.

Recently, a lot of synthetic methods for metal nanoparticles have been reported and innovated by researchers and engineers. Due to the diversification of synthetic methods, specialized knowledges for each synthetic method are required for engineers to produce metal nanoparticles. In these knowledges, the interaction between the surface of metal nanoparticles and protective agents is extremely important for the synthesis of metal nanoparticles. However, the interaction has been hardly shown in general synthetic methods because of various restraints such as low solubility of reagents and difficult reproducibility of synthetic environment. In other words, practical know-how for production of metal nanoparticles has not been based on the essential compatibility between the surface of metal nanoparticles and protective agents these days.

In the practical use of nanoparticles, the metal of the raw material is generally determined by the requirements of the final product. In addition, it is necessary to select the protective agent in accordance with the metal to be used. Although a protective agent should be determined from various aspects, its role in the synthetic process is highly important because it largely affects characteristics of obtained metal nanoparticles. Therefore, the clarification of the roles of protective agents in the synthesis of metal nanoparticles would enable us to select the suitable one in various manufacturing methods.

Section 1-2: Survey of Metal Nanoparticles

1-2-1 Characteristics of Metal Nanoparticles

Characteristics of metal nanoparticles are necessary for developing innovative devices. Metal nanoparticles are metals that are only atomized to nanosize. This atomization causes the decrease of particle diameter and the increase of the surface area per unit weight. These changes lead to changes in the handling of metal particles. Because of their small size, metal nanoparticles can disperse stably in a solvent if they are protected by effectual repulsion to aggregation such as electrostatic repulsion or steric hindrance. As metal nanoparticles dispersed in a solution can be handled as a liquid rather than as a powder, they are suitable for transporting with liquid or forming a fine pattern. On the other hand, it is possible to utilize the chemical reaction on the surface of metal nanoparticles effectively because their specific surface area of a spherical particle is inversely proportional to its diameter. These features are quite useful but they have no surprises at present. Significant features of metal nanoparticles have been discovered along with advances in science.

The first important discovery of the characteristics of metal nanoparticles is Kubo effects which was proposed in 1961 and reported in 1962 by R. Kubo [1]. This report predicts that significantly small size of particle brings different characteristics from those of metal in the bulk state because their particles have discrete energy levels of electron due to paucity of atoms constituting the particle. For example, their characteristics are specific heat and magnetic susceptibility. This report triggered full-scale application researches for metal nanoparticles.

After that, surface-enhanced Raman scattering (SERS) effect was discovered in studies on physical property of gold nanoparticles and it had a great influence on application studies. This effect originates from electromagnetic enhancement effect based on localized surface plasmon resonance (LSPR) due to collective vibration of electrons.

Depression of melting point of metal nanoparticle is a well-known feature. This depression is observed in the cases of adequately-small nanoparticles and extremely-thin film of metals [2,3].

In many application studies with metal nanoparticles, one or some of their characteristics are utilized.

1-2-2 Metals for Nanoparticles

A lot of kinds of metal nanoparticles have been examined for their applications since the scientific study was firstly shown by M. Faraday [4]. Gold and silver are considerably popular as materials for metal nanoparticles because they are relatively stable against oxidation. In many cases, they can be synthesized with chemical synthetic methods in atmosphere. For these reasons, gold and silver nanoparticles are utilized in a wide range of fields from education to industrial products. Although gold is extremely expensive, gold nanoparticles are highly compatible with biotechnology. It is relatively difficult to react with other molecules, but techniques for surface modification have been reported. Therefore, gold nanoparticles are used as a chemically-stable electrode and biomarker in the biotechnology field. In addition, it was also reported that gold nanoparticles are catalytically active [5]. It is difficult to replace gold with other materials to obtain this property. On the other hand, silver nanoparticles are mainly used in the field of electronics because they have good electrical resistivity (1.467×10^{-8} Ω m). For a reference, the electrical resistivities of gold and copper are 2.051 and 1.543×10^{-8} Ω m, respectively [6]. The balance between price and performance is also good. In addition, the melting temperature of silver is relatively low. The melting points of gold, silver, and copper are 1337, 1235, and 1358 K, respectively [6]. Printed pattern by silver nanoparticle ink can be sintered at a relatively low temperature. Although these technologies have problems such as production rate and cost, they are becoming to be utilized in terms of repair of defective products and on-demand production. For the further use of silver nanoparticles,

there are some tasks to solve such as sulfurization, electromigration of printed-wiring, and adhesiveness to substrate. The sulfidation can be solved with a suitable coating. Although they are not perfect answers, suggested solutions for the adhesiveness are surface modification and addition of binder resin. These solutions sacrifice process costs and wiring characteristics. However, in order to solve the electromigration, it is necessary to change the material of nanoparticles to another suitable one.

Copper is the most commonly used material in the field of electronics. The electrical resistivity of copper is almost the same as that of silver [6]. Moreover, copper has better electromigration resistance than silver even though the price is only one hundredth of silver. This electromigration resistance is required for power devices such as high brightness LEDs and sheet heaters because degradation based on migration has a correlation with current density. On the other hand, copper is easily oxidized by a slight amount of oxygen in the air. This oxidation proceeds rapidly with exotherm because the specific surface area of nanoparticles is significantly larger than that of bulk metal. It is difficult to solve this problem completely. At present, the studies of mix with other metals and protection with organic molecules are being conducted. These solutions for oxidization negate the advantage of cost in copper.

As described above, silver is the best choice for studies of the adsorption of organic compounds on the surface of metal nanoparticles among many kinds of metals. It is relatively stable in physical and chemical properties. In addition, the cost is reasonable for gram-scale production and measurements. And most of all, a lot of synthetic methods and researches for silver nanoparticles have been reported up to now.

1-2-3 Protective Agents for Metal Nanoparticles

The surface of metal nanoparticle is often protected by organic molecules against aggregation and fusion. These molecules are also called as the protective agent, capping agent, surfactant or ligand depending on their role and usage. The role of protective agent

is to keep enough distance between nanoparticles in the dispersion. Therefore, the protective agent is desired to have an adsorption performance on the surface of metal nanoparticles and to inhibit the approach of other particles. These protections are attained generally by steric hindrance and electrostatic repulsion. The choice of protective agents depends not only on the metals of nanoparticles but also on the solvent as the dispersant.

It is highly important to use protective agents in the synthetic process of metal nanoparticles. The reason is that it is more difficult to keep their independence than to produce nanoparticles. Therefore, metal nanoparticles need to be protected immediately after the synthesis. In the absence of protective agents, nanoparticles easily turn into coarse particles by their aggregation and fusion. In addition, the change is irreversible. For these reasons, studies on protective agents must be conducted simultaneously with the studies of synthetic methods for metal nanoparticles.

The molecular weight of protective agents is one of the determining factors for the synthesis of metal nanoparticles. In many cases, the high-molecular-weight type of protective agent is a polymer because it can have a lot of functional groups. These functional groups are used as adsorption moieties on the particle surface. Having many adsorption moieties means that the molecules can stay for a longer time onto the surface of nanoparticles due to the presence of many adsorptive moieties. In addition, these adsorption moieties are generally bulky. Therefore, these polymers work as a strong steric hindrance group. If some of the functional groups are ionized, it is also possible to use an electrostatic repulsion as a repulsive force. On the other hand, there are several disadvantages for the use of polymers as protective agents. An unnecessarily high-molecular-weight of polymer protects a plurality of nanoparticles collectively at the same time. In this case, individual particles cannot behave freely in the dispersion. In other words, nanoparticles entangled by the polymer behave like agglomerated particles. It is difficult for them to disperse in a solvent. Furthermore, a bulky protective layer decreases the concentration of metal nanoparticles in the dispersion or paste. In the case of

conductive inks, the decrease is the critical problem because the printed wire shrinks as protective agents in the printed ink are removed in the sintering process. The shrinkage induces strong stress and cracks in the printed wiring. For these reasons, the molecular weight of protective agents should be optimized according to the purpose.

On the other hand, the surface of metal nanoparticle is not homogeneous. As a metal forms a crystalline structure, some of crystal plane orientations are observed in the surface of metal nanoparticles. These crystal plane orientations are important because sometimes some of protective agents show special adsorptions on the specific crystal plane in the solution. These specific adsorptions bring about the anisotropic growth of the nanoparticles [7]. In this case, the surface of the crystal is unstable due to its smallness. In other words, it is different from the crystal plane of bulk metals.

In some cases, adsorbed molecules on the surface of metal nanoparticles play the roles of not only prevention of aggregation but also functionalization of nanoparticles.

Priorities for selecting the protective agent in the synthesis of metal nanoparticles are as follows. Firstly, the molecule has at least one suitable adsorption moiety in its functional groups. Secondly, it provides enough repulsion force between nanoparticles. Finally, it is suitable for the production process and the final products. Unless particle surfaces are protected, they cannot exist as nanoparticles in general. Therefore, adsorption of molecules on the surface of nanoparticles is the most important in the selection.

Even in the cases of polymer-type of protective agents, the compatibility with the surface of metal nanoparticles is essentially dependent on the functional group. Regardless of the molecular weight, effective functional groups are the most important for adsorption on the surface of metal nanoparticles. Conversely, when investigating adsorption ability of the functional group on the particle surface, it is desirable that the molecule has only one functional group. In addition, another moiety of the molecule must be designed so as not to influence the adsorption as much as possible. The examples of their moiety are saturated hydrocarbons which have stable and quite simple structure. In

practice, the functional group is added into the protective agent in order to increase the solubility in an organic solvent. In addition, double bonds are often added so that the protective agent is easily dissolved in many kinds of solvents.

1-2-4 Chemical Synthetic Methods

In chemical synthetic methods, chemical reactions are used for the synthesis of metal nanoparticles. It is possible to synthesize metal nanoparticles with relative ease because many of chemical synthetic methods can be conducted with general laboratory instruments. Chemical methods are classified further according to types of chemical reactions. They are the chemical reduction method, solvothermal synthetic method, sol-gel method, aerosol synthetic method, and thermal decomposition method. The details and features of these synthetic methods are described below.

Chemical Reduction Method

Reduction reaction is the simplest method for depositing metal chemically. This reaction is often used in non-electrolytic plating. In a typical reduction method, a reducing agent is added to the aqueous solution containing a metal salt. Since this method is extremely simple, it has often been used to acquire the basic knowledge of nanoparticles [8]. After the reduction, the surface of the generated nanoparticles is unstable. Therefore, the surface of nanoparticles must be covered with protective agents. In some cases, reduction agents also act as the protective agent in the synthesis. Citric reduction of $AuCl_4^-$ is the famous reaction among these methods. The adsorbed citric acid molecules are known to form an electric double layer to protect the surface of gold nanoparticles (**Figure 1-1**) [9].

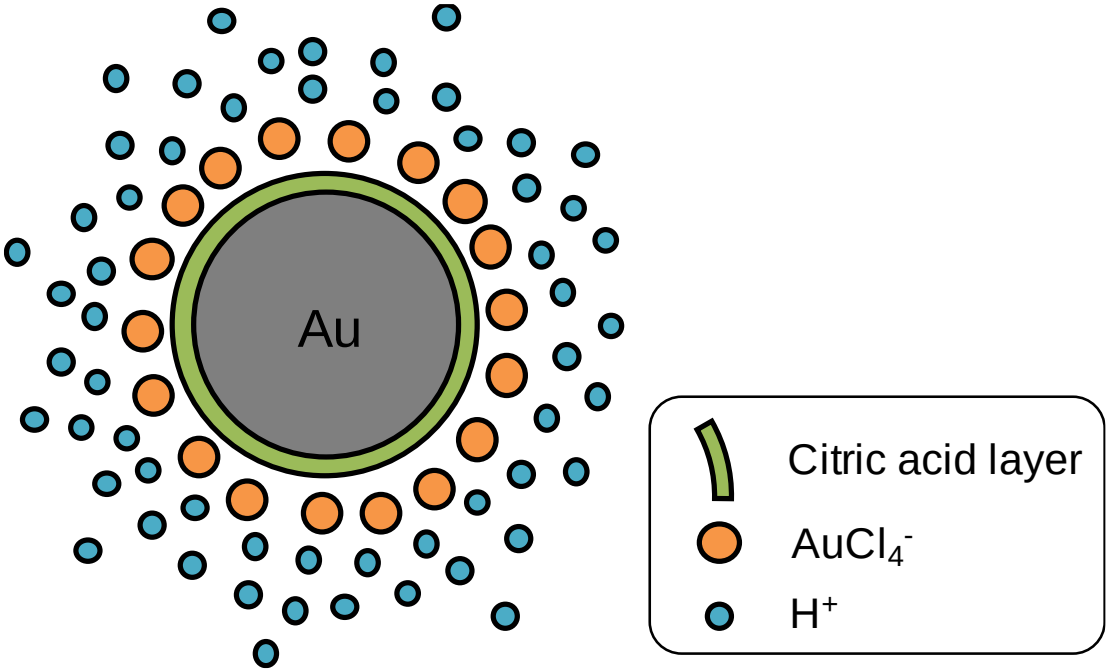

Figure 1-1. Schematic illustration of gold nanoparticles syntheized by citric reduction of $AuCl_4^-$.

Many combinations of metal salts and reducing agents have been reported in the reduction process. For instance, silver salts were reduced by *N*-methylpyrrolidone [10] and gold / silver salts were reduced by *N*,*N*-dimethylformamide [11]. In addition, it is known that polymers such as polyvinylpyrrolidone also act as a reducing agent [12].

The reduction method with polyol is called the polyol method [13]. This method does not require water as a solvent because polyol plays the roles of both solvent and reducing agent. This method is often utilized for producing metal nanoparticles dispersed in a non-aqueous system.

Solvothermal Synthetic Method

Solvothermal synthesis is used for synthesis of nanoparticles of metals, metal oxides, and semiconductors. In this method, the synthesis is carried out at a higher temperature than the boiling point of the solvent by raising the pressure to promote the reaction. In the

case of water, it is called hydrothermal synthesis method. Since the synthetic environment is special, there is a possibility for the production of nanoparticles which cannot be produced by the other synthetic methods. Therefore, these methods are generally used for studying complex metal compounds rather than simple metals. In fact, it is well-known that cadmium selenide (CdSe) quantum dots and indium tin oxide (ITO) nanoparticles are produced by the solvothermal synthetic method although they cannot be produced by the other methods [14,15].

Sol-Gel Method

In sol-gel methods, metal oxide nanoparticles can be synthesized by hydrolysis or polycondensation of metal alkoxide. For instance, amorphous silica nanoparticles are synthesized from silicon alkoxide [16]. It is possible to make various kinds of metal oxides simply by changing metal alkoxide. Therefore, these methods are utilized for metal oxide nanoparticles. In this method, a large amount of uniformly sized nanoparticles can be obtained. The particle size is precisely controlled by adjusting alkoxide type, amount of water, and catalyst type.

Aerosol Synthetic Method

The diameter of nanoparticles is controlled by nucleation and grain growth in general chemistry methods. In these cases, simultaneous nucleation and gentle grain growth are necessary for uniformly sized nanoparticles. When there is the same amount of raw material for one particle in each droplet as a reaction container, uniformly sized nanoparticles can be synthesized even if nucleation and growth rate are not properly controlled. In aerosol synthetic methods, micro-droplets are used as extremely small reaction space. Therefore, it is possible to control the size and distribution of nanoparticles by the size of droplets. Ultrasonic waves and electrostatic spraying are famous methods for making micro-droplets. In particular, the electrostatic spraying

method is excellent in controlling the size of droplets. The illustration of the electrostatic spraying method is shown in **Figure 1-2**.

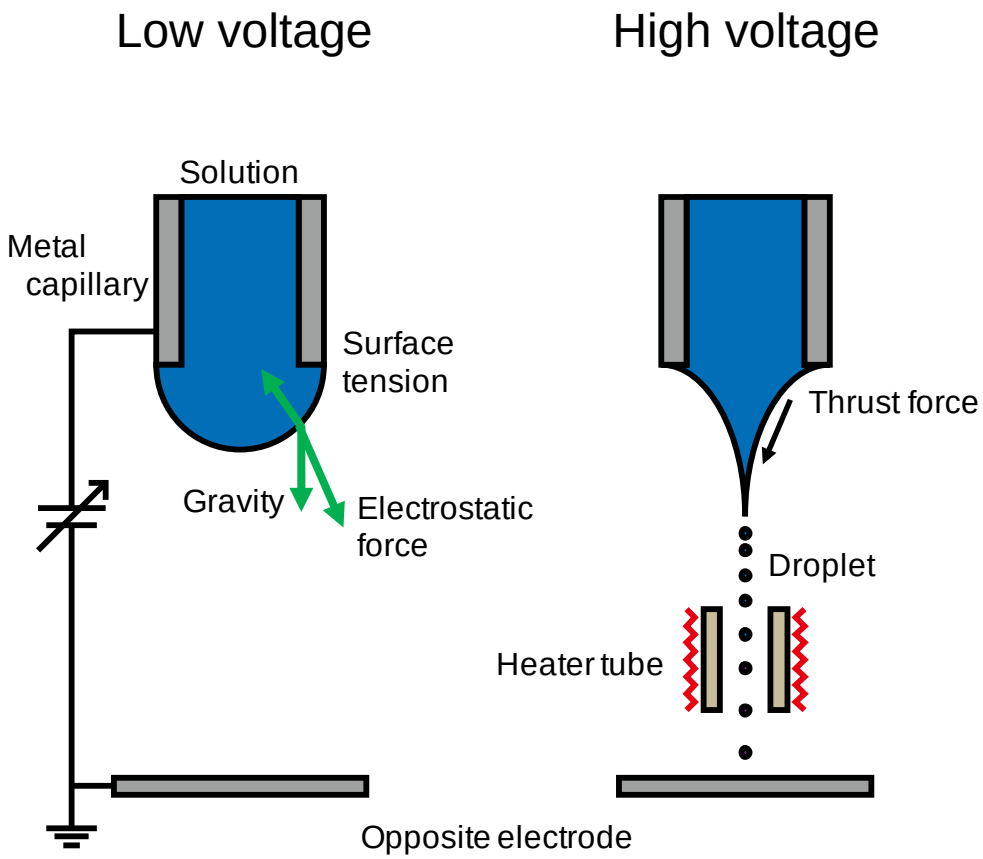

Figure 1-2. Illustration of the electrostatic spraying method [17].

The solution in the metal capillary is affected by surface tension, electrostatic force, and gravity. Then, the surface of solution at the end of capillary forms a semicircular meniscus. The resultant force is a thrust force to the opposite electrode. As the electrostatic force increases, the shape of meniscus becomes conical. When the electrostatic force exceeds the surface tension, the droplet is generated from the tip of conical meniscus. Therefore, it is possible to produce uniformly sized liquids. Furthermore, it is possible to freely adjust the droplet size by changing the physical properties of the liquid and the spraying conditions. The droplets obtained by spraying

grow up into particles as the solvent evaporates by the heating. In this reaction, the shape of the particles is also changeable depending on the evaporation time of the solvent and the diffusion time of the solute. Therefore, the aerosol synthesis is attracting much attention as a method that can produce a wide size range of particles.

Thermal Decomposition Method

Metal nanoparticles can be also produced by thermal decomposition reactions of metal complexes. In addition, this reaction does not require additives such as reducing agents. In these methods, metal ions as raw materials are complexed with organic molecules in advance. The molecules are often called the ligand. They are likely to adsorb on the metal surface of nanoparticles. Therefore, ligands can also act as protective agents for nanoparticles. This feature contributes to reducing kinds of reagents required for the synthesis. It means that the thermal decomposition requires the least reagents for the synthesis of metal nanoparticles among chemical methods.

Some of the methods do not require even any solvent in the synthesis for metal nanoparticles [18]. The metal complexes in the form of powder are used for pyrolysis. After pyrolysis, nanoparticles are obtained in a paste state because this thermal decomposition produces redundant molecules in addition to nanoparticles.

1-2-5 Physical Synthetic Methods

In physical synthetic methods, physical energy is used for atomization of bulk metal. All physical synthetic methods require more expensive equipment than chemical synthetic methods because it is necessary to generate enough physical energy to cut metal bonds. The technique used in the physical synthesis of nanoparticles is closely similar to that used in the physical vapor deposition (PVD). Typical physical synthetic methods are gas evaporation method, sputtering method, direct heating method, laser ablation method and arc plasma method. In addition, the improved vacuum evaporation on running oil

substrate (VEROS) method employed in this study is one of the physical synthetic methods.

Gas Evaporation Method

In physical synthetic methods, the gas evaporation method has been studied for a long time all over the world [19]. The nanoparticles obtained by the gas evaporation method have excellent characteristics such as ultra-purity and uniformly sized distribution. A series of reports by Uyeda and his co-workers indicated that a variety of metal nanoparticles could be obtained by using the gas evaporation method [20-25]. However, the nanoparticles produced in such a manner easily fused each other at room temperature because their surface was not covered with protective agents.

Synthetic process of the gas evaporation method is shown in **Figure 1-3**. The interior of the equipment is kept in a vacuum. During the synthesis, the pressure in the chamber is kept constant by an inert gas. The roles of this inert gas are both cooling the metallic vapor and carrying the obtained particles. The cooled metallic vapor is shown as plume around the crucible in **Figure 1-3**. The evaporation source is installed in the center of the bottom of the equipment. Evaporator boat or crucible is used as an evaporation source. The evaporated metallic vapor is cooled in the vicinity of the evaporation source. Then, the cooled metallic vapor becomes nanoparticles and the generation of nanoparticles can be observed as fumes. Therefore, the type and pressure of the inert gas and the evaporation rate of the metal are important for the generation of nanoparticles.

Generated metal nanoparticles are transported along the gas flow to the upper collector. The particles are cooled and collected in the collector. It is also possible to protect the surface of metal nanoparticles by mixing with vaporized organic molecules during the transportation. The particles obtained by this method have been very often used for crystallographic studies of nanoparticles [26].

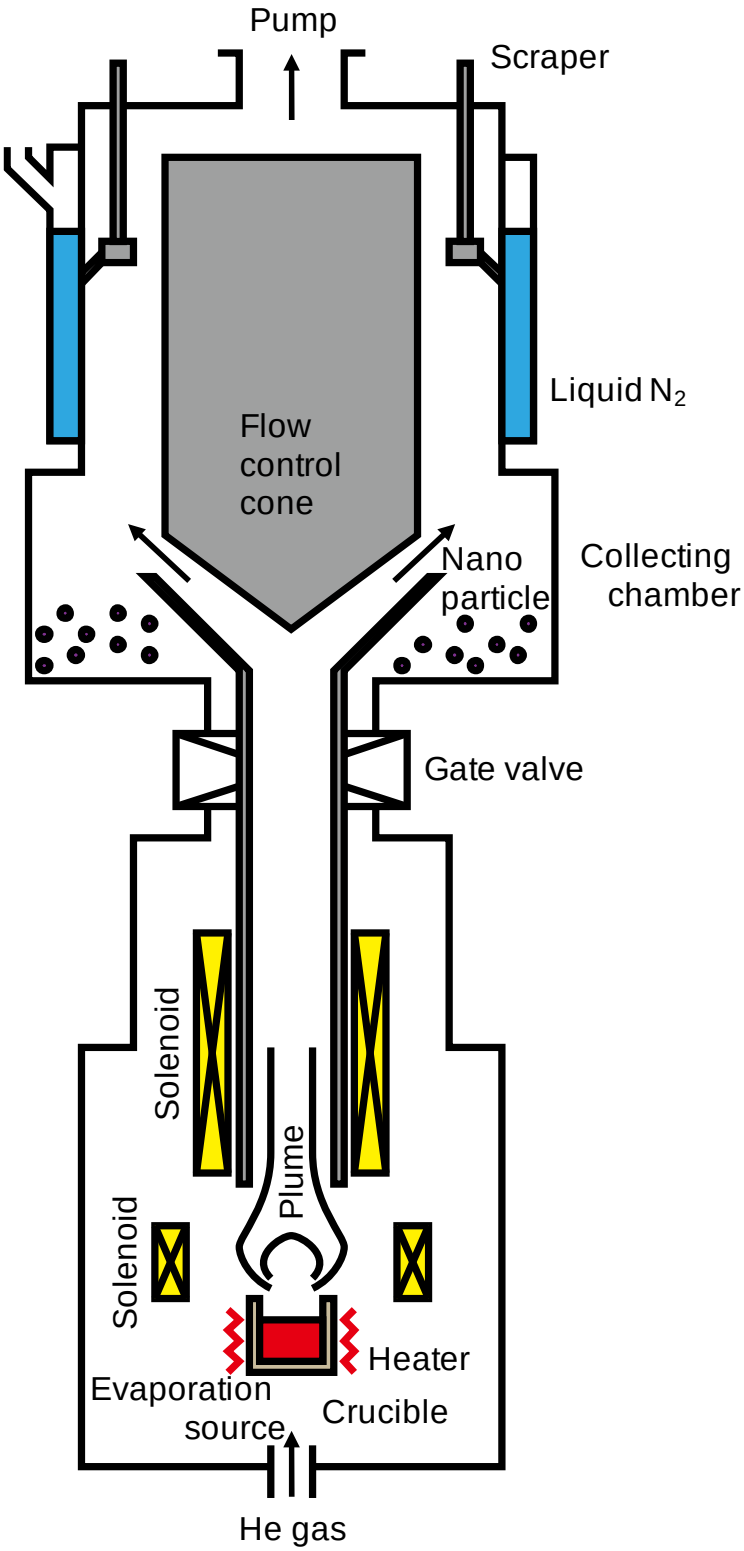

Figure 1-3. Illustration of the gas evaporation method [27].

Sputtering Method

Sputtering deposition is the well-known process in the PVD. In this method, the metal surface is bombarded by an ionized gas in a vacuum and metal atoms are sputtered to the opposite side. Plasma is often used in order to obtain an ionized gas. In this case, the source of metal is called sputtering target. Magnetron sputtering, where a magnet is placed under the sputtering target, is often used to increase the supply rate of metal. As for the feature of this method, it is possible to obtain particles having substantially the same composition ratio as the sputtering target because it is only physically sputtered off. Instead, the target has to be molded in advance, and the deposition rate is not as fast as the gas deposition method.

For obtaining metal nanoparticles, a collector is needed as a substrate to collect the generated particles. Since the source of metal is a solid metal, it can be supplied from the top to the bottom in this case. Therefore, it is possible to set up the solution downward and sputter to the liquid surface. The illustration of the sputtering method is shown in **Figure 1-4**. However, the type of solvent must be chosen properly because it is used in a vacuum. Ionic liquids and α,α'-diglycerol are known as the suitable solvents [29,30].

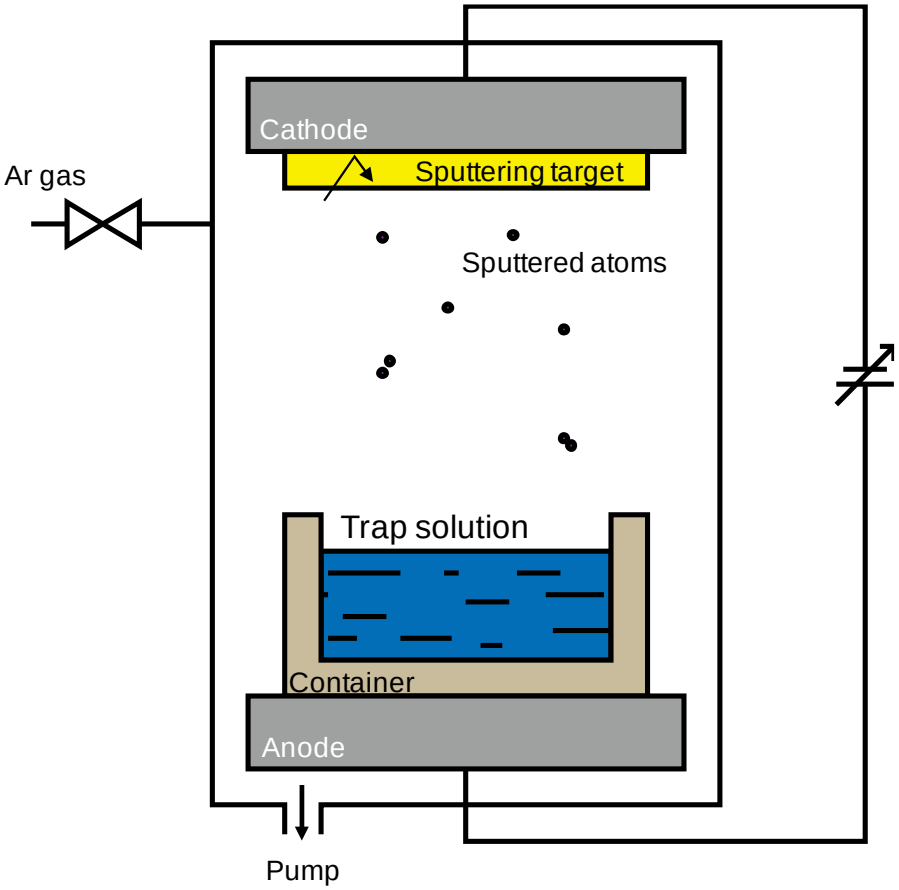

Figure 1-4. Illustration of the sputtering method [28].

Direct-Heating Method (Electrical Wire Explosion Method)

This method uses direct electrical heating of an object to evaporate it. This method is often selected for synthesizing high melting point nanoparticles. For example, heated carbon reacts easily with boats and filaments. In this case, carbon can be sublimated by flowing electricity directly.

Though this method requires more energy than in a vacuum, some nanoparticles can be obtained unless the source is in a liquid that does not conduct electricity. A small amount of particles are obtained by a spike of a high current for making a metal plasma. In the case of heating metal in a liquid, a metal wire has been frequently used as an evaporation source and a raw material [31]. This method is called the electrical wire explosion method (**Figure 1-5**).

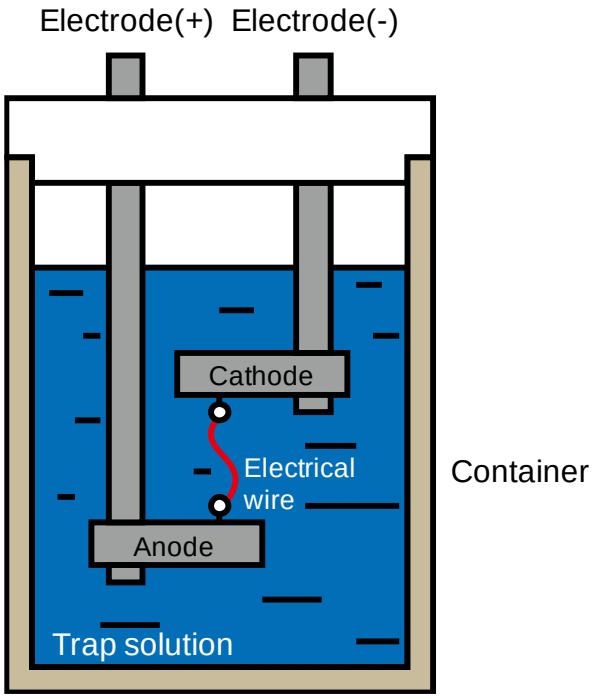

Figure 1-5. Illustration of the electrical wire explosion method [31].

Laser Ablation Method

This technology is based on the pulsed laser deposition (PLD). A pulse laser is irradiated to the surface of bulk metal or thin metallic film (**Figure 1-6**). The position is heated quickly and locally by the laser irradiation. Since the heated part is very small, it can be applied to the metal with high melting point. On the other hand, it is necessary to scan the laser to sufficiently vaporize the metal surface if a lot of particles are needed.

Laser has a single wavelength and its energy is concentrated on one point. Therefore, these ablations are carried out in the solution unless it has absorbance at the wavelength of the laser. A lot of laser ablation methods in water or in organic solvent have been reported [32].

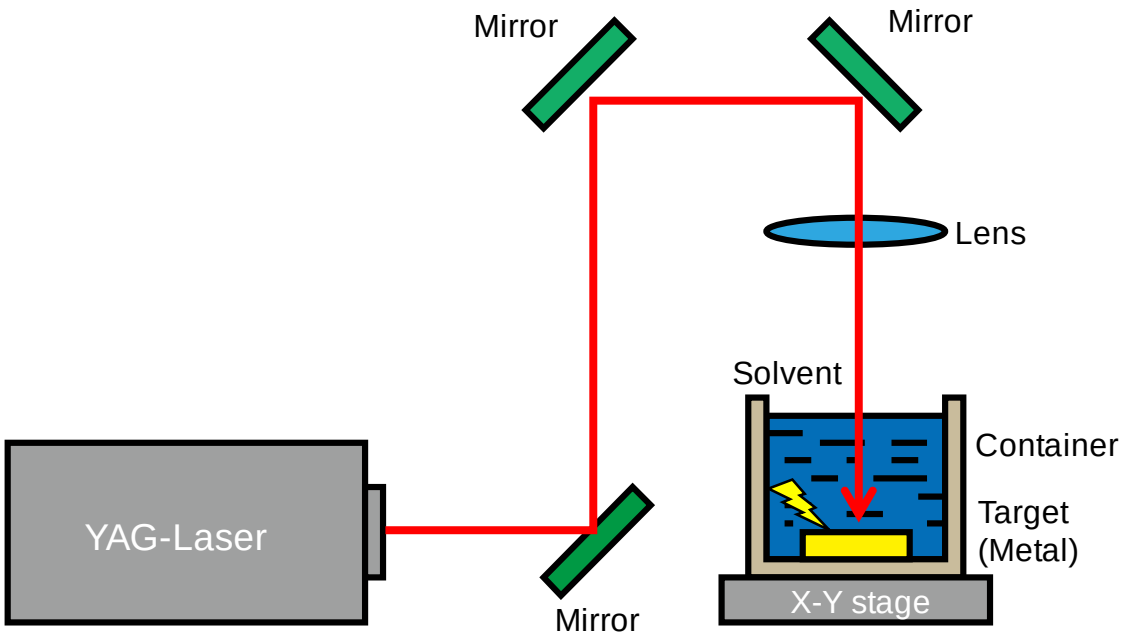

Figure 1-6. Illustration of the laser ablation method [32].

Arc Plasma Method

Electric arc is a powerful heating source. It generates heat at more than several thousand degree celsius with high energy density. In this method, it is possible to obtain a large amount of nanoparticles efficiently by blowing inert gas simultaneously with arc plasma. In some cases, the plasma used with gas is called plasma-jet. An example of the equipment using arc plasma is shown in **Figure 1-7**.

It is difficult to use a liquid for the collection of nanoparticles because this method generates a gas at very high temperature.

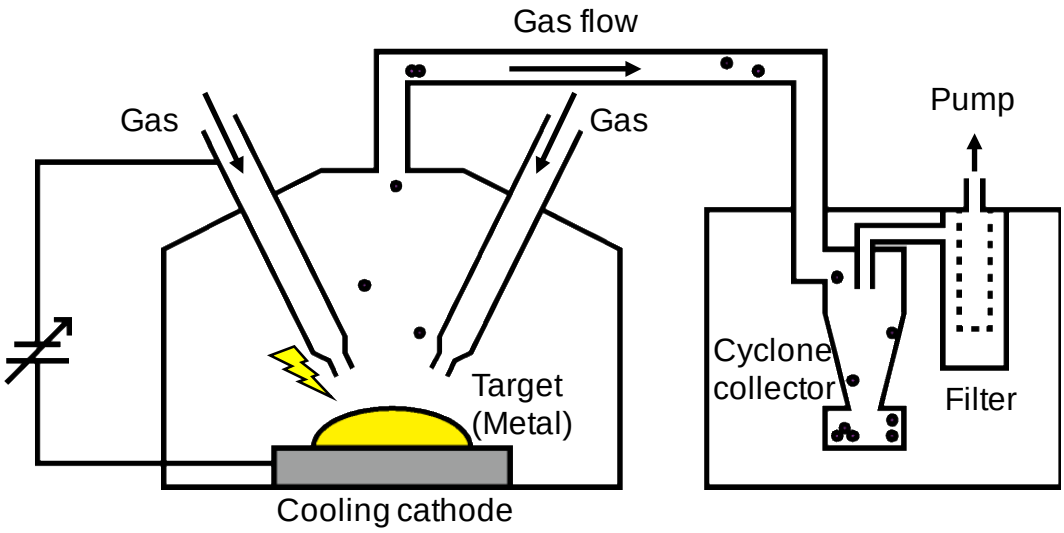

Figure 1-7. Illustration of the arc plasma method [33].

1-2-6 Improved Vacuum Evaporation on Running Oil Substrate (VEROS) Method

The improved Vacuum Evaporation on Running Oil Substrate (VEROS) method is a physical synthetic method for metal nanoparticles. The improvement of the original VEROS method was reported in 1987 by I. Nakatani *et al*. [34] The most important modification in this report is that a rotary cylindrical chamber instead of a rotary disc is used in order to form a thin oil film for collecting nanoparticles (the running trap solution). This modification enables us to produce the dispersion of nanoparticles with high concentrations.

In order to understand the improved VEROS method, the original VEROS method should be explained. The original VEROS method was established by Uyeda and co-workers based on the configuration as shown in **Figure 1-8** [35]. The lower side of the equipment is almost the same as that of the general vapor deposition. One of the greatest features of this method is the utilization of the rotating disk in the supply mechanism of the trap solution. In this method, an oil with high boiling point is adopted as a trap solution. Generally, a metal cannot be deposited on the surface of the liquid from the bottom to the

top because the liquid surface always faces upwards due to its gravity. This device allows the liquid surface to face downward by surface tension and centrifugal force. This collecting method for nanoparticles made it possible to use various evaporation sources. The trap solution containing nanoparticles is transferred to the collecting container. In addition, it became easier to add a protective agent by using a liquid in the collecting mechanism.

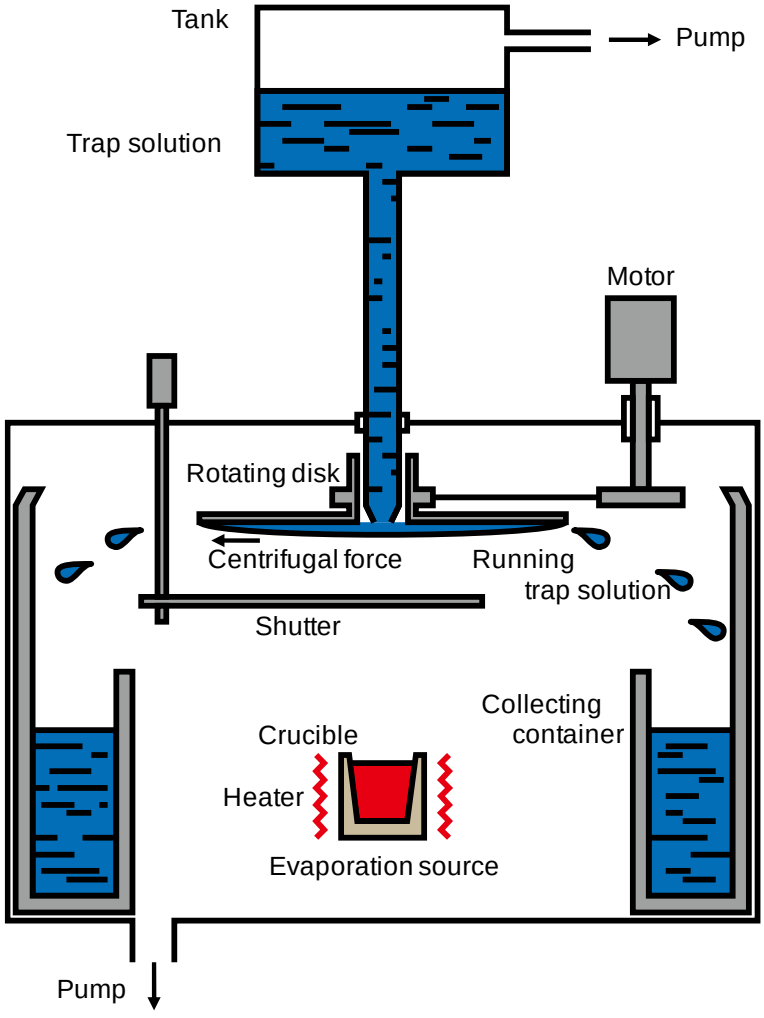

Figure 1-8. Illustration of the original VEROS method [35].

Although the VEROS method has an ability of synthesis of high-quality particles, it was difficult to make a large amount of nanoparticles at one time. The main factor is that

it was impossible to recycle the oil of the collecting liquid. Besides, when the amount of evaporation increases in order to obtain a high concentration of metal nanoparticles, the aggregation of nanoparticles on the liquid surface is likely to occur.

Significant improvements were made from the original VEROS method, which are explained in detail below. The illustration of the improved VEROS method is shown in **Figure 1-9 (a)**. In addition, the cross-section diagram of the chamber is shown in **Figure 1-9 (b)**. The chamber shape was changed from a normal disk to a cylinder. This cylindrical chamber rotates around the center. Evaporation source is installed at the center of the chamber. The oil as the collecting liquid for nanoparticles is poured into the lower part of the chamber in advance. This oil is called a trap solution in this method. An oil film is formed by the rotation of the cylindrical chamber. This oil film is called running oil or running trap solution due to its motion. Therefore, the fresh surface of the trap solution is continuously made on the inside of the chamber.

In addition, this method is potentially profitable for the synthesis of various kinds of metal nanoparticles because it can produce metal nanoparticles by vacuum evaporation regardless of synthetic environments unlike chemical synthetic methods.

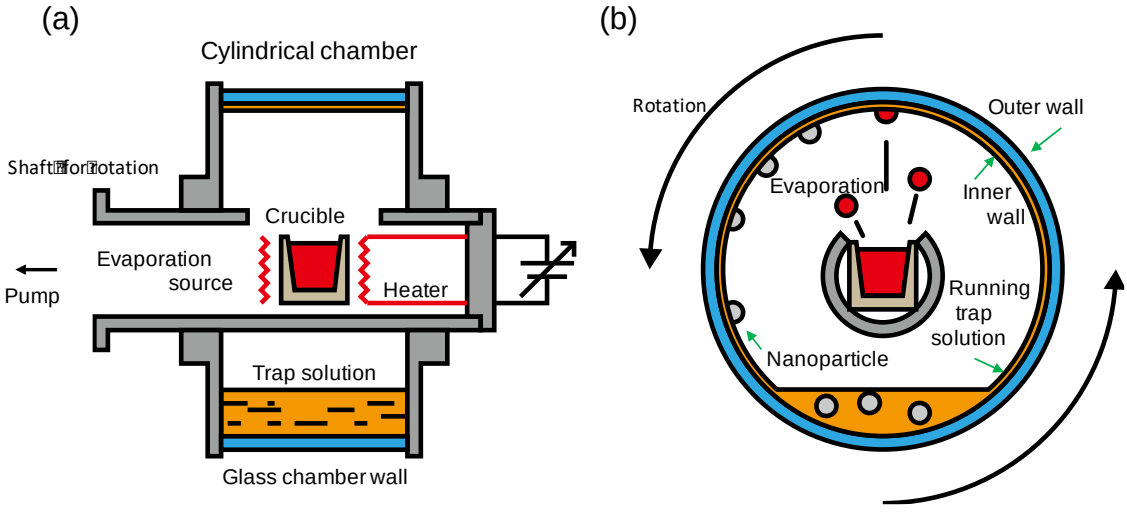

Figure 1-9. Illustration of the improved VEROS method. (a) Front view, (b) Cross-section diagram. [34]

Section 1-3: Purpose of This Study

Although there are various classifications of synthesis methods for metal nanoparticles, they are roughly divided into physical method and chemical method from the viewpoint of the supplying method of raw materials. In chemical synthetic methods, raw materials for metal nanoparticles are supplied as the metal complex, and they are soluble or dispersible and then dissociate in a polar solvent. In this situation, metallic atoms are usually ionized. Contrastingly, in physical synthetic methods, non-ionized atoms can be supplied for growing nanoparticles. For instance, evaporation of metal by heating is used for the supply of non-ionized atoms. In primary physical synthetic methods, cold substrate or wall was used as a collector for generated metal nanoparticles. Although it was effective to reveal the mechanism of particle formation, the method could not provide the sufficient amount of redispersible metal nanoparticles.

Surface protection for inhibition of aggregation and fusion between nanoparticles is required for the synthesis of these particles. Molecular adsorption of protective agents on the surface of nanoparticles is the most useful for the protection of metal nanoparticles. In addition, wet processes are preferable for the synthesis of metal nanoparticles because they are used as dispersion state in many application processes. Thus, it is important to investigate the adsorption of protective agents on the particle surface in the solution. For the above reasons, physical synthetic methods with the wet processes of collecting and protection are needed. However, it is difficult to make a system with the above features. The reasons are that a vacuum chamber is needed for the supply of non-ionized metallic atoms and that the chamber needs to have a solution for the collection and protection of metal nanoparticles.

Among a lot of physical synthetic methods, the improved VEROS method is the most suitable for this purpose. However, there have been no studies on molecular adsorption of protective agents on the surface of metal nanoparticles with the improved VEROS

method as far as the author knows. Therefore, it is important to investigate molecular adsorption of protective agents in the improved VEROS method at first. After that, the author discusses the difference between the improved VEROS method and chemical synthetic methods.

The purpose of this study is to clarify the role of protective agents in the synthesis of metal nanoparticles by the improved VEROS method, which is the simple system for synthesis of metal nanoparticles. In this method, the adsorption environment of the protective agent is quite close to that of the chemical method. This is because the non-ionized metal vapor supplied from the evaporation source is stabilized in the trap solution containing protective agents. Furthermore, the adsorption process of protective agents can be separated from the supply process of raw material.

Section 1-4: Composition of This Thesis

This thesis is constructed for the previously described purpose. Although the VEROS method requires the expensive and special equipment, the results obtained from these researches are highly useful for a lot of synthetic methods and their relevant studies. In the thesis, the VEROS method was used for the investigation of simple molecular adsorption of protective agents on the surface of metal nanoparticles.

In Chapter 1, as the general information, history of metal nanoparticles was described for the understanding of this research. Moreover, a lot of parts were devoted for comparison of synthetic methods for metal nanoparticles. The improved VEROS method used in this study was described in detail in the last part.

In Chapter 2, the effect of protective agents on the synthesis of silver nanoparticles was investigated in the improved VEROS method. After that, the concentration effect of the protective agents in the trap solution was also investigated in the synthesis of silver nanoparticles with sorbitan monooleate in order to clarify the growth mechanism of metal nanoparticles in the improved VEROS method.

In Chapter 3, the synthesis of silver nanoparticles was performed by a chemical synthetic method (thermal decomposition technique) with the same protective agents as the improved VEROS method. In addition, the adsorption states of oleic acid on the surface of silver nanoparticles synthesized by both physical and chemical synthetic methods were compared by using their IR spectra.

In Chapter 4, the comparison of physical adsorption strength to silver surface between carboxyl acid and amine compounds was carried out by the ligand exchanges with silver

nanoparticles synthesized by the improved VEROS method.

Finally, the findings obtained by experiments using the improved VEROS method were summarized. Furthermore, the forward perspective of this study was proposed from the conclusion of this thesis.

References

[1] R. Kubo, *J. Phys. Soc. Jap.* **1962**, *17*, 975-986.

[2] M. Takagi, *J. Phys. Soc. Jpn.* **1954**, *9*, 359-363.

[3] Ph. Buffet and J-P. Borel, *Phys. Rev. A* **1976**, *13*, 2287-2298.

[4] M. Faraday, *Philos. Trans. R. Soc.* **1857**, *147*,145-181.

[5] M. Haruta, T. Kobayashi, and H. Sano, N. Yamada, *Chem. Lett.* **1987**, *16*, 405-408.

[6] W. M. Haynes (Ed.), *CRC Handbook of Chemistry and Physics, 98th Edition* **2010**, CRC Press.

[7] P. R. Sajanlal, T. S. Sreeprasad, A. K. Samal, and T. Pradeep, *Nano Reviews* **2011**, *2*, 5883-5944.

[8] J. Turkevich, J. Stevenson, and P. C. Hillier, *J. Discuss. Faraday Soc.* **1951**, *11*, 55−75.

[9] H. B. Weiser, *Inorganic colloid chemistry* **1933**, *1*, 21-57.

[10] S. Jeon, P. Xu, N. H. Mack, L. Y. Chiang, L. Brown, and H. Wang, *J. Phys. Chem. C* **2010**, *114*, 36-40.

[11] M. Tsuji, R. Matsuo, P. Jiang, N. Miyamae, D. Ueyama, M. Nishio, S. Hikino, H. Kumagae, K. S. N. Kamarudin, and X. Tang, *Cryst. Growth Des.* **2008**, *8*, 2528-2536.

[12] C. E. Hoppe, M. Lazzari, I. Pardiñas-Blanco, and M. A. López-Quintela, *Langmuir* **2006**, *22*, 7027-7034.

[13] H. Dong, Y. -C. Chen, and C. Feldmann, *Green Chem.* **2015**, *17*, 4107-4132.

[14] Q. Peng,Y. Dong, Z. Deng, X. Sun, andY. Li, *Inorg. Chem.* **2001**, *40*, 3840-3841.

[15] Y. Endo, T. Sasaki, K. Kanie, A. Muramatsu, *Chem. Lett.* **2008**, *37*, 1278-1279.

[16] W. Stober, A. Fink, and E. Bohn, *J. Colloid Interface Sci.* **1968**, *26*, 62-69.

[17] J. Choi, Y. Kim, S. U. Son, K. C. An, S. Lee, *NSTI-Nanotech* **2010**, *2*, 464-467.

[18] K. Abe, T. Hanada, Y. Yoshida, N. Tanigaki, H. Takiguchi, H. Nagasawa, M. Nakamoto, T. Yamaguchi, and K. Yase, *Thin Solid Films* **1998**, *327-329*, 524-527.

[19] K. Kimoto, Y. Kamiya, M. Nonomiya, and R. Uyeda, *Jpn. J. Appl. Phys.* **1963**, 2, 702-713.

[20] S. Yatsuya, S. Kasukabe, and R. Uyeda, *Jpn. J. Appl. Phys.* **1973**, *12*, 1675-1684.

[21] S. Kasukabe, S. Yatsuya, and R. Uyeda, *Jpn. J. Appl. Phys.* **1974**, *13*, 1714-1721.

[22] T. Ohno, S. Yatsuya, and R. Uyeda, *Jpn. J. Appl. Phys.* **1976**, *15*, 1213-1217.

[23] T. Hayashi, T. Ohno, S. Yatsuya, and R. Uyeda, *Jpn. J. Appl. Phys.* **1977**, *16*, 705-717.

[24] Y. Saito, S. Yatsuya, K. Mihama, and R. Uyeda, *Jpn. J. Appl. Phys.* **1978**, *17*, 291-297.

[25] Y. Saito, K. Mihama, and R. Uyeda, *Jpn. J. Appl. Phys.* **1980**, *19*, 1603-1610.

[26] S. Kasukabe, S. Yatsuya, and R. Uyeda, *J. Cryst. Growth* **1974**, *24/25*, 315-318.

[27] M. Oda , *Dissertation (in Japanese)* **1986**, Nagoya University,115-132.

[28] Y. Ishida, R. Nakabayashi, M. Matsubara, and T. Yonezawa, *New J. Chem.* **2015**, *39*, 4227-4230.

[29] K. Okazaki, T. Kiyama, K. Hirahara, N. Tanaka, S. Kuwabata, and T. Torimoto, *Chem. Commun.* **2008**, *6*, 691-693.

[30] I. Akita, Y. Ishida, and T. Yonezawa, *Bull. Chem. Soc. Jpn.* **2016**, *89*, 1054–1056.

[31] G. Kawamura, S. Alvarez, I. E. Stewart, M. Catenacci, Z. Chen, and Y. -C. Ha, *Sci. Rep.* **2015**, *5*,18333.

[32] V. Amendola, and M. Meneghetti, *Phys. Chem. Chem. Phys.* **2013**, *15*, 3027-3046.

[33] M. Uda, *Bull. Japan Inst. Metals* **1983**, *22*, 412-420.

[34] I. Nakatani, T. Furubayashi, T. Takahashi, and H. Hanaoka, *J. Magn. Magn. Mater.* **1987**, *65*, 261-264.

[35] S. Yatsuya, K. Mihama, and R. Uyeda, *Jpn. J. Appl. Phys.* **1974**, *13*, 749-750.

Chapter 2: Effects of Protective Agents in the Synthesis of Silver Nanoparticles by the Improved VEROS Method.

Section 2-1: Introduction

Today, metal nanoparticles are becoming more valuable by the modification with organic molecules on their surfaces. Typical application fields of metal nanoparticles are conductive ink [1-3], storage media [4], biosensor [5-7], catalyst [8-11], conductivity flude [12], drug delivery [13-16] system, and optical devices [17]. In these fields, the extremely large surface area per unit mass compared with its bulk material is quite valuable. As the surface of metal nanoparticles becomes more sensitive with the increase in the surface energy, they can adsorb a lot of molecules. In addition, they show specific spectroscopic properties [18] and their optical properties are easily affected by the surface state of metal nanoparticles.

In the most cases, the surface of metal nanoparticles is covered with protective agents, which inhibits the aggregation and fusion between the nanoparticles. Furthermore, protective agents can endow the nanoparticles with some types of functionality such as solvent dispersibility, reactivity, and stability [19]. Even though the selection of protective agents is especially important for obtaining high quality nanoparticles, it is highly difficult to investigate the effect of protective agents on the production of metal nanoparticles systematically. This is because there are a lot of parameters such as metal precursor, solvent, and reducing agent in general chemical synthetic methods. These parameters affect each other in the reaction medium, which brings about the difficulty in the clarification of the performance of protective agents.

In addition to characteristics brought by adsorption of protective agents, it is important

to investigate the effect of protective agents in the synthesis process of nanoparticles. The elucidation of the effect enables researchers to synthesize metal nanoparticles with adsorption of any protective agents. Especially, it is expected that the adsorption moiety affects the production of metal nanoparticles highly. This is because the adsorption strength of protective agents for the nanoparticle is strongly related to the sojourn time of protective agent on the surface of nanoparticles and the stability of obtained nanoparticles.

Based on these backgrounds, the purpose of this chapter is investigation of the influence of the protective agents in the synthetic process of metal nanoparticles. For the objective, the author adopted the synthesis of silver nanoparticle by a physical synthetic method because silver is an easy-to-handle material in the consideration of its cost and stability. The experiments with silver nanoparticles are discussed in a lot of references. As the characteristics of silver nanoparticles are highly dependent on their size and shape [2-5], it is necessary to investigate the influence of protective agents on the particle growth before evaluating the adsorption phenomenon. In addition, protective agents never affect metal sources in physical synthetic methods. By contrast, metal sources are almost affected by protective agents in chemical synthetic methods because they are mixed with protective agents in the reaction solution. These factors complicate the discussion on the adsorption behavior of the protective agent. As general features of physical syntetic methods, these methods require expensive equipment but they also bring some merits. For instance, a metal can be used at a granular state as a source material. After the source material is atomized into nanoparticles by physical energy, the surface of metal nanoparticles is covered with protective agents immediately. The covering with protective agents is attributed to physical adsorption.

The analytical techniques for investigating the interaction between protective agents and the surface of metal nanoparticles have been developed. For instance, the quartz crystal microbalance (QCM) method has been used for the analysis of molecular adsorption and desorption [20-22]. It is frequently utilized for observing the adsorption

process of protective agents on the metal surfaces but this method has two serious problems. One is the difference in the curvature factor because the surface of the sensor tip is generally flat even though nanoparticles have high curvature. Even if metal nanoparticles are fixed on the sensor tip, the surface of the sensor tip is not the same as that of nanoparticle because metal nanoparticles tend to fuse each other on the sensor tip. The other problem is the lack of the cleanliness on the metal surface due to the adsorption of unwanted molecules such as water in the atmosphere. Accordingly, the QCM method cannot be the best approach to investigate the adsorption process of protective agents on the surfaces of metal nanoparticles. Recently, an interesting research about the ligand effect on the formation of gold nanoparticles via sputtering deposition over a liquid matrix has been also reported [23]. The diameter of gold nanoparticles produced by sputtering process could be controlled by varying the kinds of protective agents in this report. However, analytical methods for characterizing nanoparticles are limited due to the low production output of this sputtering deposition method.

In order to achieve the investigation of influence of protective agents, the VEROS method with a cylindrical glass chamber (improved VEROS method) [24] was employed in this study. In the VEROS method, metal vapors are made by vacuum evaporation and they form the nanoparticles before entering into the running trap solution containing protective agents. The protective agents cover their surfaces as soon as the nanoparticles enter into the trap solution. In this process, an extremely clean surface of metal nanoparticles is covered by protective agents right after the formation of metal nanoparticles, unlike QCM method. Thus, the two processes, which are the formation of metal nanoparticles and the adsorption of protective agents on the surface of metal nanoparticles, are completely independent in the VEROS method and all the parameters concerning the nanoparticle formation can be ignored in terms of considering the effect of protective agents. In other words, protective agents act only in adsorption process, which enables a systematic investigation of effect of protective agents on the surface of

metal nanoparticles. These features were well adapted for this study. Furthermore, this method is appropriate for the mass production of metal nanoparticles. In this experiment, five types of compounds shown in **Figure 2-1** were employed as protective agents. There are two reasons for the choice of these oleyl compounds: One is that all the compounds have an oleyl group for improving the solubility in alkylnaphthalene used as a solvent. The other is that only hydrophilic moieties in the five compounds are different for each of them. For this reason, the difference enables this research to compare the effect of the hydrophilic moiety in protective agents on the surface of metal nanoparticles.

Moreover, a size-determining factor of silver nanoparticles is an important clue for understanding the growth mechanism because it limits the growth of silver nanoparticles. Of course, ample studies have reported many techniques for size control. For example, the pH of the reaction medium played an important role in determining the morphology of silver nanoparticles [25]. Further, the particle size of silver nanoparticles was regulated by heat treatment in the solid state or the solution [26]. The mechanism of particle size determination has been poorly understood in the VEROS method, although several mechanisms have been suggested [27]. For the discussion of the mechanism, the effect of protective agent concentration in the trap solution was investigated in the improved VEROS method with a suitable protective agent. The concentration of protective agents in the synthetic process is related to the frequency of contact between the nanoparticle surface and protective agents. This frequency seems to affect the growth behavior of nanoparticles in the synthetic process. In other words, the complete protection of the particles means the end of particle growth. Of course, the actual synthetic process is not simple, but the investigation would help to discuss the behavior of protective agents in the synthetic process.

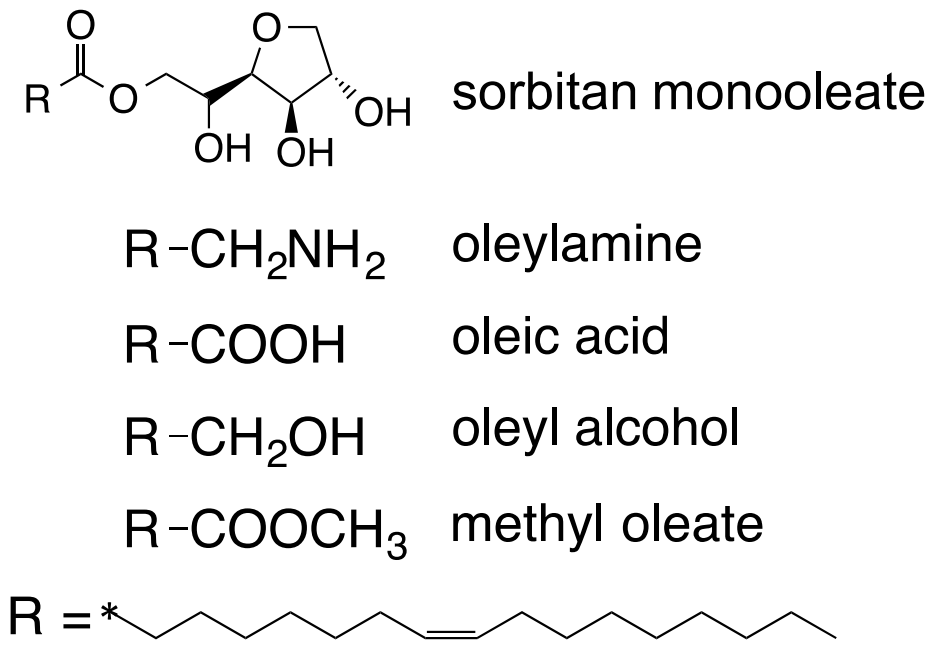

Figure 2-1. Chemical structures of protective agents employed in this study.

Section 2-2: Results and Discussion

2-2-1 Design of Advanced Equipment for the Improved VEROS Method

There has been no major change in the equipment for the improved VEROS method since the improvement of original VEROS method was reported in 1987 [24]. Although, the improvement of the equipment in the report was sufficient to bring about the significant results at the time, further modifications were needed for the purpose of the author's study. Most of modifications were designed for the improvement of experimental reproducibility. Especially, computerized numerical control of the equipment and recent advanced design for evaporation source are highly important in the modifications. These technologies have not been applied to the equipment for the improved VEROS method, despite the remarkable progress of general vapor deposition equipment in the past 30 years. These improvements should be also incorporated into the improved VEROS method. Therefore, the author remakes and updates the equipment from scratch.

Power control of evaporation source is the most important for constant evaporation rate. In the resistive heating, this power is determined based on the voltage multiplied by current. However, the resistance value of filament is not constant because it has inescapable temperature dependency in the temperature range of metal evaporation used in this study. Thus, general electric power (constant voltage or current) of the general evaporation source cannot be controlled at the constant value. This problem was completely solved by the computer control of the electric power source. The computer calculates electric power more than 10 times per second and performs feedback so as to obtain a constant electric power. This system stabilized the experimental conditions extremely and as a result it remarkably improved the reproducibility of experiments. In addition, this system also contributed to the control of the rotation speed of the cylindrical chamber.

For constant evaporation of metal, the most important point after the power control is

the design of evaporation source. There are two important points for the design of evaporation source. One is the shape of the crucible and the other is balance for heat insulation and heat transfer. They are closely related to uniformity of evaporation rate in an experiment.

The shape of the crucible used in the reported equipment was the inverted cone shape (**Figure 2-2**) [24]. This shape has some merits. For example, the remaining amount of metal can be seen visually from the top. Unfortunately, these merits are useful for machine development but not for synthesis of metal nanoparticles. The stability of the evaporation rate is deteriorated by this shape because it is largely affected by the front area of evaporation. Then, the surface of the crucible becomes exposed as the amount of the raw material decreases. This exposed area unnecessarily heats the trap solution by radiation heat futilely. Therefore, the shape of the crucible was modified to the inverted top hat shown in **Figure 2-3**. In this shape, the front area of evaporation is constant until the raw material disappears. Of course, this benefit is valid so long as the temperature of the crucible is constant.

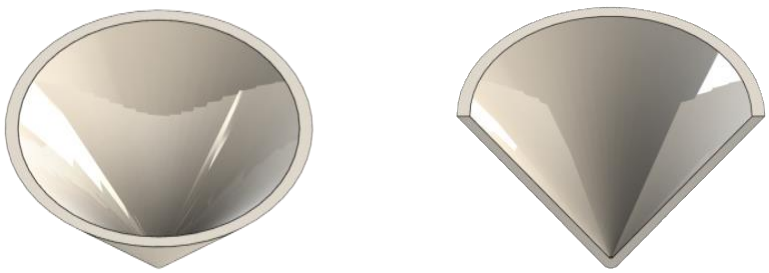

Figure 2-2. Appearances and cross-section diagrams of the crucible with the inverted cone shape used in the conventional improved VEROS method.

Figure 2-3. Appearances and cross-section diagrams of the crucible with the inverted top hat shape used in the newly-designed improved VEROS method.

The optimal evaporation source varies depending on the purpose. In this study, the temperature control of the evaporation source is the most important. From this point of view, the conventional equipment has some serious problems in its heater and insulation zone. The appearance and cross-section diagrams of the evaporation unit in the conventional equipment are shown in **Figure 2-4**. This figure shows a model in which heated filament is dipped in the molten metal. The contact of the filament with the molten metal is excellent in terms of efficient heat transfer, but it is not suitable for uniform heating because of local heating. Moreover, this unit adopts a cup-shape insulation made of alumina called shroud. This insulation is not suitable in a vacuum because thermal conductivity of alumina is not enough low. In other words, the effect of this design is to protect the surrounding parts by diffusing heat with alumina. Its design is more effective in the atmosphere. By contrast, the author's design makes it possible to confine energy using a shield called reflector. The evaporation unit designed by the author is shown in **Figure 2-5**. The crucible is covered with the reflector except for the metal vapor outlet. There are the three types of heat transfers (conduction, convection, and radiation) in the vacuum conditions. The influence of conduction can be quite reduced by minimizing the

contact area. The design of thermal insulation in vacuum is optimized for radiation heat. However, energy of radiation is mainly determined by temperature, material, and surface area. Thus, it must be designed to negate the radiated energy instead of reducing the radiated energy. The component for the purpose is the reflector made of molybdenum. The shiny surface of the metal reflects the radiated light energy directly to the crucible. Moreover, the inner wall of the reflector emits half of absorbed energy as radiation heat to the crucible. At this time, another half of the energy is released to the outside. For the radiation of absorbed energy, the inner wall of the reflector has to heat up soon. For that reason, an extremely thin metal plate was used as the inner wall of the reflector for easy temperature change. This reflector has a multilayered structure in order to return the leaked energy to the inside as much as possible. In this unit, a three-layer reflector was adopted (**Figure 2-6**). As a result, the energy to escape outside is reduced, and the internal temperature becomes uniform.

Due to the accumulation of these improvements, the evaporation source newly-designed by the author is superior to the conventional one in terms of temperature control. These improvements made it possible to compare synthetic results based on trivial differences such as changes in components of trap solutions.

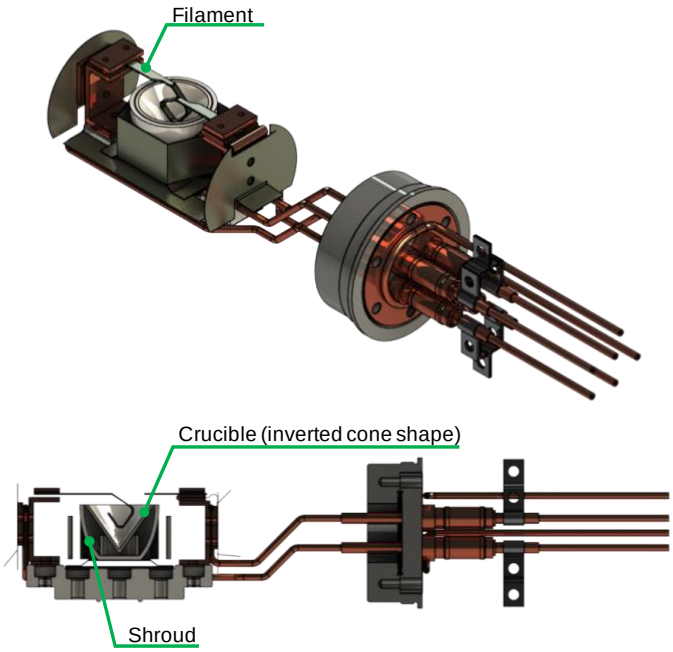

Figure 2-4. Appearances and cross-section diagrams of the evaporation unit used in the conventional improved VEROS method.

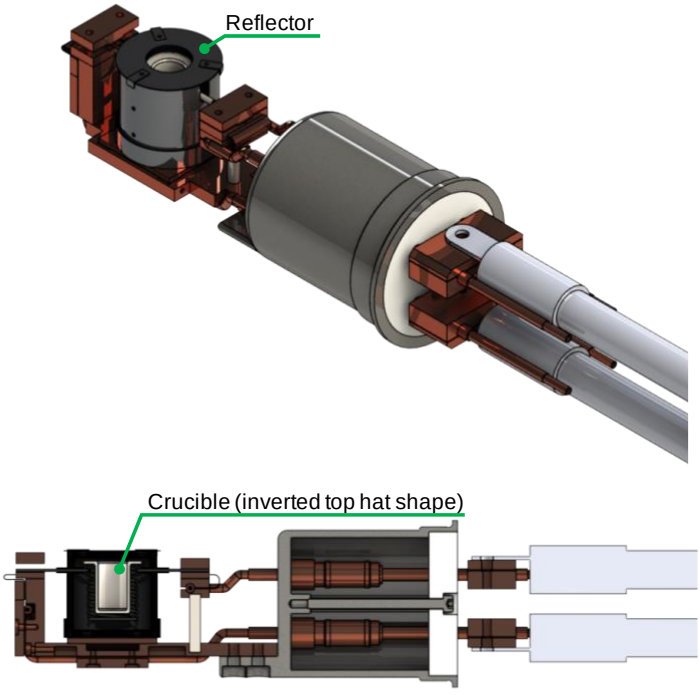

Figure 2-5. Appearances and cross-section diagrams of the evaporation unit used in the newly-designed improved VEROS method.

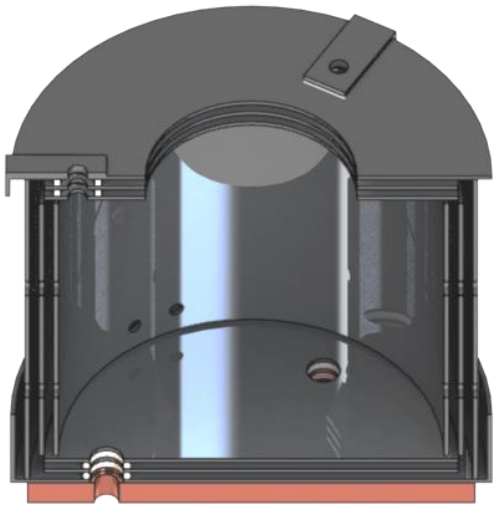

Figure 2-6. The cross-section diagram of the three-layer reflector for the newly-designed evaporation unit.

2-2-2 Effect of Adsorption Moiety of Protective Agent

Silver nanoparticles were synthesized by the improved VEROS method with the five trap solutions. **Figure 1-9** shows a diagram of the equipment used in this study. The trap solutions were prepared by mixing alkylnaphthalene and a protective agent. Alkylnaphthalene, which is a general oil showing high thermal stability and excellent chemical tolerance, was used as a solvent for providing moderate fluidity. The five protective agents with different hydrophilic groups were selected. Those are sorbitan monooleate, oleylamine, oleic acid, oleyl alcohol, and methyl oleate. Here, all the protective agents have an oleyl group, which bestows high fluidity and boiling point on the protective agents. Therefore, the composition ratios of the trap solutions hardly changed under the vacuum conditions. The concentration of the protective agent was set at about 20 wt% (at the same molar amount among protective agents). Synthetic conditions of silver nanoparticles with five protective agents are shown in **Table 2-1**. The samples synthesized using sorbitan monooleate, oleylamine, oleic acid, oleyl alcohol, and

methyl oleate are symbolized as sorbitol, amino, carboxy, hydroxy, and ester, respectively, in the following figures.

Table 2-1. Synthetic conditions of silver nanoparticle with five protective agents by the improved VEROS method.

Protective agents	Amount of Protective agent / g	Total amount of trap solution / g	Supply amount of silver / g
Sorbitan monooleate	21.43	121.43	10
Oleylamine	13.37	113.37	10
Oleic acid	14.12	114.12	10
Oleyl alcohol	13.42	113.42	10
Metyl oleate	14.82	114.82	10

Figure 2-7 shows the appearances of the trap solutions after the synthesis. The appearances were distinctly different although the same amount of silver was evaporated under the vacuum conditions. It is noteworthy that the colors of the attachment on the sidewall of the bottles were different. The samples were roughly divided into two groups. The samples, where a yellow liquid film was observed on the sidewall of the bottle, in the cases using sorbitan monooleate, oleic acid, and oleylamine were categorized into one group. In the other group, a cloudy color liquid film was observed in the cases using oleic alcohol and methyl oleate. This difference in color is derived from the plasmon color peculiar to nanoparticles. In the case of silver nanoparticle, the plasmon color is yellow. On the other hand, the disappearance of plasmon color means the size increases of nanoparticles due to their aggregation and fusion. This result indicates the difference in the size of obtained silver particles.

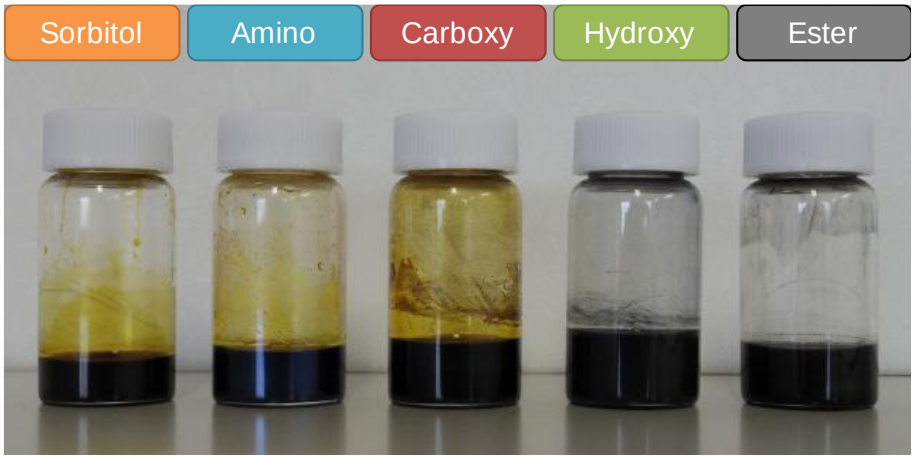

Figure 2-7. Appearances of the trap solutions after the synthesis by the improved VEROS method with the five trap solutions.

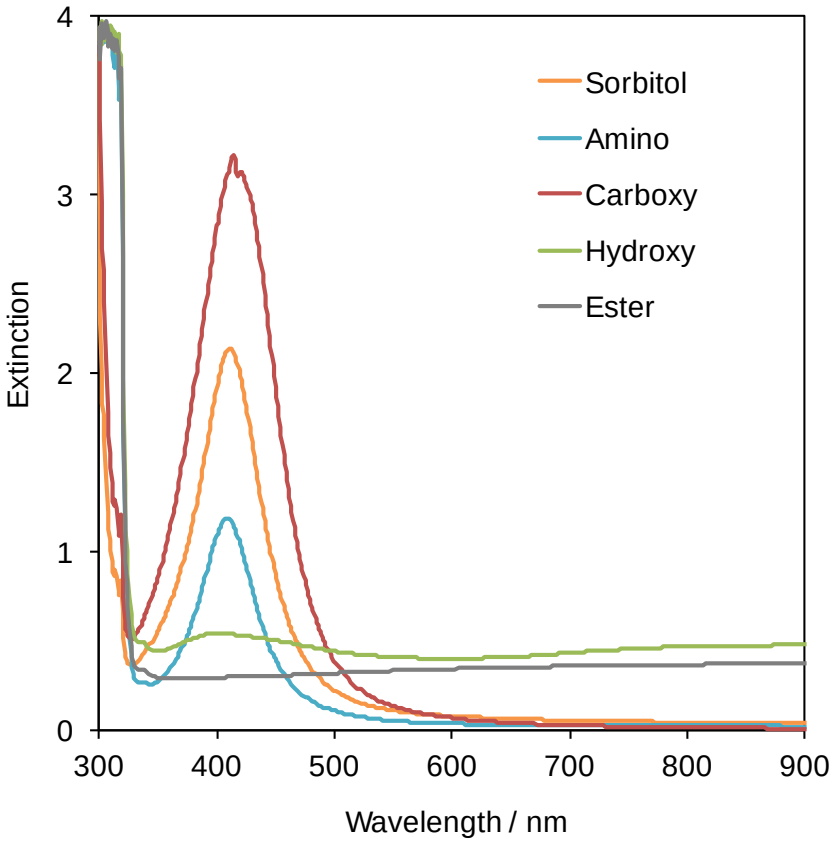

Figure 2-8. Extinction spectra of the trap solutions after the synthesis by the improved VEROS method with the five trap solutions.

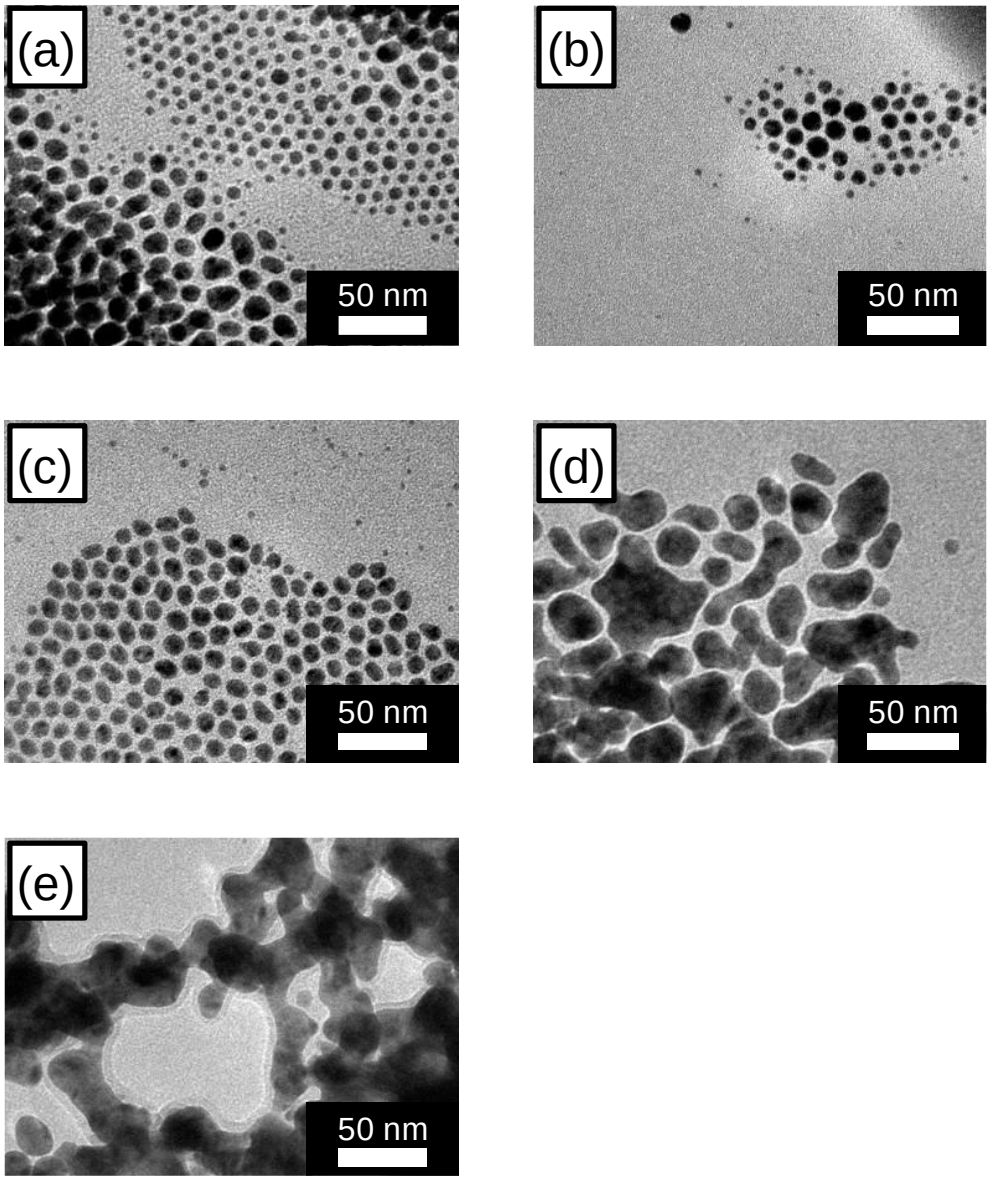

Figure 2-9. TEM images of silver nanoparticles synthesized by the improved VEROS method. Silver nanoparticles (a), (b), (c), (d), and (e) were synthesized using sorbitan monooleate, oleylamine, oleic acid, oleyl alcohol, and methyl oleate, respectively.

Table 2-2. Maximum extinction wavelength and FWHM of five silver nanoparticles in the extinction spectra of their dispersed *n*-dodecane solutions.

Protective agent	λ_{max} / nm	FWHM / nm
Sorbitol	412	67
Amino	409	60
Carboxy	418	84
Hydroxy	403	n.d.
Ester	n.d.	n.d.

Note: n.d., not determined.
λ_{max}, maximum extinction wavelength
FWHM, full width at half maximum.

Next, the extinction spectra of the trap solutions after the synthesis were measured (**Figure 2-8**) and the maximum extinction wavelength and full width at half maximum (FWHM) were indicated in **Table 2-2**. It is well known that metal nanoparticles show characteristic absorption peaks, whose particular wavelength is highly dependent on the size of nanoparticles [28,29]. The trap solutions were diluted at the same ratio with *n*-dodecane before the measurements. Furthermore, the samples synthesized using sorbitan monooleate and oleic acid were diluted ten times with *n*-dodecane because their spectra were saturated. A sharp extinction peak around 400 nm was observed in the cases using sorbitan monooleate, oleic acid, and oleylamine. This result demonstrates that silver nanoparticles could be obtained in those cases. In the cases using oleic alcohol and methyl oleate, the presence of silver nanoparticles was vanishingly small in their extinction spectra although the amounts of protective agents were sufficient for the formation of nanoparticles. Alternatively, the increase of the background was observed at more than 600 nm. This phenomenon would be originated from the increase of the light scattering based on the occurrence of coarse particles. **Figure 2-9** shows the TEM images of silver

nanoparticles synthesized by the improved VEROS method with the five trap solutions. Many spherical and independent particles were observed in **Figures 2-9 (a)-(c)**. On the other hand, the shape of most particles was highly complicated due to the fusion in **Figure 2-9 (d) and (e)**. The particle diameters of silver nanoparticles in the TEM images were quantitatively analyzed by digital image analysis software (**Figure 2-10**). **Table 2-3** shows the yield of silver nanoparticles, average diameter, and average circularity of obtained silver nanoparticles. In this table, the values of hydroxy and ester should be roughly treated for reference because their values certainly include the results of particles which are obviously larger than nano-size. In **Figures 2-10**, the ranges of the particle size distributions of silver nanoparticles were almost the same in three of the samples and their average diameters were 6.9 ± 3.3 nm, 6.0 ± 3.3 nm, and 8.2 ± 3.0 nm, respectively. The order of diameters of the three samples was in agreement with the order of maximum extinction wavelengths observed in UV-vis spectra. On the contrary, coarse particles were observed in the cases using oleic alcohol and methyl oleate. In these samples, it is too difficult to determine the particle size because the shapes of the particles were highly complex. Probably, they are generated by the fusion of small nanoparticles. As a reference, the nano-structure of silver was not observed at all in the case of the trap solution without any protective agent (**Figure 2-11**). In this case, silver nanoparticles easily agglutinated and formed coarse particles at the microscale.

These particle sizes shown in **Figure 2-10** seem to be bimodal or more distributions. The author anticipates that there are two main factors in the growth of particles. One of the factors is of course the supply of silver atoms by evaporation. The other factor is the fusion by agglomeration of particles. The author thinks that the different factor brings about the different growth of particles.

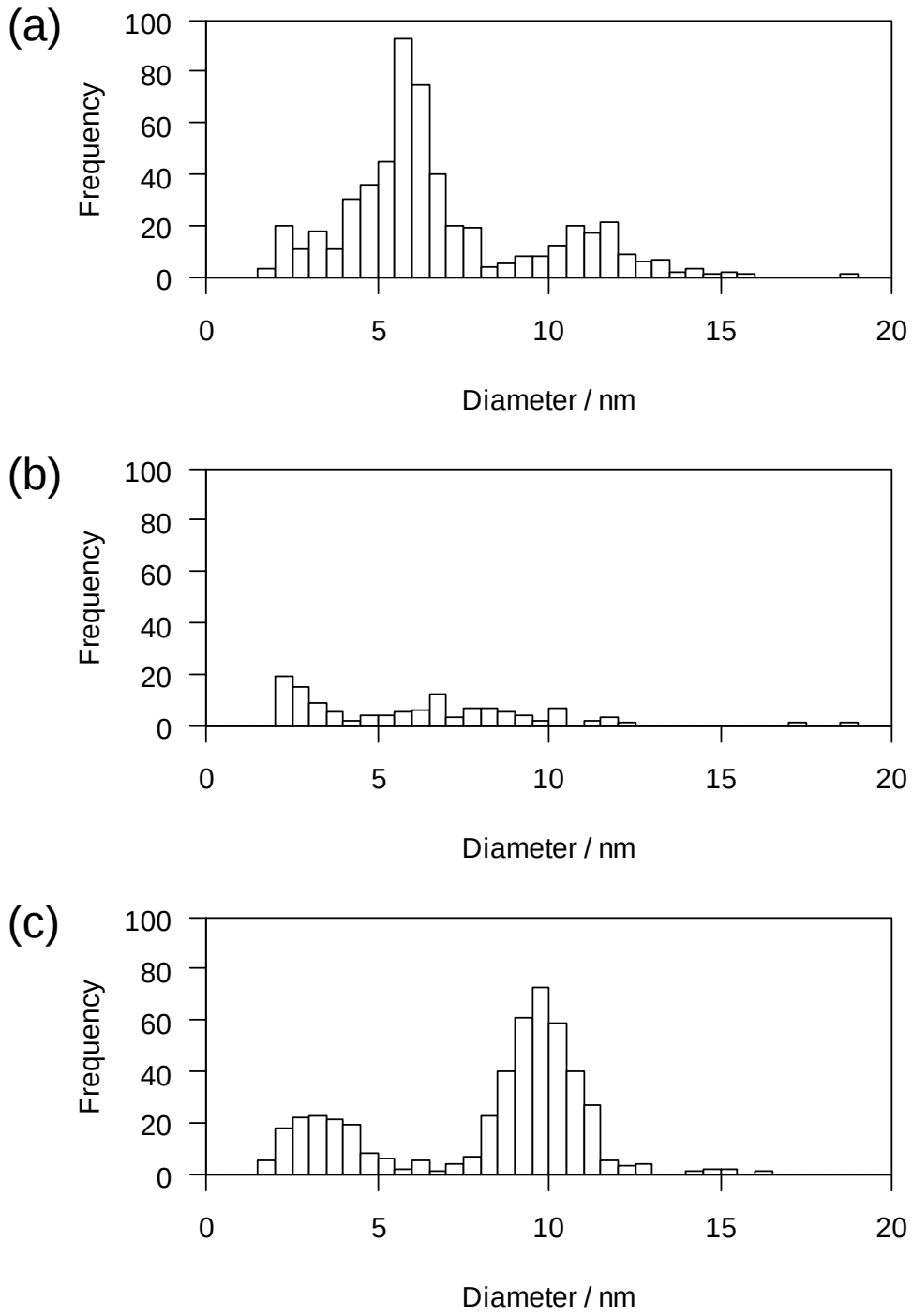

Figure 2-10. Particle size distributions of silver nanoparticles synthesized by the improved VEROS method with the three trap solutions. The samples (a), (b), and (c) were synthesized using sorbitan monooleate, oleylamine, and oleic acid, respectively.

Table 2-3. Yield of silver nanoparticles, average diameter, and average circularity of silver nanoparticles obtained by the improved VEROS method.

Protective agent	Yield of silver nanoparticles / %	Diameter / nm	Circularity
Sorbitol	29.7	6.9 ± 3.3	0.8 ± 0.1
Amino	0.4	6.0 ± 3.3	0.7 ± 0.1
Carboxy	25.7	8.2 ± 3.0	0.7 ± 0.1
Hydroxy	(15.4)*1	n.d.	n.d.
Ester	(7.5)*1	n.d.	n.d.

Note: n.d., not determined.
*1, Rough value for reference.

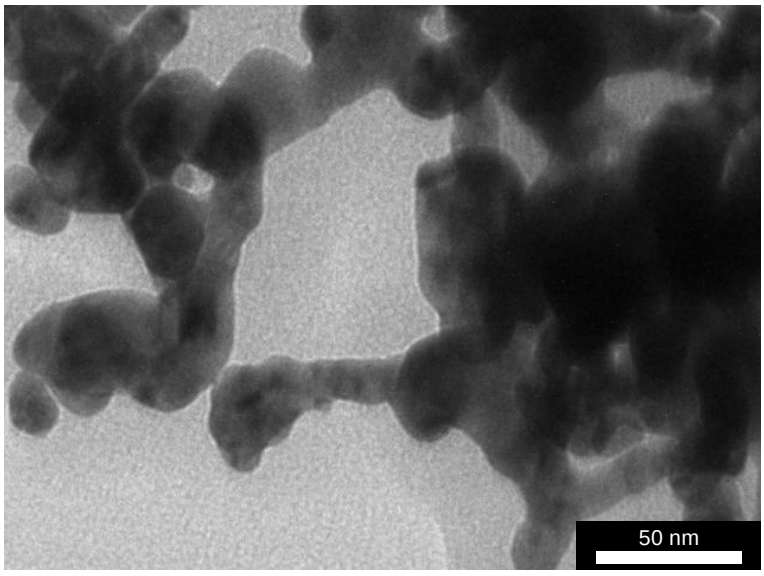

Figure 2-11. TEM image of the sample synthesized by the improved VEROS method using the trap solution without any protective agent.

The productivity in the physical process is evaluated by the utilization efficiency of the raw material. The yields of silver nanoparticles were calculated from the weight loss obtained by TGA and the input amount of silver. Here, the remaining weight ratios of the trap solutions after heating at 500˚C equals to the weight ratios of silver nanoparticles dispersed in the trap solution. Surprisingly, the yield was extremely low only when oleylamine was used as a protective agent. This result demonstrates that the aggregates of silver, which are too large for TEM observation, were generated at the majority instead of nanoparticles. Similarly, as some aggregates were formed in the cases using oleic alcohol and methyl oleate, their material efficiencies were also low. Whereas, the yields in the cases of sorbitan monooleate and oleic acid were significantly higher than those of other cases. This result shows that only sorbitol and carboxy groups could adsorb on the surface of silver nanoparticles effectively. In the cases of using sorbitan monooleate and oleic acid, about 30 % and 26 % of silver as a source material formed the nanoparticles under the experimental conditions used in this study, respectively. The yield is not so high from the viewpoint of effective utilization of materials. This is because more than 50 wt% of silver as a source material adsorbs on the inner wall of the apparatus. However, they can be reused for the next synthesis of silver nanoparticles. This problem would be solved by lengthening the distance between the evaporation source and the inner wall of the apparatus. Therefore, it is not an essential problem of the improved VEROS method.

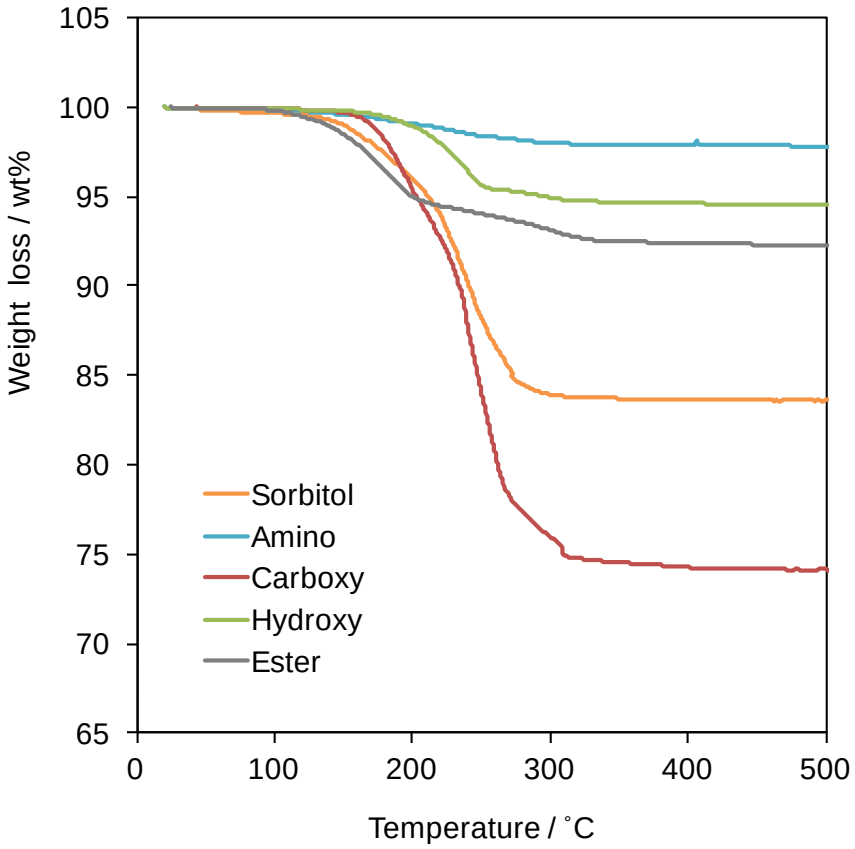

Figure 2-12. TGA curves of silver nanoparticles synthesized by the improved VEROS method.

Table 2-4. Maximum extinction wavelength and FWHM of the five kinds of silver nanoparticles in the extinction spectra of their redispersed *n*-hexane solutions.

Protective agent	λ_{max} / nm	FWHM / nm
Sorbitol	404	101
Amino	406	77
Carboxy	414	83
Hydroxy	n.d.	n.d.
Ester	n.d.	n.d.

Note: n.d., not determined.
λ_{max}, maximum extinction wavelength
FWHM, full width at half maximum.

The amount of protective agents existing on the surface of the particles was evaluated by TGA using silver nanoparticles isolated from the trap solutions. The isolation was carried out with decantation for the removal of the excess of the protective agent and solvent. **Figure 2-12** shows the TGA curves of silver nanoparticles which were synthesized with the five protective agents. In the cases of oleylamine, oleic alcohol, and methyl oleate, the weight loss ratios after heating at 500˚C were much lower than those in the cases of sorbitan monooleate and oleic acid. This result shows that these protective agents hardly existed in the isolated silver nanoparticles. Among the five protective agents, the weight loss ratio was the highest in the case of oleic acid. This result shows that oleic acid most effectively adsorbs on the surface of silver nanoparticles in the improved VEROS method. Furthermore, the isolated samples were redispersed at the concentration of 1 mg (silver) per 36 mL (*n*-hexane). **Figure 2-13** shows the extinction spectra of these solutions and the maximum extinction wavelength and FWHM are shown in **Table 2-4**. The absorbance originated from silver nanoparticles was the highest in the case of oleic

acid. These spectra indicate that the sample synthesized using oleic acid shows the best dispersibility in *n*-hexane. This result may be mainly due to the fact that the amount of protective agent on the surface of silver nanoparticles after the isolation was the highest in the case of oleic acid. The maximum extinction wavelength and FWHM of the spectrum hardly changed after the isolation process with decantation in the case of oleic acid. On the other hand, no peak was observed in the cases of oleic alcohol and methyl oleate. This result means that most of the particles could not redisperse in the solution.

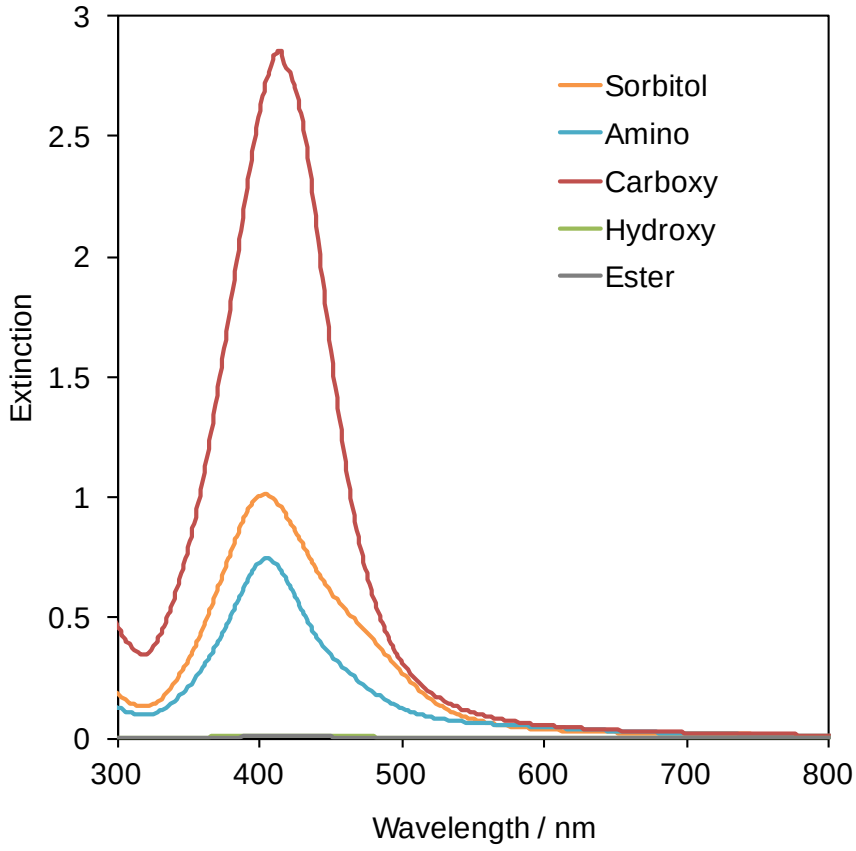

Figure 2-13. Extinction spectra of redispersed silver nanoparticle solutions.

2-2-3 Effect of Concentration of Protective Agent in the Trap Solution

The experimental results of the concentration effect of protective agent in the trap

solution were described below. Here, sorbitan monoolate was selected from the five protective agents in **Figure 2-1** because the silver nanoparticles synthesized with sorbitan monooleate showed the best yield and good redispersibility. Synthetic conditions of silver nanoparticle are shown in **Table 2-5**. The typical TEM images are shown in **Figure 2-14**. In the case of Entry 1 (Protective agent concentration: 1 wt%), many coarse particles were observed as shown in **Figure 2-14 (a)**. These coarse particles are very large and heteromorphic. They must be secondary particles generated by the fusion of primary particles. On the other hand, small and spherical particles were observed in **Figures 2-14 (b)-(d)** in the cases of Entry 2-4 (Protective agent concentrations: 5, 10, and 20 wt%). The primary particles were more frequently observed along with the increase in the protective agent concentration. Remarkably, the secondary particles were hardly observed in the case of the highest protective agent concentration (Entry 4 (Protective agent concentration: 20 wt%), **Figure 2-14 (d)**). These results indicate that aggregation among the silver nanoparticles was effectively inhibited by the increase of the protective agent concentration. In addition, the silver nanoparticles synthesized under the optimum synthetic conditions could redisperse in a solution after the washing and drying process except irreversible aggregated particles.

Table 2-5. Synthetic conditions of silver nanoparticles by the improved VEROS method

Entry	Protective agent concentration / wt%	Total amount of trap solution / g	Supply amount of silver / g
1	1	100	10
2	5	100	10
3	10	100	10
4	20	100	10

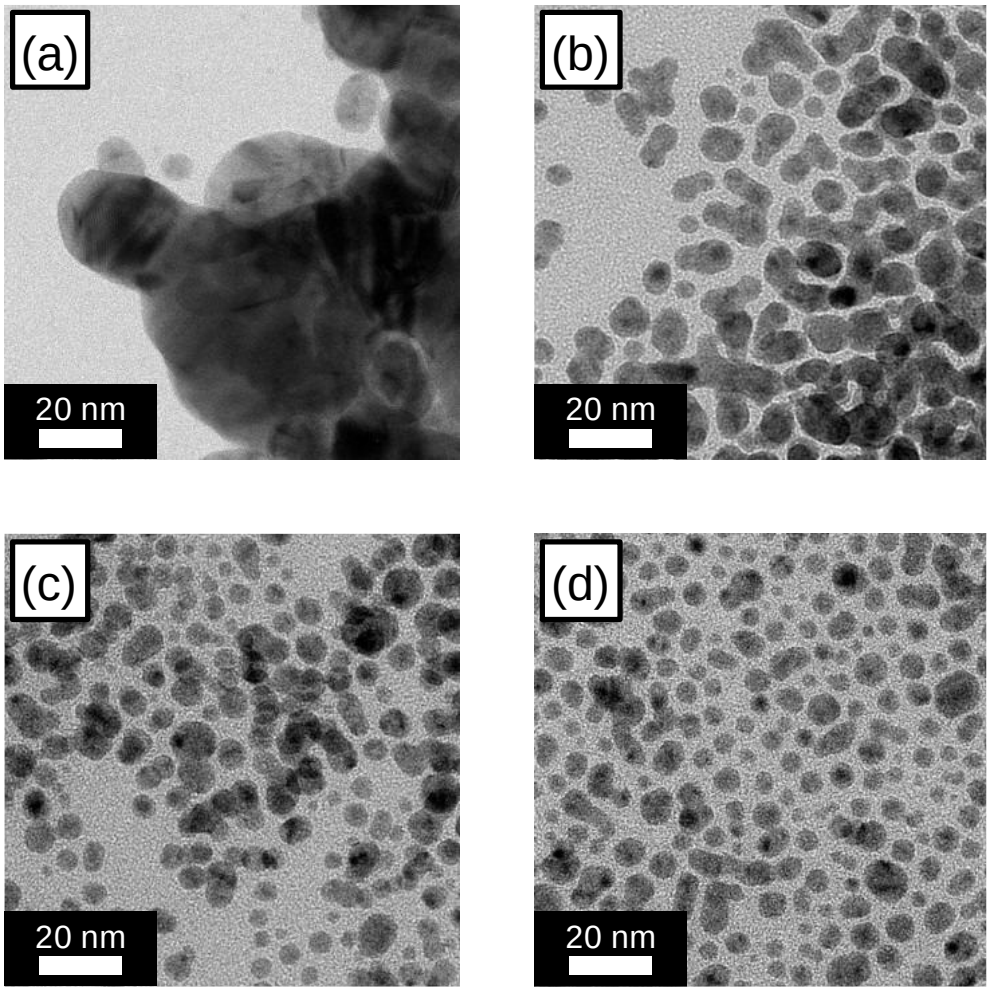

Figure 2-14. TEM images of silver nanoparticles synthesized at different concentrations of sorbitan monooleate: (a) 1 wt%, (b) 5 wt%, (c) 10 wt%, and (d) 20 wt%.

The effect of the protective agent concentration on the size of the primary particles was quantitatively evaluated by a digital image analysis software from pictures of over five points on the grids. In this analysis, the TEM images were converted to binary images based on a threshold value. After that, each particle was detected in the binary images. Calculations of the projected area diameter and the circularity of the particles are conducted. The projected area diameter is calculated from the projection area of particle, assuming that the particle shape is a perfect sphere. Circularity is defined as the ratio of the projected area diameter to the diameter calculated from the perimeter of the projection area. The size (projected area diameter) distributions of the nanoparticles were determined by using only primary particles, which is defined as the particle with circularity of 0.6 or more in this study (**Figure 2-15**). As a result, all particles larger than 20 nm in diameter were excluded from the analysis of primary particles. In **Figure 2-15 (a)**, the author rarely counted nanoparticles because most of the particles aggregated severely. In **Figures 2-15 (b)**, **(c)**, and **(d)**, the sizes of the nanoparticles synthesized under the three synthetic conditions were very close, and the average diameters were 6.8 ± 2.7 nm, 5.2 ± 2.2 nm, and 5.4 ± 2.0 nm, respectively. In addition, the size distributions had almost the same range from about 2 nm to 15 nm. These results indicate that the size of the primary particles is hardly affected by the protective agent concentration in the trap solution.

It is well known that metal nanoparticles show particular absorption spectra by local surface plasmon resonance and their maximum absorption wavelength is highly dependent on the size of their nanoparticles [30]. Accordingly, a change in the particle size brings about a peak shift of plasmon absorption. The trap solutions containing silver nanoparticles with different concentrations of sorbitan monooleate were diluted by cyclohexane, and their solutions were measured at room temperature. **Figure 2-16** shows extinction spectra normalized at the maximum extinction of around 410 nm. In the case of Entry 1, a broad peak and the rise of background level were observed, which is due to

scattering by coarse particles. On the other hand, the wavelength at maximum extinction hardly changed among the other samples (Entry 2-4). These results support the conclusion obtained by TEM observations that the protective agent concentration rarely affects the size of the primary particles in the improved VEROS method.

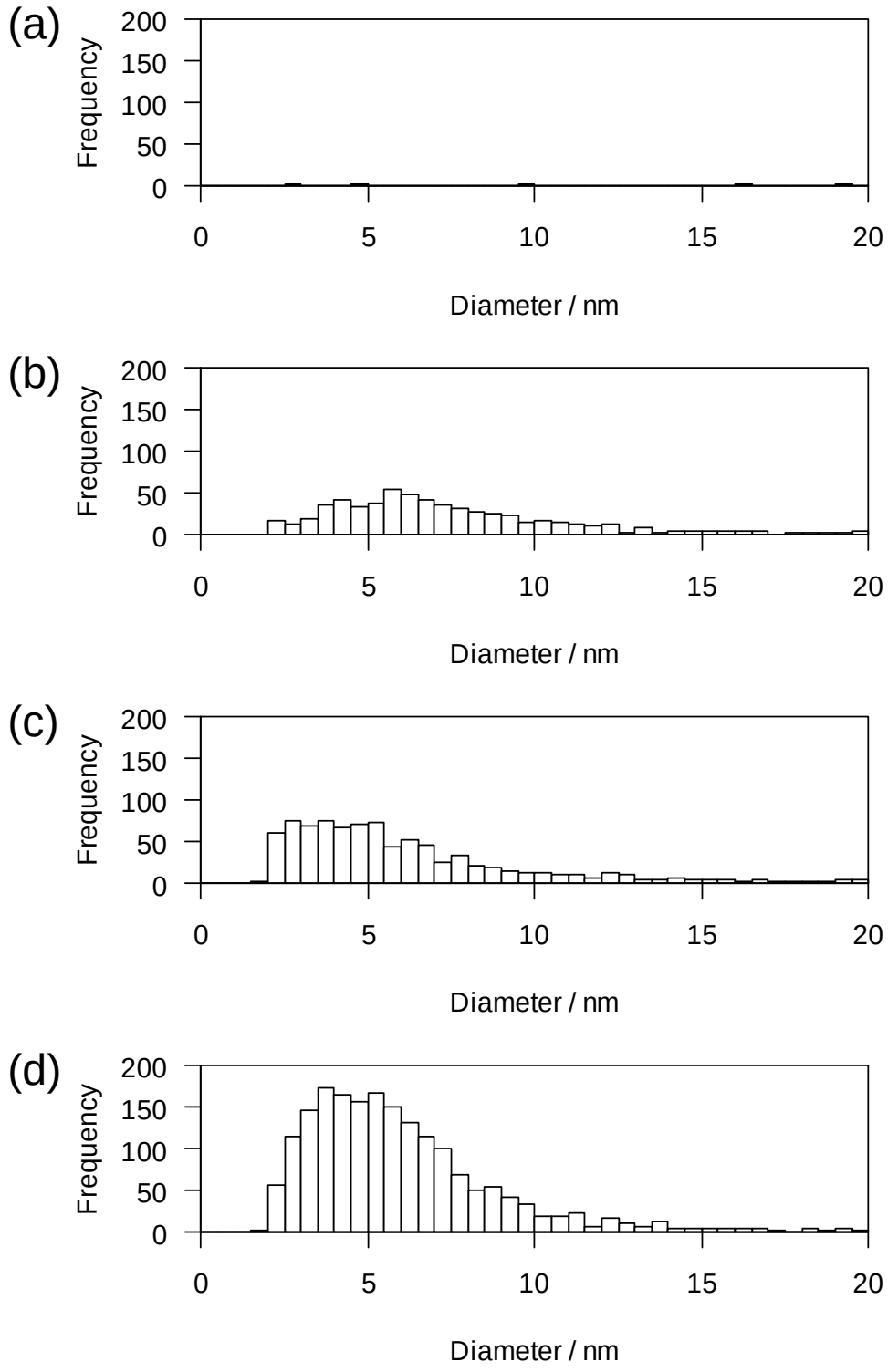

Figure 2-15. Particle size distribution of primary silver nanoparticles synthesized at different concentrations of sorbitan monooleate: (a) 1 wt%, (b) 5 wt%, (c) 10 wt%, and (d) 20 wt%.

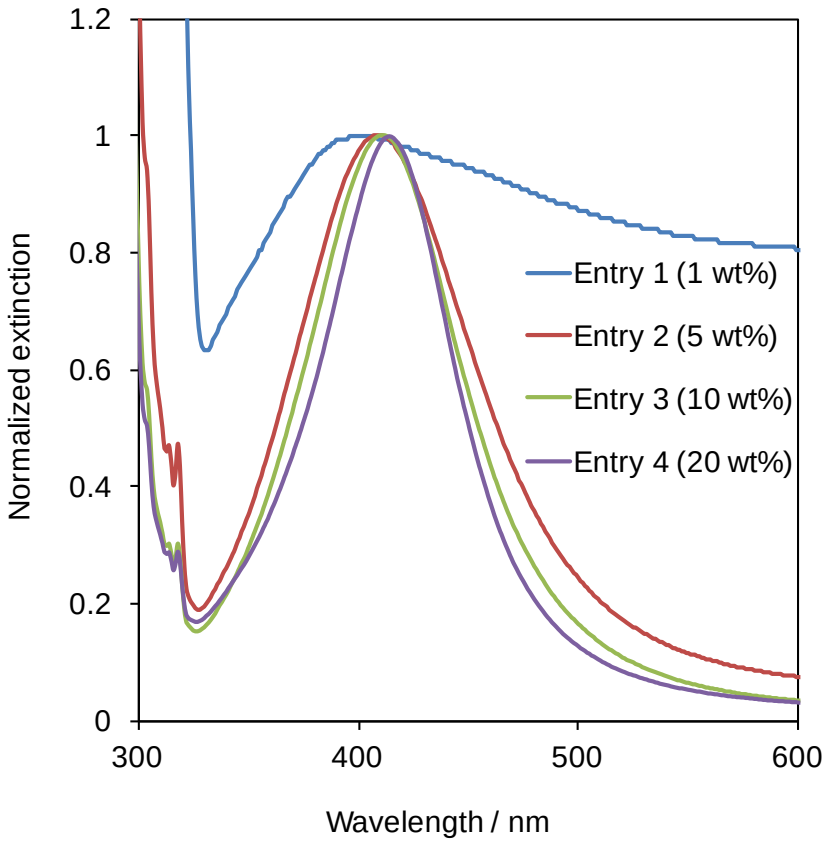

Figure 2-16. Normalized extinction spectra of silver nanoparticles synthesized at different concentrations of sorbitan monooleate in cyclohexane.

Thermogravimetric (TG) analyses of the trap solutions containing silver nanoparticles were carried out for the determination of silver content in the solution. In the case of Entry 4, the remaining weight ratio of the sample was 3.3 wt%, which equals the weight ratio of silver in the trap solution. Namely, it was shown that 36 wt% of silver in the raw material formed monodispersed spherical nanoparticles under the experimental conditions used in this study. The yield of silver nanoparticles in the improved VEROS method is relatively high among the physical methods for the production of metal nanoparticles.

2-2-4 Consideration of Formation Mechanism of Silver Nanoparticles in the Improved VEROS Method

Two important experimental facts were demonstrated by the synthesis of silver nanoparticles with the improved VEROS method. One is that the concentration of sorbitan monooleate in the trap solution significantly affects the probability of aggregation among the nanoparticles. The other is that the concentration hardly affects the size of the primary particles. From these results, the author proposes the formation mechanism of silver nanoparticles in the improved VEROS method as follows. The silver atoms generated by heating rarely collide with each other in space and reach the interface of the trap solution because the distance from the crucible to the interface of the trap solution is too short, taking into account the mean free path under these experimental conditions. Then, the silver atoms grow into nanoparticles around the air-liquid interface of the trap solution. Alternatively, the silver atoms enter into the trap solution with atom or cluster state and they grow into nanoparticles in the trap solution. However, the possibility of growth in the trap solution is excluded because the particle size determination process is not directly affected by the protective agent concentration in the trap solution. As the solution is stirred by the rotation of the chamber in the improved VEROS method, the nanoparticles cannot stay at the air-liquid interface of the trap solution after the rotation. Subsequently, the silver nanoparticles enter the trap solution and are immediately covered with the protective agents. At this time, the insufficiency of protective agents in the trap solution raises the aggregation of silver nanoparticles. If the nanoparticle formation at the air-liquid interface is dominant in the size control of primary particles, the size should depend on the supply rate of silver atoms at the interface. In fact, a previous study showed that the deposition rate largely influenced the particle size in the original VEROS method [27]. This result supports the author's plausible mechanism. Naturally, further studies are needed in order to elucidate the mechanism of the particle size determination completely.

Section 2-3: Experiments

2-3-1 Materials

All chemicals and solvents were obtained commercially and used without further purification. Alkylnaphthalene (LION A) was obtained from Lion Corporation. In the experiment for effect of concentration, alkylnaphthalene (C=16,18) was purchased from Wako Pure Chemical Industries. Sorbitan monooleate (IONET S-80) was purchased from Sanyo Chemical Industries, Ltd. Oleylamine (purity: > 50 %) was obtained from Tokyo Chemical Industry Co., Ltd. Oleic acid, oleyl alcohol (purity: > 65 %), and methyl oleate were obtained from Wako Pure Chemical Industries, Ltd. Granular state silver (purity: > 99.9 %) was obtained from GENERGY Co., Ltd.

2-3-2 Synthesis of Silver Nanoparticles by the Improved VEROS Method

A schematic diagram of the improved VEROS method is shown in **Figure 1-9**. The improved VEROS method consists of below-mentioned steps for obtaining metal nanoparticles. Firstly, silver was placed in the center of the chamber with a crucible. Silver as a source material was at a granular state with the size of about one mm. The distance between the evaporation source and the inner wall was about 100 mm. After the trap solution was stirred for 1 h at 100˚C, it was poured into the cylindrical chamber and located at the bottom of the chamber. The internal air was evacuated from the chamber at a pressure less than 10^{-2} Pa by a diffusion pump. After the evacuation, the cylindrical chamber was rotated. Hence, the inner wall of the cylindrical chamber was covered with the thin film of the trap solution. The outer wall temperature of the cylindrical chamber was controlled by cooling water at 20˚C. Next, silver was evaporated from the crucible by heating with the tungsten filament at 400 W. The metallic vapors formed nanoparticles before entering into the trap solution. Then, the protective agents inhibited the growth of

silver into the aggregate like a bulk material in the trap solution. The processes were continuously repeated up to the exhaustion of silver in the crucible. After the insoluble silver aggregates were removed, the trap solutions containing silver nanoparticles were collected from the cylindrical chamber as elaborately as possible.

In the experiment with five protective agents, protective agents are sorbitan monooleate, oleylamine, oleic acid, oleyl alcohol, and methyl oleate. The base oil for trap solutions was 100 g and the molar amount of the protective agent in the trap solution was 0.05 mol. In addition, the supply amount of silver was 10 g and the rotation speed of cylindrical chamber was eight rpm.

In the experiments with different concentrations of the protective agent, silver nanoparticles were synthesized using trap solutions (total amount: 100 g) at different concentrations of the protective agent (1, 5, 10, and 20 wt%). As a protective agent, a nonionic surfactant, sorbitan monooleate, was used because it is highly soluble in the hydrocarbon solution and it showed good dispersibility. The rotation speed of cylindrical chamber is six rpm. The viscosities of the trap solutions were almost the same, regardless of the protective agent concentration. Silver (10 g) was supplied as a vapor into the trap solution by vacuum evaporation at an almost constant speed (about 30 mg min^{-1}).

2-3-3 Characterization

The extinction spectra were recorded using a UV-1800 UV-vis spectrophotometer (Shimadzu, Japan) at room temperature. The samples obtained by the improved VEROS method were observed by a JEM-2100 transmission electron microscope (JEOL, Japan). The samples for TEM observation were cast on ultrathin amorphous carbon films supported by copper grids COL-C15 (Okenshoji, Japan) and dried *in vacuo* before the observations. The size and shape of silver nanoparticles were analyzed by a digital image analysis software LAS Image Analysis (Leica, Germany). The mean particle diameters and size distributions were determined based on the pictures of over five points on the

grids. TGA was carried out using a TG/DTA 7300 system (SII Nanotechnology, Japan). Heating was performed in air at a rate of 5˚C min^{-1}, in the temperature range from 25 to 500˚C. When the samples were the trap solutions, the remaining weight ratios of the samples were regarded as the weight ratio of silver in the trap solutions, here.

Section 2-4: Summary

The effect of adsorption moiety of protective agents on silver nanoparticle synthesis was investigated in the improved VEROS method based on the inhibition of the aggregation between nanoparticles. This research was achieved using various analytical methods with the sufficient amounts of nanoparticles synthesized by the improved VEROS method. The TEM and UV-Vis spectral analyses indicate that sorbitan monooleate and oleic acid showed the better protection performance towards silver nanoparticles than oleylamine, oleyl alcohol, and methyl oleate in the hydrocarbon solution. Especially, silver nanoparticles showed the excellent redispersibility in the case of oleic acid. Based on these results, the author identified the affinity of protective agents on the surface of silver nanoparticles. Although the performance order of protective agents is varied by the change of source material and solvent, our systematic investigation would be applicable for the synthesis of various kinds of metal nanoparticles.

Furthermore, it was shown that the protective agent concentration in the trap solution rarely affected the primary particle size but decisively contributed to blocking of the aggregation between the nanoparticles. The present results suggest that the nanoparticles might be covered with protective agents after their size was determined. However, further investigations on other size determining factors such as evaporation rate of the metal, viscosity and surface free energy of the trap solution, and degree of vacuum in the chamber should be carried out in the future for realizing more precise size control of the metal nanoparticles in the improved VEROS method.

References

[1] A. Kosmala, R. Wright, Q. Zhang, and P. Kirby, *Mater. Chem. Phys.* **2011**, *129*, 1075-1080.

[2] S. Magdassi, M. Grouchko, O. Berezin, and A. Kamyshny, *ACS Nano* **2010**, *4*, 1943-1948.

[3] H. C. Jung, S.-H. Cho, J. W. Joung, and Y.-S. Oh, *J. Electron. Mater.* **2007**, *36*, 1211-1218.

[4] S. Sun, *Adv. Mater.* **2006**, *18*, 393-403.

[5] E. Y. Sun, L. Josephson, K. A. Kelly, and R. Weissleder, *Bioconjugate Chem.* **2006**, *17*, 109-113.

[6] W. P. Hall, J. Modica, J. Anker, Y. Lin, M. Mrksich, and R. P. Van Duyne, *Nano Lett.* **2011**, *11*, 1098-1105.

[7] K.-S. Lee and M. A. El-Sayed, *J. Phys. Chem. B* **2006**, *110*, 19220-19225.

[8] M. Kumar and S. Deka, *ACS Appl. Mater. Interfaces* **2014**, *6*, 16071-16081.

[9] A. Mondal and N. R. Jana, *ACS Catal.* **2014**, *4*, 593-599.

[10] C. W. Xu, H. Wang, P. K. Shen, and S. P. Jiang, *Adv. Mater.* **2007**, *19*, 4256-4259.

[11] M. Haruta, T. Kobayashi, H. Sano, and N. Yamada, *Chem. Lett.* **1987**, *16*, 405-408.

[12] N. Shalkevich, W. Escher, T. Bürgi, B. Michel, L. Si-Ahmed, and D. Poulikakos, *Langmuir* **2010**, *26*, 663-670.

[13] E. Yamamoto and K. Kuroda, *Bull. Chem. Soc. Jpn.* **2016**, *89*, 501-539.

[14] T. C. Johnstone, K. Suntharalingam, and S. J. Lippard, *Chem. Rev.* **2016**, *116*, 3436-3486.

[15] N. Kamaly, B. Yameen, J. Wu, and O. C. Farokhzad, *Chem. Rev.* **2016**, *116*, 2602-2663.

[16] N. Livneh, M. G. Harats, D. Istrati, H. S. Eisenberg, and R. Rapaport, *Nano Lett.* **2016**, *16*, 2527-2532.

[17] K. M. Mayer and J. H. Hafner, *Chem. Rev.* **2011**, *111*, 3828-3857.

[18] V. Malgras, J. Qingmin, Y. Kamachi, T. Mori, F.-K. Shieh, W. Wu, K. Ariga, and Y. Yamauchi, *Bull. Chem. Soc. Jpn.* **2015**, *88*, 1171-1200.

[19] X. Wang, R. D. Tilley, and J. J. Watkins, *Langmuir* **2014**, *30*, 1514-1521.

[20] M. A. Plunkett, Z. Wang, M. W. Rutland, and D. Johannsmann, *Langmuir* **2003**, *19*, 6837-6844.

[21] A. Naderi and P. M. Claesson, *Langmuir* **2006**, *22*, 7639-7645.

[22] E. Mansfield, K. M. Tyner, C. M. Poling, and J. L. Blacklock, *Anal. Chem.* **2014**, *86*, 1478-1484.

[23] I. Akita, Y. Ishida, and T. Yonezawa, *Bull. Chem. Soc. Jpn.* **2016**, *89*, 1054-1056.

[24] I. Nakatani, T. Furubayashi, T. Takahashi, and H. Hanaoka, *J. Magn. Magn. Mater.* **1987**, *65*, 261-264.

[25] D. Li, B. Hong, W. Fang, Y. Guo, and R. Lin, *Ind. Eng. Chem. Res.* **2010**, *49*, 1697-1702.

[26] M. Yamamoto, Y. Kashiwagi, and M. Nakamoto, *Langmuir* **2006**, *22*, 8581-8586.

[27] S. Yatsuya, Y. Tsukasaki, K. Yamauchi, and K. Mihama, *J. Cryst. Growth* **1984**, *70*, 533-535.

[28] A. W. Orbaek, M. M. McHale, and A. R. Barron, *J. Chem. Educ.* **2015**, *92*, 339-344.

[29] S. Mourdikoudis and L. M. Liz-Marzán, *Chem. Mater.* **2013**, *25*, 1465-1476.

[30] S. Link and M. A. El-Sayed, *J. Phys. Chem. B* **1999**, *103*, 4212-4217.

Chapter 3: Comparison of Silver Nanoparticles Synthesized by Physical and Chemical Synthetic Methods

Section 3-1: Introduction

Silver nanoparticles synthesized by the improved VEROS method with five protective agents showed the difference in their characteristics and yields. In the improved VEROS method, the only difference in the synthesis conditions is obviously the adsorption moiety of protective agents. Therefore, the difference seems to be derived from the adsorption ability of protective agents. These investigations could be conducted by taking the full advantage of the improved VEROS method. Of course, this experiment would be also accomplished by chemical methods. What matters here is the effect of protective agents on the nucleation and growth of metal nanoparticles. In the improved VEROS method, the supply rate of metal is determined by the temperature and pressure in the chamber. These parameters are hardly affected in the cases of protective agents with sufficiently-high boiling temperature. By contrast, there may be interactions between metallic precursors and protecting agents before the formation of nanoparticles in most chemical methods. The presence of protective agents in the process of metal supply may adversely affect the adsorption of protective agents on the surface of metal nanoparticles in chemical synthetic methods.

Nowadays, various chemical synthetic methods for obtaining metal nanoparticles have been reported [1-4]. Among them, a thermal decomposition technique has attracted much attention because this method is very simple; i.e., it requires only thermally degradable metal complexes and solvents without reducing agents. This feature is quite similar to that of the improved VEROS method. Recently, Viswanath and co-workers reported [5]

that monodisperse silver nanoparticles could be obtained by the thermal decomposition of silver (I) oxalate using poly(vinyl alcohol) as the protective agent. Also, Kurihara and co-workers reported [6] that oleylamine was used for the protection of silver nanoparticles in the similar synthetic technique to the Viswanath's method. Therefore, there is a possibility that various protective agents are usable for the synthesis of metal nanoparticles under the same experimental conditions in the Viswanath's method.

Additionally, it is also necessary to investigate the adsorption states of protective agents in physical and chemical synthetic methods. The thermal decomposition technique developed by Nakamoto and his co-workers is suitable for obtaining nanoparticles protected by oleic acid. In the Nakamoto's method, only silver oleate is used as a raw material for silver nanoparticles. His group has also studied the adsorption and exchange of protection agents in detail. Therefore, there is no doubt about the adsorption of oleic acid on the surface of silver nanoparticle. In order to compare the adsorption states of protective agents between chemical and physical methods, oleic-acid-capped silver nanoparticles seem to be the most suitable because they could be successfully synthesized by both the Nakamoto's method and the improved VEROS method, and the structure of oleic acid is very simple.

In this chapter, the author compared the silver nanoparticles synthesized by physical method (improved VEROS method) and chemical method (thermal decomposition technique). For this objective, the synthesis of silver nanoparticles was carried out using the same solvent and protective agents by the thermal decomposition technique (Viswanath's method) as the improved VEROS method. In addition, the adsorption states of protective agents were compared between oleic-acid-capped synthesized by both the improved VEROS method and the thermal decomposition technique (Nakamoto's method). By clarifying the adsorption states of protective agents in physical and chemical synthetic methods, it would be possible to make use of mutual benefits between the physical and chemical synthetic methods.

Section 3-2: Results and discussion

3-2-1 Effect of Protective Agent in the Thermal Decomposition Technique

The improved VEROS method differs from general chemical synthetic methods in the synthetic process. There is a necessity to clarify the effect of synthetic process. Hence, silver nanoparticles were also synthesized by the thermal decomposition technique using the same chemicals as those used in the improved VEROS method. The synthesized samples were observed by the optical microscope with epi-illumination (**Figure 3-1**) and transmitted illumination (**Figure 3-2**) because most of silver particles synthesized by the thermal decomposition technique were too large for TEM observation. In the sample synthesized using oleylamine, purple particles were observed in the optical microscope image with epi-illumination (**Figure 3-1 (b)**). The purple color is originated from the plasmon absorption of silver nanoparticles [6,7]. In addition, this sample was easily dispersible in organic solvents such as *n*-hexane. These results demonstrate that most of the samples synthesized using oleylamine consist of silver nanoparticles. The size of these nanoparticles was determined to be 10.3 ± 2.3 nm by TEM observation (**Figure 3-3**). However, in the cases of other samples, white particles were observed in the optical microscope image with epi-illumination (**Figures 3-1 (a) and (c)–(e)**). Furthermore, light passed through these samples synthesized using oleic acid, oleyl alcohol, and methyl oleate under the same observation conditions (**Figures 3-2 (c)–(e)**). These results clearly show that silver (I) oxalate was imperfectly decomposed in those cases. In the case of sorbitan monooleate, the black images were observed in the optical microscope image with transmitted illumination, which means that light did not pass through the sample (**Figure 3-2 (a)**), but the purple color was not observed by the optical microscope with epi-illumination (**Figure 3-1 (a)**). These results show that silver (I) oxalate became the aggregate of silver by thermal decomposition. In this synthetic technique, it is known that

silver (I) oxalate forms a complex with the protective agent before the thermal decomposition. As the decomposition temperature is largely affected by the thermal stability of the complex, it is very difficult to evaluate the performance of protective agents directly by this method. In other words, this method was not suitable for the purpose of this study to compare the effect of protective agents systematically without changing experimental conditions.

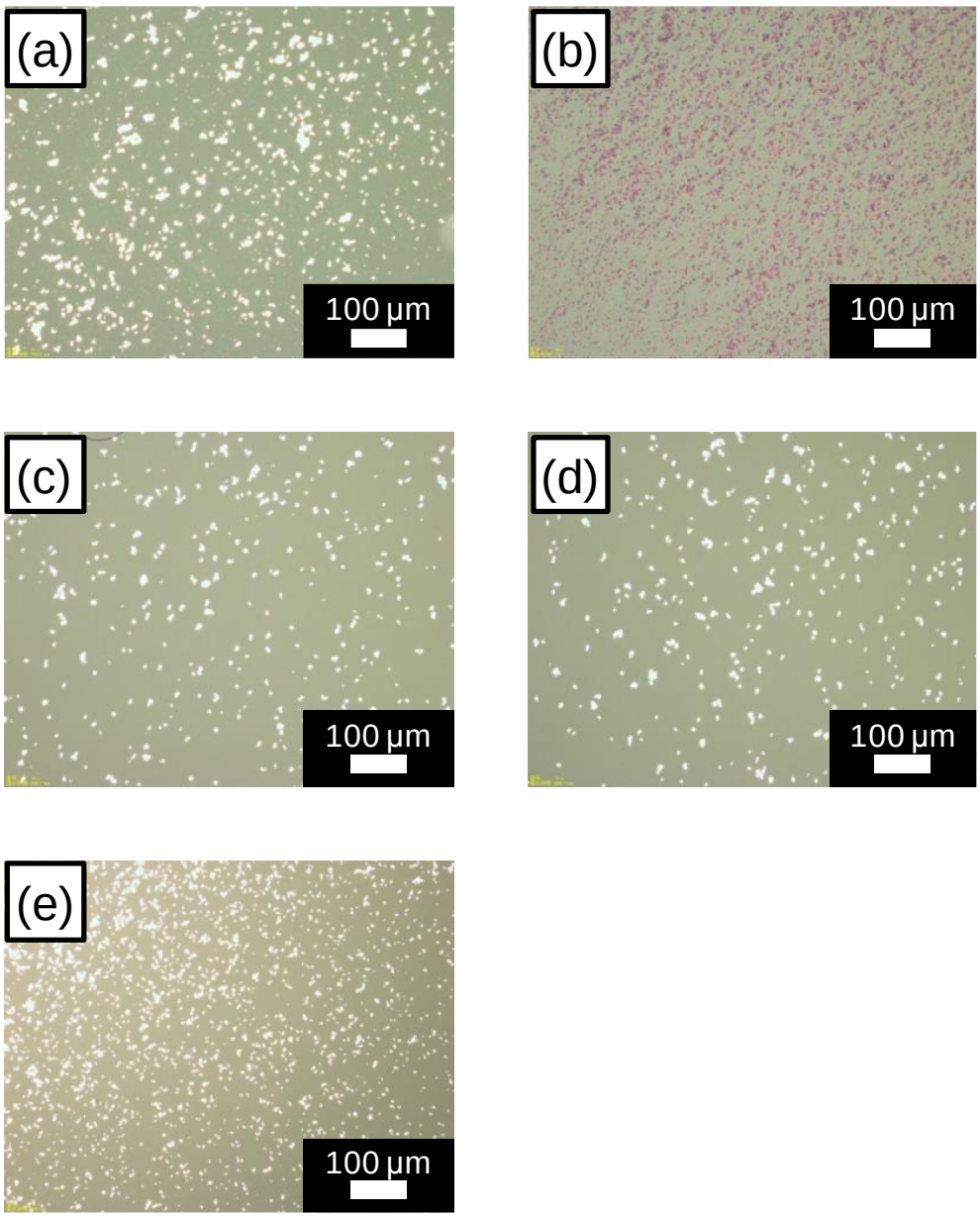

Figure 3-1. Optical microscope images with epi-illumination of the samples synthesized by the thermal decomposition technique. The samples (a), (b), (c), (d), and (e) were synthesized using sorbitan monooleate, oleylamine, oleic acid, oleyl alcohol, and methyl oleate, respectively.

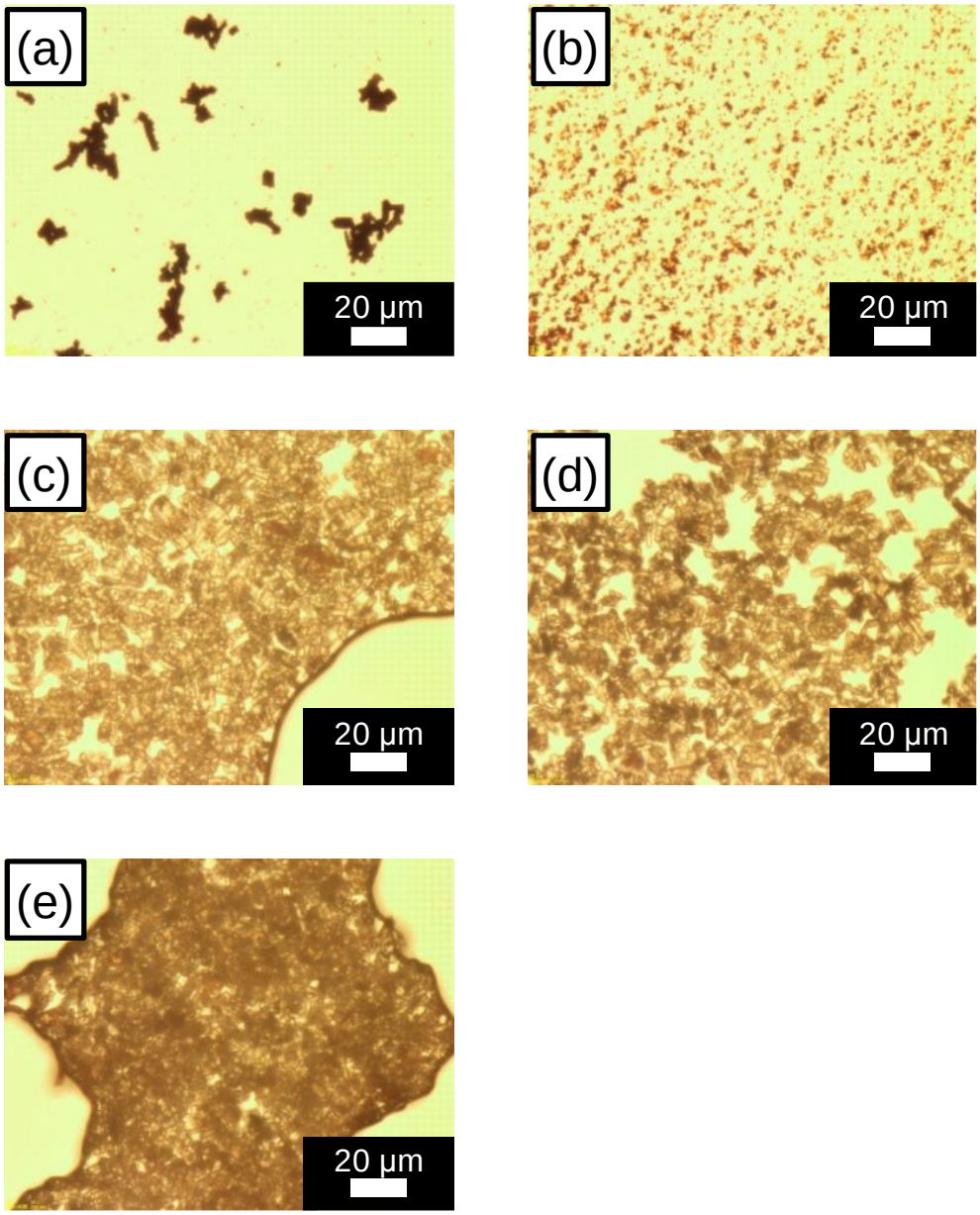

Figure 3-2. Optical microscope images with transmitted illumination of the synthesized samples by the thermal decomposition technique. The samples (a), (b), (c), (d), and (e) were synthesized using sorbitan monooleate, oleylamine, oleic acid, oleyl alcohol, and methyl oleate, respectively.

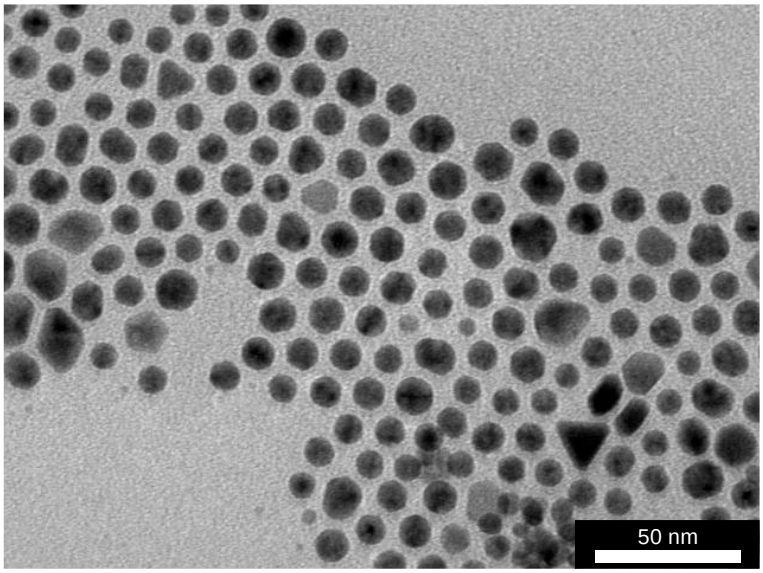

Figure 3-3. TEM image of the sample synthesized by the thermal decomposition technique (Viswanath's method) with oleylamine.

3-2-2 Difference in Synthesis of Silver Nanoparticles Between the Improved VEROS Method and the Thermal Decomposition Technique

Although oleylamine is well known as an effective protective agent for silver nanoparticles in chemical synthetic methods [8], the yield of silver nanoparticles in the case of oleylamine was extremely low in the improved VEROS method (Chapter 2). The reason why the difference between the improved VEROS method and the thermal decomposition technique occurred was speculated as follows: This result may be originated from the different process time after the generation of nanoparticles. In the improved VEROS, nanoparticles produced at the beginning of the process are exposed for a long time to the severe environments such as radiation heat from evaporation source and collision between unprotected particles because they are produced successively. On the other hand, nanoparticles are exposed for a shorter time in the thermal decomposition technique because they are formed concurrently. This process time increases as the amount of the source material increases. In this study, it took several hours to exhaust silver completely in the improved VEROS method. In contrast, it took about 30 minutes

to complete the thermolytic reaction in the thermal decomposition technique. Of course, the yield of silver nanoparticles would be associated with not only the process time but also the affinity of the protective agent with the metal surface. In consideration of the experimental results obtained in this study, the affinity of oleylamine is relatively weaker than that of oleic acid and sorbitan monooleate. Therefore, silver nanoparticles covered with oleylamine could be effectively obtained only by the thermal decomposition technique, which does not require a long process time after the generation of nanoparticles.

3-2-3 Comparison of Adsorption States of Oleic Acid on the Surface of Silver Nanoparticles Between the Improved VEROS Method and the Thermal Decomposition Technique

In this chapter, silver nanoparticles capped by the same protective agent are needed in order to compare the adsorption states between physical and chemical synthetic methods. Oleic-acid-capped silver nanoparticles were not obtained by the aforementioned synthetic technique (Viswanath's method) unlike the improved VEROS method. On the other hand, oleylamine-capped silver nanoparticles were slightly synthesized by the improved VEROS method. Therefore, the synthesis of oleic-acid-capped silver nanoparticles was carried out by the thermal decomposition technique (Nakamoto's method).

A typical TEM image of oleic-acid-capped silver nanoparticle synthesized by the Nakamoto's method is shown in **Figure 3-4**. The mean diameter of these nanoparticles was determined to be 4.7 ± 1.4 nm by image analysis. This value is different from that of silver nanoparticles synthesized by the improved VEROS method with oleic acid. It is highly difficult to coincide perfectly with the mean diameter between two different synthetic methods. However, the discussion on the size of silver nanoparticles is not required in this chapter.

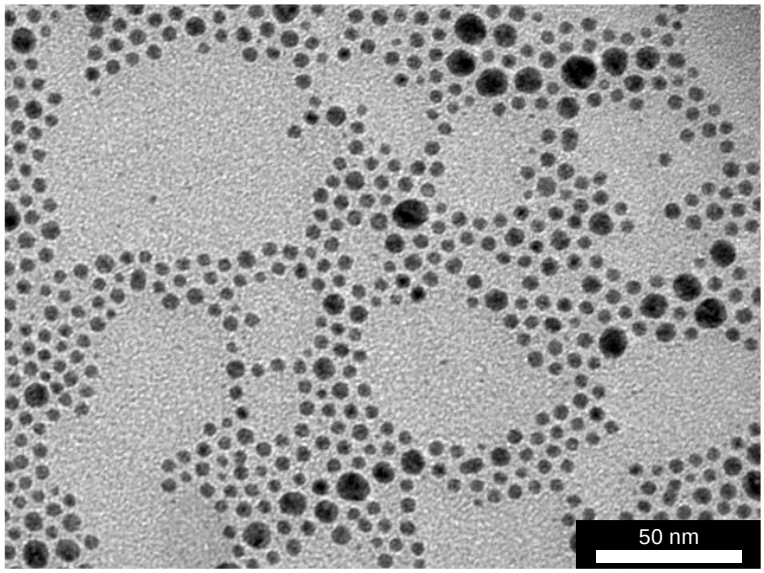

Figure 3-4. TEM image of the sample synthesized by the thermal decomposition technique (Nakamoto's method) with oleic acid.

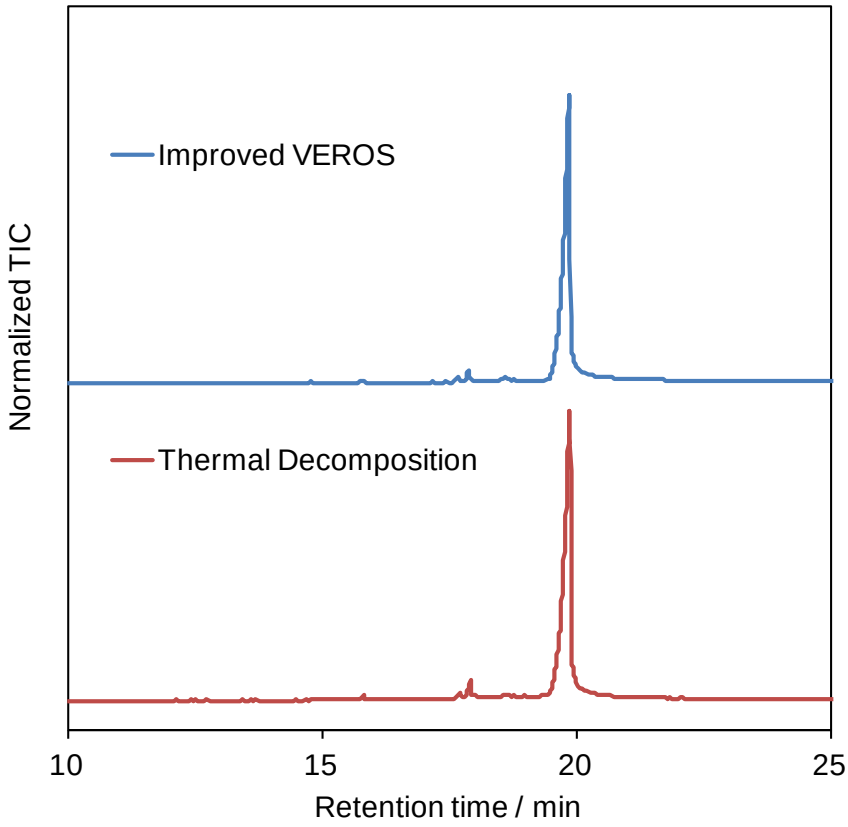

Figure 3-5. TICs of samples of oleic-acid-capped silver nanoparticles synthesized by the improved VEROS method and thermal decomposition technique.

In this discussion, it is important to confirm whether oleic acid is really adsorbed on the surface of silver nanoparticles. This adsorption was confirmed by a pyrolysis-GC-MS. Total ion chromatograms (TICs) of samples are shown in **Figure 3-5**. TIC of oleic-acid-capped silver nanoparticles synthesized by the thermal decomposition technique are almost the same as that of the improved VEROS method. Therefore, it is considered that the same molecule is adsorbed on the surface of silver nanoparticles in both cases.

Next, IR spectra were measured to obtain information on the adsorption states of oleic acid on the surface of silver nanoparticles. As these samples contain not only organic molecules but also a large amount of silver nanoparticles, the ATR method was chosen to minimize the interference such as scattering of metal particles. In addition, it was necessary to use a germanium prism because it has the highest refractive index among prisms for ATR. IR spectra of samples synthesized by the improved VEROS method and thermal decomposition technique are shown in **Figure 3-6**. Two IR spectra were almost the same in the range from 1000 to 3500 cm^{-1}. Therefore, the adsorption states of oleic acid on the surface of silver nanoparticles are almost the same even though the adsorption process of the protective agent is completely different between two synthetic methods.

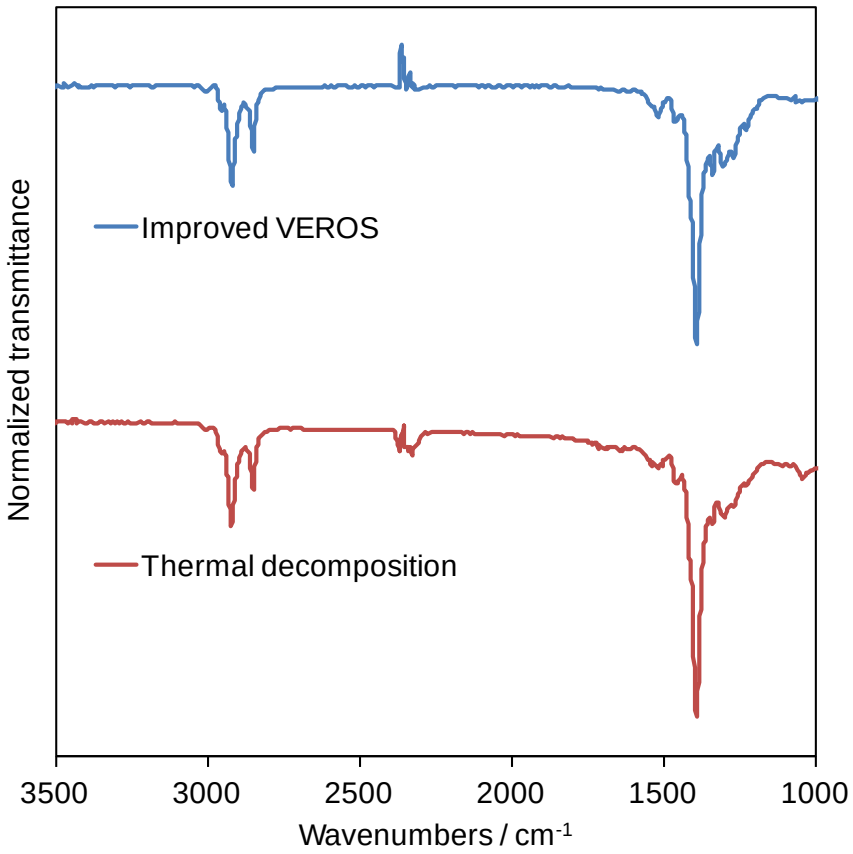

Figure 3-6. IR spectra of oleic acid on the surface of silver nanoparticles synthesized by the improved VEROS method and thermal decomposition technique.

3-2-4 Investigation of Adsorption States of Oleic Acid on the Surface of Silver Nanoparticles by Comparison with Oleic Acid Derivatives

Oleic acid on the surface of silver nanoparticle obtained by two synthetic methods showed almost the same IR spectra. Therefore, it was discussed on the premise that the adsorption states of oleic acid are almost the same between the two synthesized samples.

For the further discussion, the IR spectrum of oleic acid on the surface of silver nanoparticles was compared with those of oleic acid derivatives (**Figure 3-7**). The oleic acid derivatives are sodium oleate, potassium oleate, and silver oleate. The peaks around 2900 cm^{-1} are derived from the C-H stretching vibration of the alkyl chain. In this range,

all the peaks were almost the same in the five samples. On the other hand, IR spectra of these samples differed in the range from 1200 to 1800 cm^{-1}. **Figure 3-8** is the magnified view of this region in **Figure 3-7**.

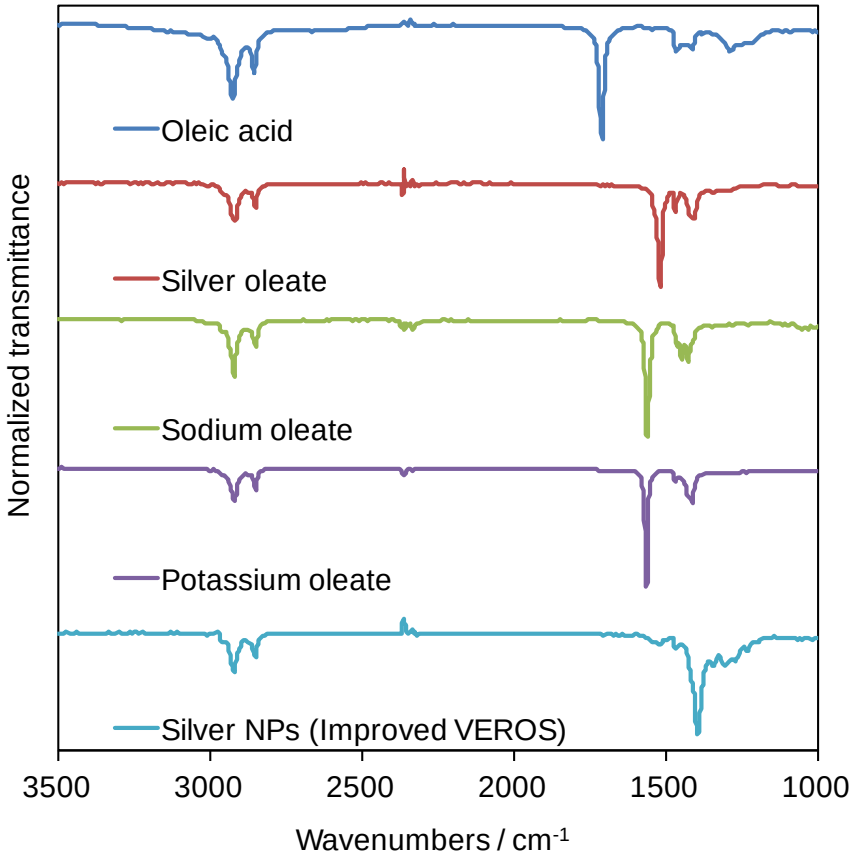

Figure 3-7. IR spectra of oleic acid on the surface of silver nanoparticles and oleic acid derivatives.

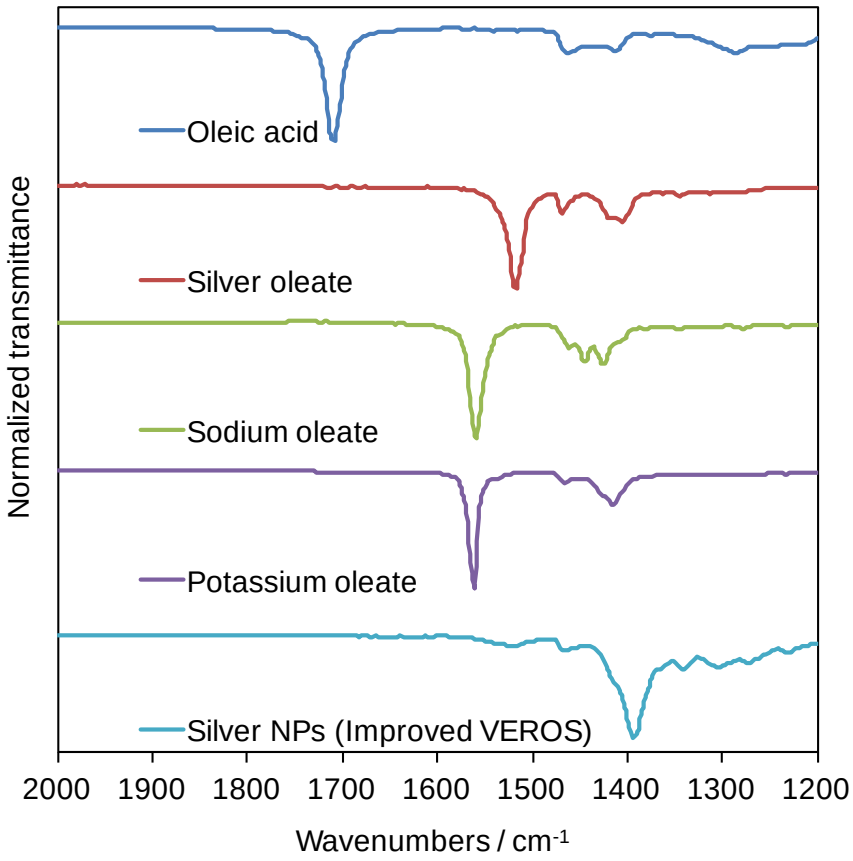

Figure 3-8. Magnified view of IR spectra of oleic acid on the surface of silver nanoparticles and oleic acid derivatives.

In the case of oleic acid, a particular peak was observed at 1710 cm^{-1}. This peak is derived from C=O stretching vibration of carboxyl group in oleic acid. In the cases of oleic acid derivatives, this peak disappeared and other peaks were observed at 1516 and 1560 cm^{-1} instead. These wavenumbers of peaks coincide with asymmetrical stretching vibration of COO^-. The reason for the shorter wavenumber shift is that the interaction strengths of carboxylate with metal ions are different. However, these peaks were hardly observed in the case of oleic acid on the surface of silver nanoparticles. Although a peak was slightly observed at 1516 cm^{-1}, this peak is not derived from silver oleate because silver oleate is not used as a raw material in the improved VEROS method. The most

prominent peak in this spectrum was observed at 1390 cm^{-1}. This peak is not consistent with any typical peak in the IR spectrum.

Interestingly, based on the peak intensity at around 2900 cm^{-1} originated from the C-H stretching vibration of the alkyl chain, the peak at 1390 cm^{-1} is almost as large as the peaks of C=O stretching vibration and COO^- asymmetrical stretching vibration. The broadening of the peak is due to overlapping with other peaks because several peaks were observed in this range in all the cases. Although the adsorption states of oleic acid on the surface of silver nanoparticles need to be elucidated in further studies, some of adsorption states can be at least discussed from these results at this present stage. Most of carboxy groups contribute to the adsorption on the surface of silver nanoparticle because the peak originated from C=O stretching vibration completely disappears in the case of silver nanoparticle. The largest wavenumber of the peak originated from oleic acid on the surface of silver nanoparticles is different from those of the peaks originated from oleic acid derivatives. In other words, the adsorption states of oleic acid on the surface of silver nanoparticle are greatly different from that of oleic acid bonded with silver ion. Otherwise, the spectrum would be affected by the local electrical field of silver nanoparticles.

In conclusion, the adsorption states of oleic acid on the surface of silver nanoparticles were almost the same between the two samples synthesized by different methods. The author speculates that the peak at 1390 cm^{-1} relates closely to the asymmetric stretching vibration of carboxylate. The basis of speciation is the disappearance of the peak originated from C=O stretching vibration at 1710 cm^{-1} and the shift of the peaks originated from COO^- asymmetric stretching vibration, depending on counter metal ions. This phenomenon takes place regardless of prior ionization of oleic acid.

Section 3-3: Experiments

3-3-1 Materials

All chemicals and solvents were obtained commercially and used without further purification. Alkylnaphthalene (LION A) was obtained from Lion Corporation. Sorbitan monooleate (IONET S-80) was purchased from Sanyo Chemical Industries, Ltd. Oleylamine (purity: > 50 %) was obtained from Tokyo Chemical Industry Co., Ltd. Oleic acid, oleyl alcohol (purity: > 65 %), and methyl oleate were obtained from Wako Pure Chemical Industries, Ltd. Silver nitrate ($AgNO_3$) and ammonium oxalate monohydrate $(NH_4)_2(C_2O_4)\cdot H_2O$ were purchased from Kanto Chemical Co., Inc. Silver nitrate was of special grade. Sodium oleate (purity: > 60 %) was purchased from Wako Pure Chemical Industries, Ltd. Triethylamine (purity: > 99 %) was purchased from Tokyo Chemical Industry Co., Ltd. Sodium oleate (purity: > 97 %) and potassium oleate (purity: > 98 %) was purchased from Tokyo Chemical Industry Co., Ltd. The oleic-acid-capped silver nanoparticles by the improved VEROS method were obtained from experiments in Chapter 2.

3-3-2 Synthesis of Silver Nanoparticles by the Thermal Decomposition Technique with Five Protective Agents (Viswanath's method)

The synthesis of silver nanoparticles by the Viswanath's method was carried out based on the paper reported by the other research group [20,21,29]. The author made minor modifications to some of the components in this method in order to use identical compounds to the improved VEROS method as much as possible. Firstly, silver (I) oxalate was synthesized from silver nitrate and ammonium oxalate monohydrate according to the previous paper [9]. Next, silver (I) oxalate (3.04 g, 10.0 mmol) was added to the mixture of alkylnaphthalene (15.2 g), methanol (10 mL), and the protective agent (40.0 mmol). Additionally, water (2 mL) was added into the mixture. Then, the mixture

was stirred for 24 h in the dark at room temperature. Most of methanol was removed in advance from the mixture by the evaporation at 40˚C under the reducing pressure. In the decomposition step, the mixture was heated at below-mentioned three stages. At the first stage, methanol was completely eliminated by heating for 30 min at 100˚C. At the second stage, water was eliminated by heating for 30 min at 125˚C. At the final stage, silver (I) oxalate was decomposed by heating for 1 h at 150˚C. After the processes, the mixture containing silver nanoparticles was gradually cooled to room temperature.

3-3-3 Synthesis of Oleic-Acid-Capped Silver Nanoparticles by the Thermal Decomposition Technique (Nakamoto's method)

The synthesis of silver nanoparticles synthesized from silver oleate was carried out based on the paper reported by the other research group [10-13]. Firstly, silver (I) oleate was synthesized from silver nitrate and sodium oleate according to the previous paper [12]. Next, silver (I) oleate (3.89 g, 10.0 mmol) was added to triethylamine (29 mL, 200 mmol) in a 100 mL flask. In the decomposition step, the mixture was heated for 2 h at 80˚C. After the processes, the mixture containing silver nanoparticles was gradually cooled to room temperature. Coarse particles in the obtained dispersion were removed by centrifugation with 50 mL centrifuge tube. After that, the synthesized silver nanoparticles were washed with 10 mL of ethanol.

3-3-4 Characterization

The samples obtained by thermal decomposition techniques were observed by a JEM-2100 transmission electron microscope (JEOL, Japan). The samples for TEM observation were cast on ultrathin amorphous carbon films supported by copper grids COL-C15 (Okenshoji, Japan) and dried fully under high vacuum conditions before the measurements. When the samples were the trap solutions, the remaining weight ratios of the samples were regarded as the weight ratio of silver in the trap solutions, here. The

samples obtained by the thermal decomposition technique (Viswanath's method) were observed in detail by a MX61 optical microscope (Olympus, Japan). TICs for determination of protective agents adsorbed on the silver nanoparticles were obtained from a gas chromatograph mass spectrometer QP2010 Plus and QP2010SE (Shimadzu, Japan). Ultra ALLOY UA5-30M-0.25F (Frontier Laboratories, Japan) column was used. The samples for GC-MS were heated by a PY-3030D pyrolyzer (Frontier Laboratories, Japan) at 300˚C before the injection. The IR spectra of samples were measured in the wavenumber range from 1000 to 3500 cm^{-1} by a FT/IR-4100 spectrometer with germanium attenuated total reflectance (ATR) unit (JASCO, Japan). The obtained spectra were normalized based on the largest peak and baseline.

Section 3-4: Summary

The effect of the protective agents was investigated by a thermal decomposition technique, which is the most similar method to the improved VEROS method in chemical synthetic methods in the viewpoint of used reagents as far as the author knows. Nevertheless, the adsorption of protective agents on the surface of silver nanoparticles could not be investigated because the protective agent affected the synthetic process of the nanoparticles seriously. Therefore, it can be said that the improved VEROS method as a physical synthetic method has a significant advantage for such investigation over chemical synthetic methods.

Moreover, only silver nanoparticles with oleylamine were synthesized among the five protective agents by the thermal decomposition technique. The result differs from that in the improved VEROS method. The author thinks that oleylamine in the preliminary complex effectively acts as a protective agent in the thermal decomposition technique. However, as the synthesized silver nanoparticles are exposed for a long time to the severe environments in the improved VEROS method, they could be rarely obtained due to the weakness of interaction between oleyamine and silver nanoparticles.

The adsorption states of oleic acid on the surface of silver nanoparticles were compared between the samples synthesized by two different methods. The IR spectra originated from oleic acid were almost the same regardless of the ionization of oleic acid in the synthetic process. In addition, the peak originated from C=O stretch vibration observed in non-ionized oleic acid was not obtained from the spectrum of oleic acid on the surface of silver nanoparticles. Therefore, it is speculated that the adsorption states are determined only by the interaction between oleic acid and silver nanoparticles.

References

[1] Y. Yang, S. Matsubara, L. Xiong, T. Hayakawa, and M. Nogami, *J. Phys. Chem. C* **2007**, *111*, 9095-9104.

[2] M. C. Daniel and D. Astruc, *Chem. Rev.* **2004**, *104*, 293-346.

[3] F. Mafune, J. Kohno, Y. Takeda, T. Kondow, and H. Sawabe, *J. Phys. Chem. B* **2000**, *104*, 9111-9117.

[4] M. Porta, M. T. Nguyen, T. Yonezawa, T. Tokunaga, Y. Ishida, H. Tsukamoto, Y. Shishinoc, and Y. Hatakeyamad, *New J. Chem.* **2016**, *40*, 9337-9343.

[5] S. Navaladian, B. Viswanathan, R. P. Viswanath, and T. K. Varadarajan, *Nanoscale Res. Lett.* **2007**, *2*, 44-48.

[6] M. Itoh, T. Kakuta, M. Nagaoka, Y. Koyama, M. Sakamoto, S. Kawasaki, N. Umeda, and M. Kurihara, *J. Nanosci. Nanotechnol.* **2009**, *9*, 6655-6660.

[7] S. Mourdikoudis and L. M. Liz-Marzán, *Chem. Mater.* **2013**, *25*, 1465-1476.

[8] D. Y. Naumov, N. V. Podberezskaya, A. V. Virovets, and E. V. Boldyreva, *J. Struct. Chem.* **1994**, *35*, 890-898.

[9] P. Mulvaney, *Langmuir* **1996**, *12*, 788-800.

[10] K. Abe, T. Hanada, Y. Yoshida, N. Tanigaki, H. Takiguchi, H. Nagasawa, M. Nakamoto, T. Yamaguchi, and K. Yase, Thin Solid Films **1998**, *327-329*,524-527.

[11] M. Yamamoto and M. Nakamoto, *J. Mater. Chem.* **2003**, *13*, 2064-2065.

[12] M. Yamamoto, Y. Kashiwagi, and M. Nakamoto, *Langmuir* **2006**, *22*, 8581-8586.

[13] Y. Kashiwagi, M. Yamamoto, and M. Nakamoto, *J. Colloid Interface Sci.* **2006**, *300*, 169-175.

Chapter 4: Comparison of Physical Adsorption Strength of Protective Agents via Ligand Exchange of Silver Nanoparticles Synthesized by the Improved VEROS Method

Section 4-1: Introduction

Unique features and characteristics of metal nanoparticles are utilized in the electronic [1-3], optical [4,5], magnetic [6], and catalytic [7-9] fields. Particularly, melting point depression is the well-known feature among them. [10] Due to this property, metal nanoparticles coalesce together to form thin metallic film by heating at a comparatively low temperature. As this coalescence is an irreversible change, these metallic films can be directly patterned by various printing processes such as screen printing and inkjet printing [11-15]. Typical examples of applications based on this technology are antenna for radio-frequency [16,17], electrode of various batteries [18,19], electromagnetic shielding [20], appearance for metallic luster [21], and biomarker [22]. Although specific features of metal nanoparticles bring many advantages to industrial products, they are often subject to the restrictions such as solvent solubility and anti-aggregation from the point of view of their use purposes. In those cases, metal nanoparticles have to be functionalized by organic compounds existing on their surfaces, which are called as a protective agent. The selection of ligands is extremely important for the application of metal nanoparticles. However, the combinations of ligand and metal nanoparticle are strictly limited by experimental conditions in the synthesis of chemical methods. Even though chemical synthetic methods enable the mass production of metal nanoparticles, they are inappropriate for basic investigation because the complex chemical synthetic reaction could not provide the ideally clean nanoparticle surface.

As for the synthesis of metal nanoparticles, physical methods generally enable a wide range of experimental conditions. In other words, various combinations of metal and protective agents are feasible. The vacuum evaporation on running oil substrate (VEROS) method was firstly developed in 1974 [23,24]. It is a physical method with above-mentioned features. In this method, the rotary disk provides the thin film of oil on the disk and the metal vapor evaporated under vacuum conditions moves into the oil film and forms nanoparticles at once. However, the concentration of metal nanoparticles in the oil is extremely low because the running oil is exposed to the metal evaporation area only once. It was highly difficult to obtain metal nanoparticles effectively in this method. This synthetic method was improved to solve the problem [25]. This improved method uses a cylindrical chamber for the formation of the oil film containing protective agents. The thin oil film is exposed to metal vapor many times with the rotation of the cylindrical chamber. Therefore, sufficient amount of metal nanoparticles can be obtained in the single step. In fact, several tens of grams of metal nanoparticles are produced by the improved VEROS method even in a day in the laboratory scale equipment. The purity of synthesized metal nanoparticles is quite high because all the processes for the synthesis are carried out under vacuum conditions and the improved VEROS method needs only a few materials, which are bulk metal, oil (solvent), and protective agent for the synthesis. In addition, the supply speed of metal vapor for the growth of metal nanoparticles can be easily changed.

Protective agents play a significant role in the synthesis of metal nanoparticles. The protective agents not only protect the metal surface from the fusion of metal nanoparticles but also affect a lot of characteristics such as stability and solvent dispersibility. In Chapters 2 and 3, The author described the effect of protective agents on the synthesis of silver nanoparticles by the improved VEROS method [26,27]. Therein, silver nanoparticles were effectively synthesized in the case of oleic acid. On the other hand, they were rarely obtained in the case of oleylamine although it is well known as a suitable

protective agent in the chemical synthesis of silver nanoparticles. These results were very interesting but they were not fully explained at that time.

Surface of metal nanoparticles can be modified after their synthesis. One of the modification methods is the addition of the molecules, which can interact with protective agents adsorbed on the metal surface [28]. On the other hand, protective agents on the surface of metal nanoparticle can be changed via ligand exchange process [29,30]. The simplest ligand exchange process is only to mix metal nanoparticles with additive protective agents in the solution. For example, carboxylates on the surface of silver nanoparticles were exchanged by 1-alkanethiols in *n*-hexane [31]. Generally, simple ligand exchange is closely related to the adsorption strength of protective agents on the surface of metal nanoparticles. Namely, the protective agents on the metal surface are replaced by additive protective agents with stronger adsorption strength. Therefore, the study on ligand exchange seems to contribute to the understanding of physical adsorption strength of protective agents. Physical adsorption of protective agents is indispensable for the protection of metal nanoparticles synthesized by physical methods. Thus, it is useful for the selection of suitable protective agents to clarify physical adsorption strength. Although there are extensive studies about ligand exchanges, ligand exchanges for the comparison of physical adsorption strength of protective agents have not been reported yet as far as the author knows.

In order to compare physical adsorption strength of protective agents via ligand exchanges, metal nanoparticles capped by protective agents with physical adsorption are required as the starting material. Specifically, the silver nanoparticles synthesized by the improved VEROS method are the most appropriate for this purpose. In this method, protective agents are non-ionized at least before their contact with silver nanoparticles, and they are used in the nonpolar solvent for capping the clean surface of silver nanoparticles immediately after generation. Therefore, these nanoparticles can be assumed to be protected with physical adsorption instead of chemisorption even though

this assumption requires further validation. On the other hand, silver nanoparticles synthesized by chemical synthetic methods with the ionization process of protective agents are inappropriate. The reason is that the adsorption of protective agents in the chemical synthetic methods is induced by the combination of several interactions such as electrostatic interaction.

In this chapter, the author compared the physical adsorption strength of protective agents on the silver surface via ligand exchange of silver nanoparticles synthesized by the improved VEROS method. To accomplish this purpose, all the experiments were designed for the protective agent not to ionize as much as possible. Silver nanoparticles capped by oleic acid with physical adsorption were synthesized and the ligand exchange from oleic acid to octanoic acid on the surface of silver nanoparticles was carried out in *n*-heptane. The reverse exchange from octanoic acid to oleic acid was also examined. As another type of ligand, *n*-octylamine was used in the same experimental conditions. The reason why carboxy and amino groups were selected is that they are the well-known adsorption moieties of protective agents. In addition, these results were compared with performance of protective agents (oleic acid and oleylamine) on the synthesis of silver nanoparticles by the improved VEROS method in Chapter 3.

Section 4-2: Results and Discussion

4-2-1 Synthesis of Oleic-Acid-Capped Silver Nanoparticles by the Improved VEROS Method

The oleic-acid-capped silver nanoparticles were synthesized by the improved VEROS method for all the ligand exchanges. The schematic illustration of synthesis of oleic-acid-capped silver nanoparticles by the improved VEROS method is shown in **Figure 4-1**. Notably, there is a distinct difference in the adsorption process of protective agents on the metal surface between the improved VEROS method and general chemical synthetic methods such as reductive method and thermal decomposition method. In chemical methods, adsorption of protective agents is far from physical adsorption because silver salts and ionized protective agents are used in the synthetic and adsorption processes. Therefore, the main driving force of adsorption on the metal surface is electrostatic interaction in general. On the other hand, metallic vapor is directly supplied to the trap solution containing protective agents in the improved VEROS method. Since the protective agent is not ionized before the evaporation of silver, the interaction between protective agents and evaporated silver is clearly different from that in the cases of chemical synthetic methods. Therefore, the driving force of the adsorption at the nanoparticle-formation stage of the improved VEROS method is physical adsorption. Oleic acid was selected among several protective agents because oleic-acid-capped silver nanoparticles can finely disperse in a nonpolar solvent according to Chapter 3. Oleic acid works not only as a protective agent but also as a solvent in this synthetic process.

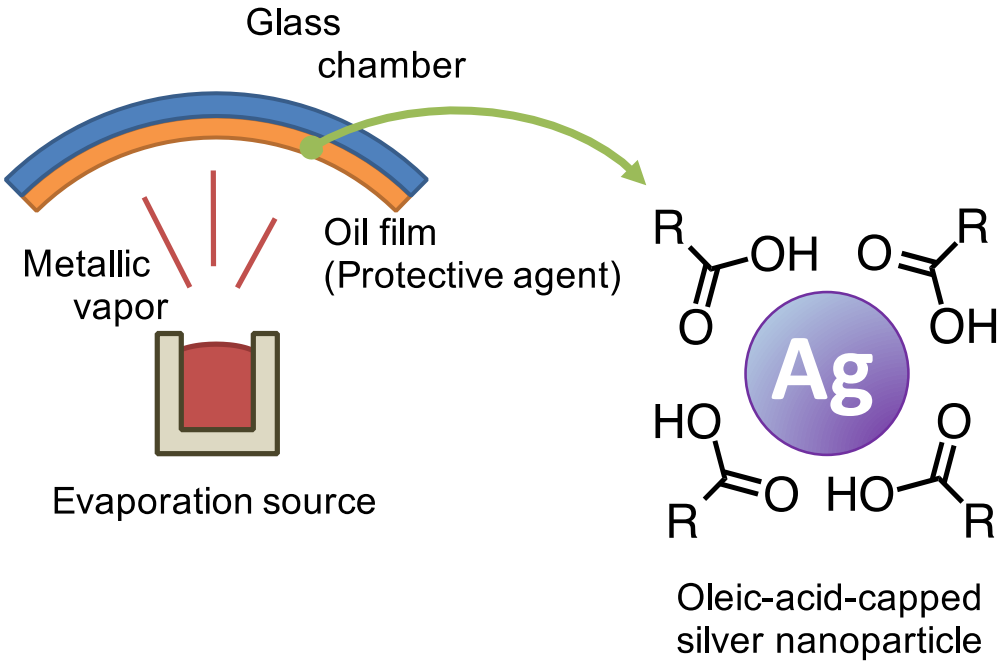

Figure 4-1. Schematic illustration of synthesis of oleic-acid-capped silver nanoparticles by the improved VEROS method.

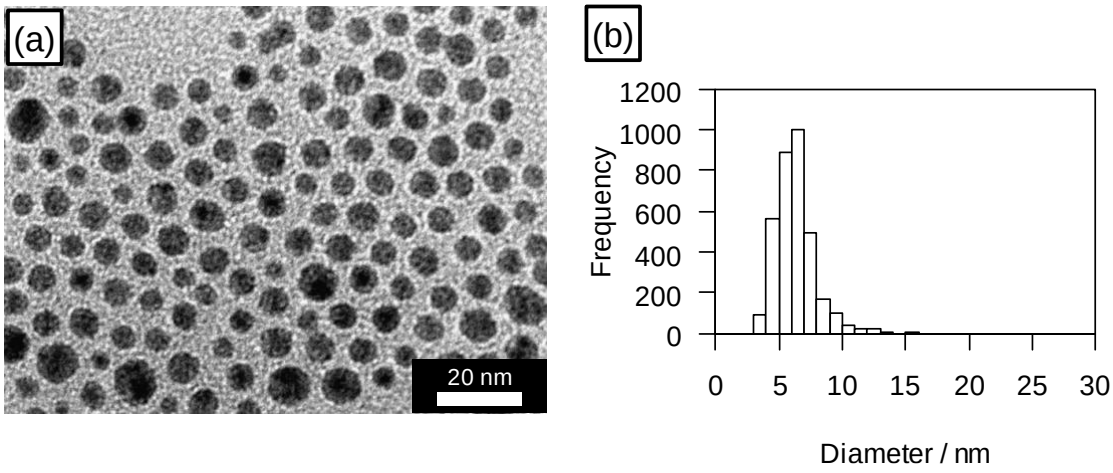

Figure 4-2. (a) TEM image and (b) particle size distribution of oleic-acid-capped silver nanoparticles synthesized by the improved VEROS method.

Figure 4-2 shows the TEM image and particle size distribution of oleic-acid-capped silver nanoparticle synthesized by the improved VEROS method. The many spherical

particles were independently observed with a constant interval but a few large particles were also confirmed from the TEM image. The mean diameter of silver nanoparticles was 6.3 ± 1.5 nm. In addition, the amount of oleic acid in the silver nanoparticle was determined by TGA. The weight ratio of oleic acid was 17 wt% in the nanoparticles. The cross-sectional area per one molecule calculated from the mean diameter of silver nanoparticles and the weight loss of oleic acid is 2.0×10^{-15} cm^2, which is almost in agreement with the molecular occupied area (2.1×10^{-15} cm^2) at the monolayer of stearic acid [32]. This result shows that oleic acid is closely packed on the surface of silver nanoparticles.

4-2-2 Ligand Exchange from Oleic Acid to Octanoic Acid

The ligand exchanges were carried out using octanoic acid as the additive protective agent and the optimal addition amount was determined in the first step of this study. Octanoic acid has the same hydrophilic group (carboxyl group) as oleic acid but has the different length of alkyl chain. The schematic illustration of this ligand exchange is shown in **Figure 4-3**. The addition amounts of octanoic acid in the ligand exchange are summarized in **Table 4-1**.

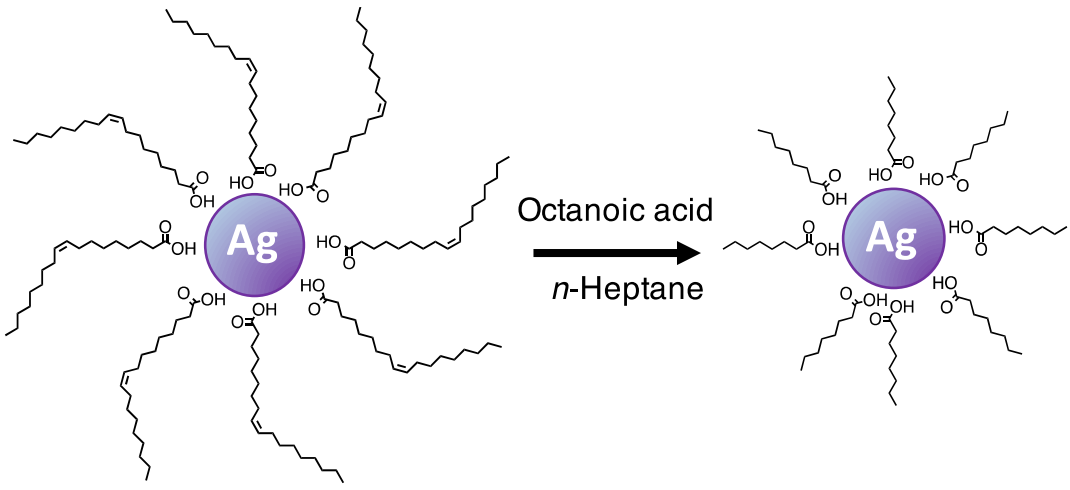

Figure 4-3. Schematic illustration of ligand exchange using octanoic acid.

Table 4-1. Reaction conditions and results of ligand exchange with octanoic acid.

Entry	Molar ratio of additive octanoic acid to oleic acid on the silver nanoparticles	Maximum extinction	λ_{max} / nm	FWHM / nm	Ligand exchange ratio / %
1	Before ligand exchange	2.23	411	64	0.0
2	1.5	2.00	414	77	53.2
3	4	1.52	413	85	67.2
4	10	1.73	414	84	93.2
5	20	1.58	415	83	95.7
6	30	0.85	412	73	97.1
7	40	0.23	420	81	100.0
8	50	0.45	423	89	100.0

Note: Amount of oleic acid in capped silver nanoparticles (50 mg) is 30 mmol.
λ_{max}, maximum extinction wavelength
FWHM, full width at half maximum

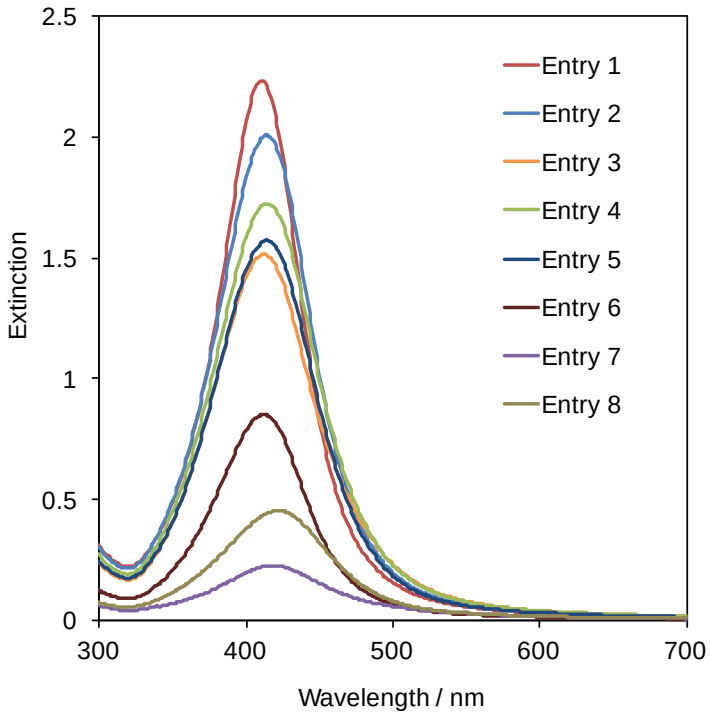

Figure 4-4. Extinction spectra of silver nanoparticles in cyclohexane before and after ligand exchange with different addition amounts of octanoic acid.

Figure 4-4 exhibits extinction spectra of silver nanoparticles in cyclohexane before and after the ligand exchange with several different addition amounts of octanoic acid. The extinction peak around 400 nm is originated from localized surface plasmon resonance of silver nanoparticles [33]. The shift of maximum extinction wavelength means the change of the particle diameter. In **Table 4-1**, the maximum extinction wavelength hardly changed in the cases of Entry 1-6. This result shows that the independence of nanoparticles mostly maintains even after the ligand exchange. However, the maximum extinction wavelengths in the cases of Entry 7 and 8 are longer by approximately 10 nm compared with that before the ligand exchange (Entry 1). It indicates that the size of silver nanoparticles becomes larger. On the other hand, the extinction is proportional to the particle concentration unless dielectric constant around the particle and particle diameter change. Although there is a variation in the maximum extinctions, the extinction decreased with the increase of the amount of the additive protective agent as the overall trend. The decrease of extinction indicates that the number of the dispersed silver nanoparticles decreases in the solution. The shift to longer wavelength and the decrease of extinction in the cases of Entry 7 and 8 can be explained that the number of dispersed particles decreases due to the aggregation and fusion of silver nanoparticles. In fact, black precipitates were observed in the solution in these cases. Many coarse particles were observed in the TEM image of the precipitate (**Figure 4-5**). The precipitated particles are clearly larger than those before ligand exchange. In this case, silver for particle growth must be supplied from a nanoparticle. In other words, the growth of nanoparticles is always triggered by the aggregation of nanoparticles. This aggregation of some silver nanoparticles may be due to the change in the solvent polarity by the addition of octanoic acid. For the above reasons, the amount of the additive protective agent should be optimized in order to proceed the ligand exchange efficiently.

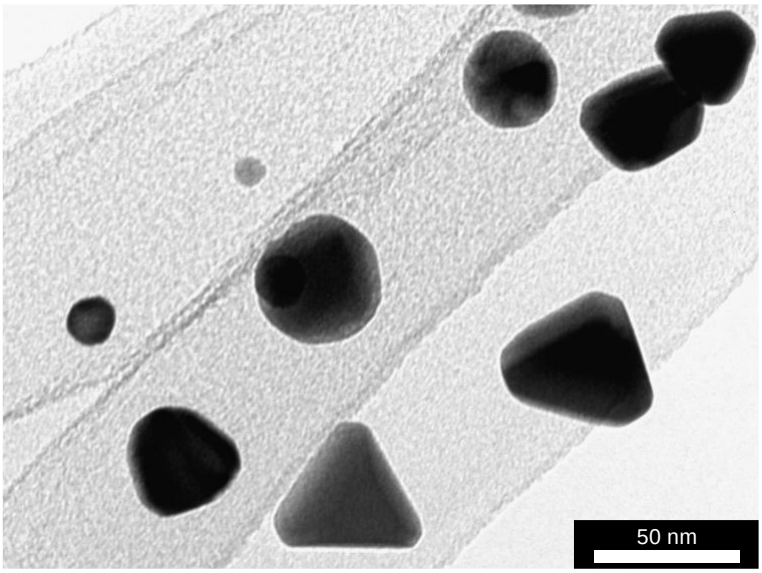

Figure 4-5. TEM image of precipitate generated in ligand exchange with octanoic acid.

The exchange rate of protective agents was determined by a pyrolysis-GC-MS. The solid samples (silver nanoparticles) were heated by pyrolyzer at 300˚C and the compounds desorbed from the samples were detected by GC-MS. Typical TICs are shown in **Figure 4-6**. The peak of oleic acid was detected around 22 min of retention time in the sample before the ligand exchange (Entry 1). In the samples after the ligand exchange, a new peak of octanoic acid appeared around 10 min (Entry 2, 4, and 7). The peak positions of oleic acid and octanoic acid were confirmed by their individual chromatograms, respectively (**Figure 4-7**). The peak of octanoic acid relative to that of oleic acid increased with the increase of the addition amount of octanoic acid. Since the excess of protective agents are fully removed in the purification process, the peak ratio reflects the existence ratio of protective agent on the surface of silver nanoparticles. In the case of Entry 7, oleic acid was completely exchanged by octanoic acid because the peak of oleic acid disappeared. As a result, it was shown that oleic acid on the surface of silver nanoparticle is perfectly exchanged by octanoic acid when the addition amount is sufficient.

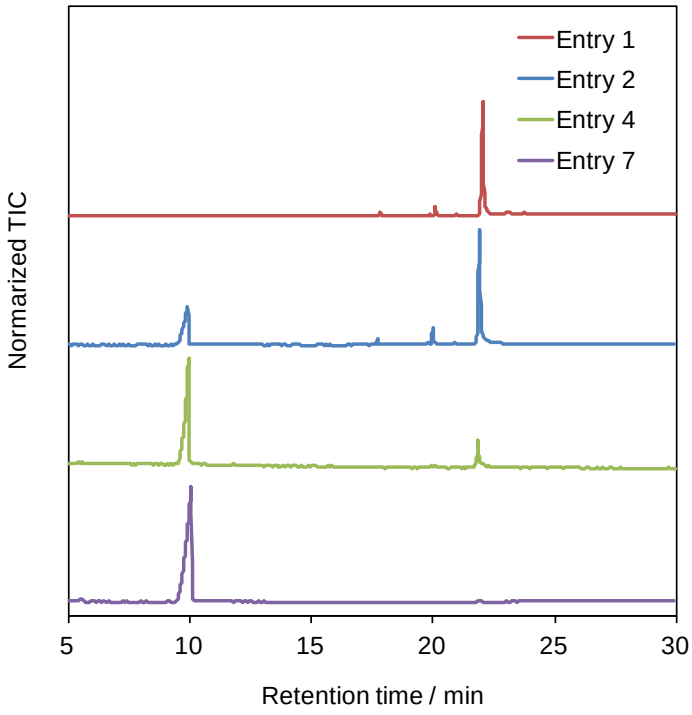

Figure 4-6. TICs of silver nanoparticles before (Entry 1) and after ligand exchange with octanoic acid (Entry 2,4, and 7). In the cases of Entry 2, 4, and 7, molar ratios of octanoic acid to oleic acid are 1.5, 10, and 40, respectively.

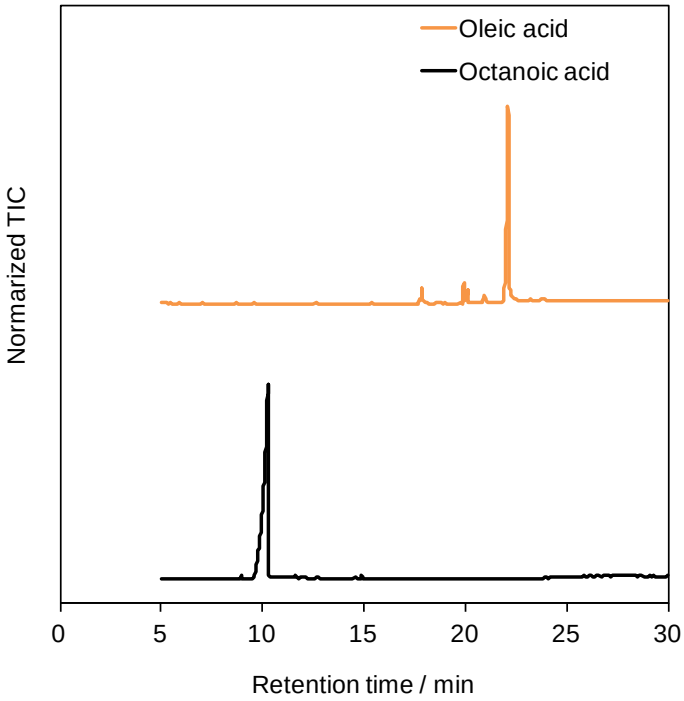

Figure 4-7. TICs of oleic acid and octanoic acid.

The results of extinction spectra and TICs are shown in **Table 4-1**. In order to obtain completely exchanged nanoparticles efficiently, lower addition amount of octanoic acid is desirable for prevention of the aggregation of nanoparticles but higher addition amount is required for the complete exchange of protective agents. The lowest addition amount of octanoic acid in the perfect exchange was 174 mg. This value corresponds to 40 times as large as the amount of oleic acid adsorbed on the surface of silver nanoparticles used in the ligand exchanges. Thus, the following ligand exchanges were carried out using 40 times of the additive protective agent relative to the protective agent adsorbed on the surface of silver nanoparticles before the ligand exchange.

As for silver nanoparticles before (Entry 1) and after the ligand exchange with octanoic acid (Entry 7), the weight loss after calcination and desorption temperature of protective agent were evaluated by TGA. The TGA curves are shown in **Figure 4-8**. The weight losses at 500˚C before and after the ligand exchange were 17 wt% and 11 wt% respectively. The molar amount (0.76 mmol g^{-1}) of octanoic acid was larger than that (0.60 mmol g^{-1}) of oleic acid. It is due to the fact that octanoic acid is less bulky than oleic acid. Interestingly, the desorption temperature of octanoic acid on the surface of silver nanoparticles was almost the same as that of oleic acid. This is significantly higher than the temperatures reached when the weight loss of pure octanoic acid and oleic acid hit the bottom under the same measurement conditions (**Figure 4-9**). This increase of desorption temperature may be originated from the stabilization by the interaction between the carboxyl group and the silver surface.

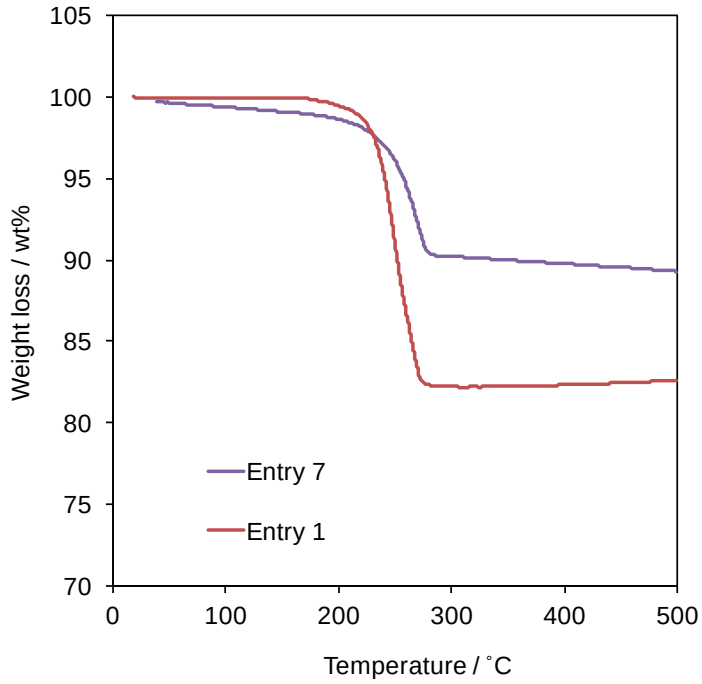

Figure 4-8. TGA curves of silver nanoparticles before (Entry 1) and after complete ligand exchange with octanoic acid (Entry 7) in a helium atmosphere.

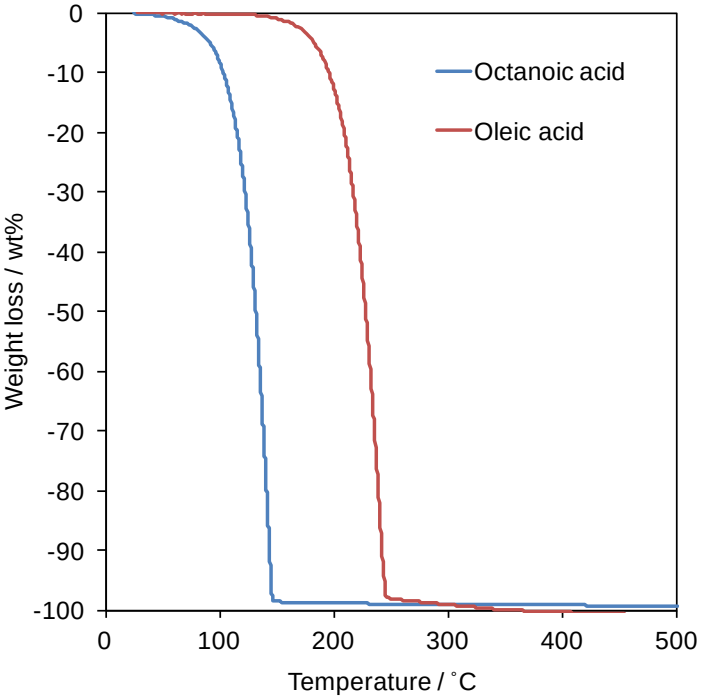

Figure 4-9. TGA curves of octanoic acid and oleic acid in a helium atmosphere.

4-2-3 Reverse Ligand Exchange from Octanoic Acid to Oleic Acid

In the previous section, the ligand exchange from oleic acid to octanoic acid on the surface of silver nanoparticles was completely carried out. Here is one question whether octanoic acid on the silver surface is exchanged by oleic acid reversely. In order to answer this question, the ligand exchange from octanoic acid to oleic acid was performed. The octanoic-acid-capped silver nanoparticles were synthesized by the ligand exchange with octanoic acid from oleic-acid-capped silver nanoparticles. The ligand exchange from octanoic acid to oleic acid was carried out using oleic acid whose amount of oleic acid is 40 times as large as that of octanoic acid adsorbed on the surface of original silver nanoparticles. **Figure 4-10** shows the schematic illustration of this reverse ligand exchange using oleic acid.

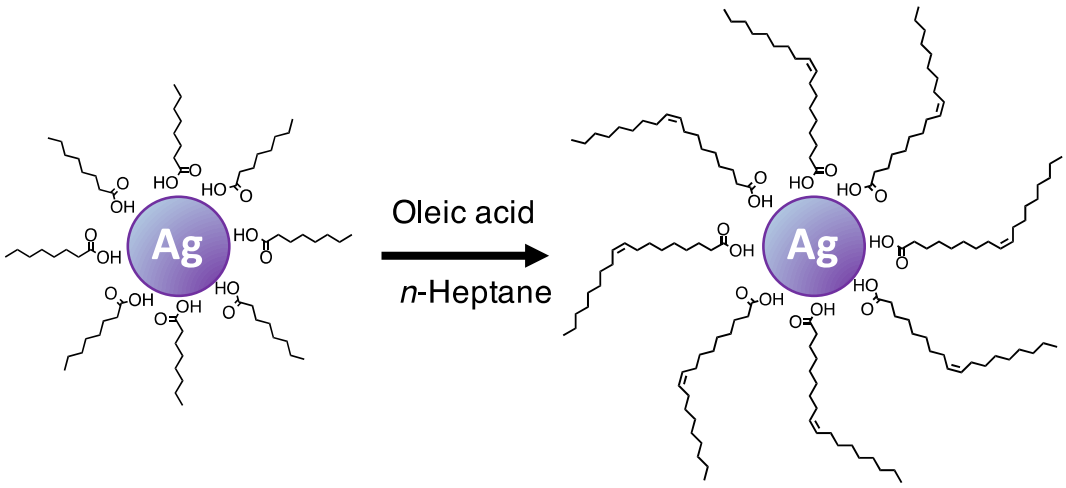

Figure 4-10. Schematic illustration of reverse ligand exchange using oleic acid.

TEM images and size distributions of the obtained silver nanoparticles are shown in **Figure 4-11** and **4-12**. In the case of octanoic acid, spherical nanoparticles with uniform size were mostly observed and their mean diameter was 6.0 ± 0.8 nm (**Figure 4-11 (a)** and **(b)**). The distribution (6.0 ± 0.8 nm) of reverse-ligand-exchanged silver nanoparticles is narrower than that (6.3 ± 1.5 nm, **Figure 4-2 (b)**) of oleic acid capped silver

nanoparticle synthesized by the improved VEROS method. It is considered that larger particles with octanoic acid aggregated and precipitated in the ligand exchange process because the ligand exchange process from oleic acid to octanoic acid lowers the solvent dispersibility of nanoparticles due to the decrease of alkyl chain length. Therefore, larger particles were selectively removed and the distribution became narrow after the ligand exchange. In contrast, various sizes of nanoparticles in size were observed in the case of the reverse ligand exchange and the mean diameter was 6.2 ± 1.1 nm (**Figure 4-12 (a)** and **(b)**). This mean diameter is slightly larger than that of octanoic-acid-capped silver nanoparticles. It may be due to the solvent dispersibility of nanoparticles improved by the reverse ligand exchange. The improvement resulted in the dispersion of the larger particles made by fusion because oleic acid allows silver nanoparticles to have the high dispersion ability owing to its long-alkyl-chain. Therefore, the distribution spread to the larger side.

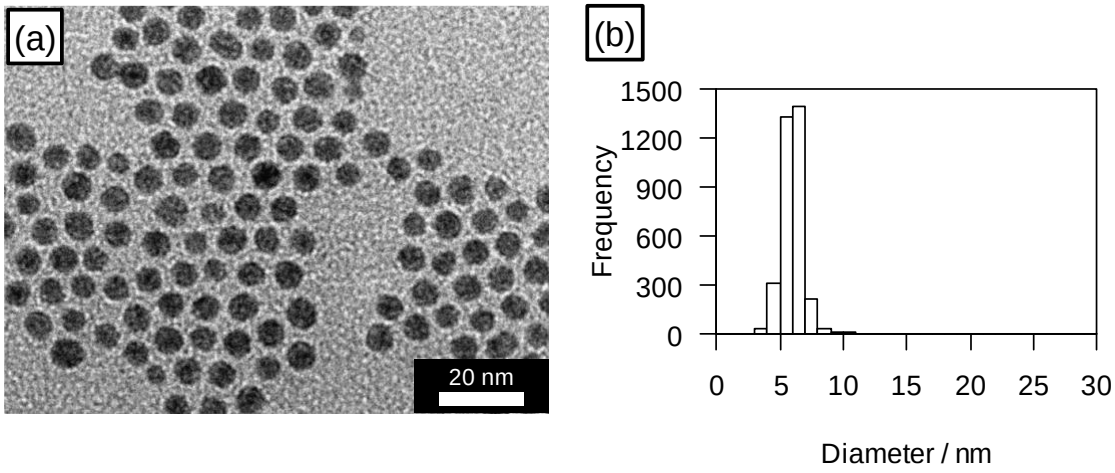

Figure 4-11. (a) TEM image and (b) particle size distribution of silver nanoparticles after ligand exchange with octanoic acid.

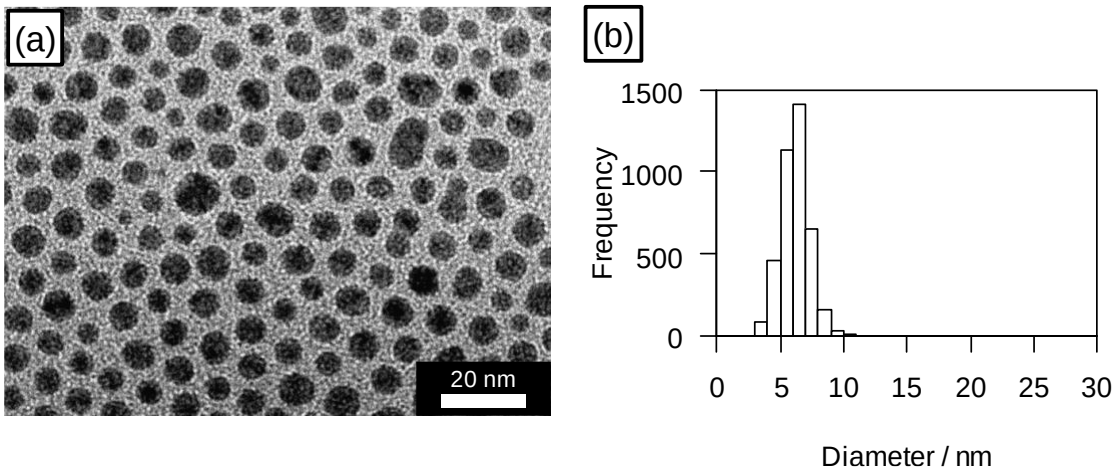

Figure 4-12. (a) TEM image and (b) particle size distribution of silver nanoparticles after reverse ligand exchange with oleic acid.

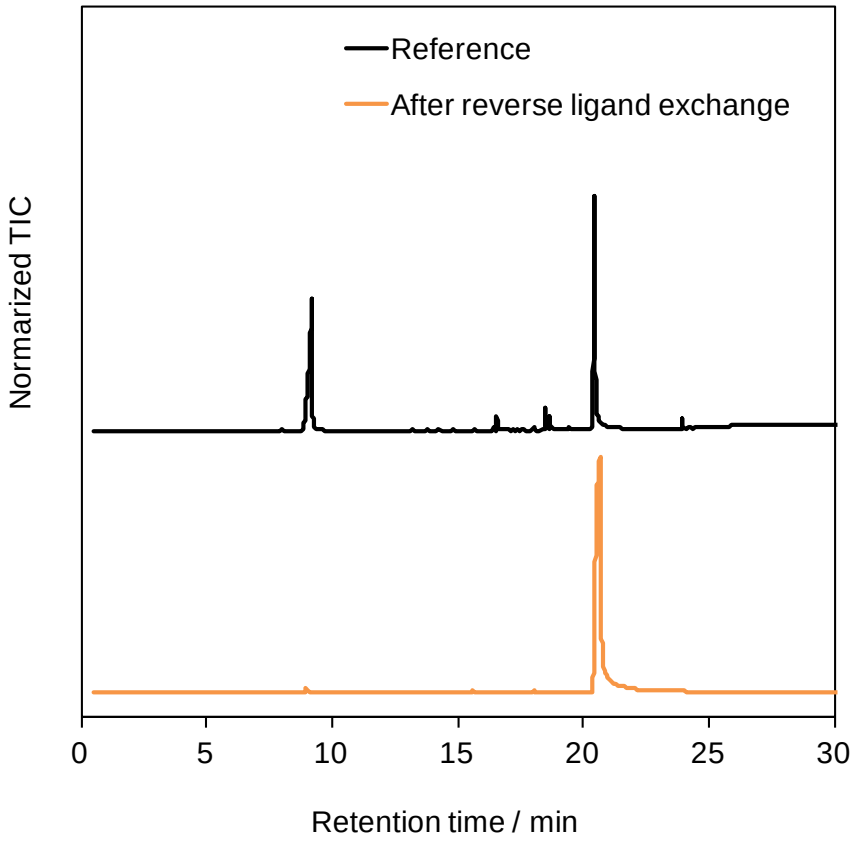

Figure 4-13. TICs of reference (mixture of octanoic acid and oleic acid) and silver nanoparticles after reverse ligand exchange with oleic acid.

The adsorbed molecules on the surface of the silver nanoparticle were determined by a pyrolysis-GC-MS as well (**Figure 4-13**). The mixture of octanoic acid and oleic acid was measured for a reference, and two strong peaks were detected around 8 min and 21 min in the chromatogram. They are octanoic acid and oleic acid respectively. In the case of silver nanoparticles after the reverse ligand exchange with oleic acid, a strong peak of oleic acid was detected around 21 min in the chromatogram and any of the other peaks were vanishingly small. This result demonstrates that octanoic acid is exchanged by oleic acid on the surface of silver nanoparticles. In fact, oleic acid and octanoic acid are exchanged each other. From these results, oleic acid and octanoic acid probably have the similar adsorption strength on the surface of silver nanoparticles. The similar desorption temperature evaluated by TGA also supports this assumption. The difference in the alkyl chain hardly affects the adsorption strength.

4-2-4 Ligand Exchange from Oleic Acid to *n*-Octylamine

As the exchange ratio reflects the difference in the adsorption ability of protective agents, the ligand exchange was also performed using *n*-octylamine with a different hydrophilic group.

Figure 4-14 shows TICs of *n*-octylamine, oleic acid and the silver nanoparticle after the experiment with *n*-octylamine. The peaks of *n*-octylamine and oleic acid appeared around 13 min and 21 min, respectively, with the column. The peak of *n*-octylamine was not detected at all although the peak of oleic acid was clearly observed in the chromatogram of silver nanoparticle after the ligand exchange. This result indicates that oleic acid on the surface of silver nanoparticles is not exchanged by *n*-octylamine. Accordingly, the author concludes that carboxyl groups interact with the silver surface more strongly than amino groups.

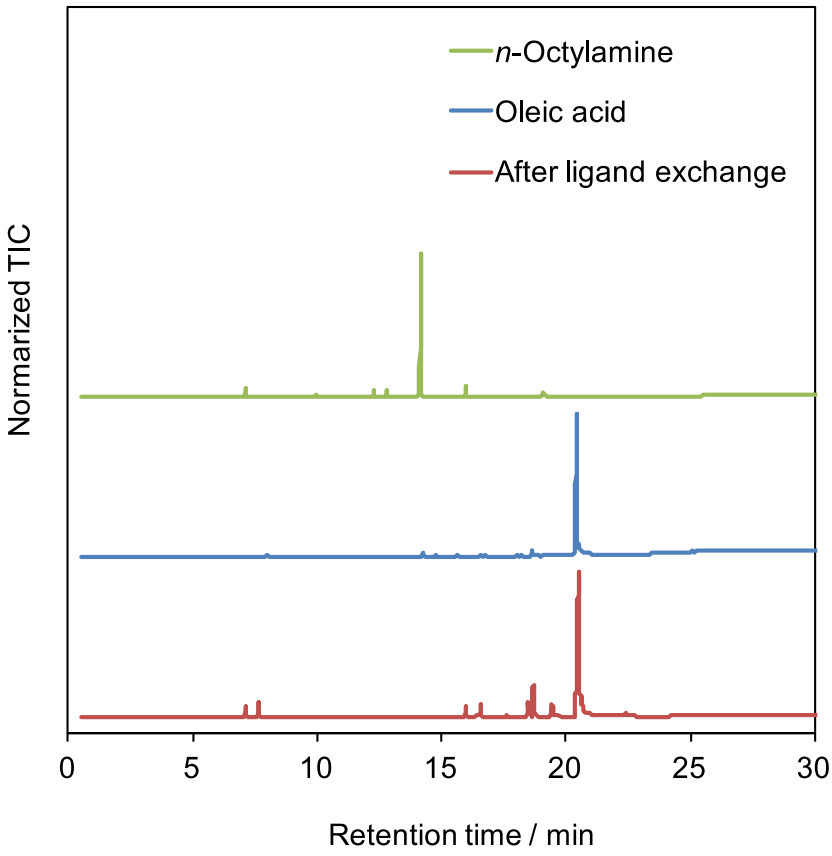

Figure 4-14. TICs of *n*-octylamine, oleic acid, and silver nanoparticles after the experiment with *n*-octylamine.

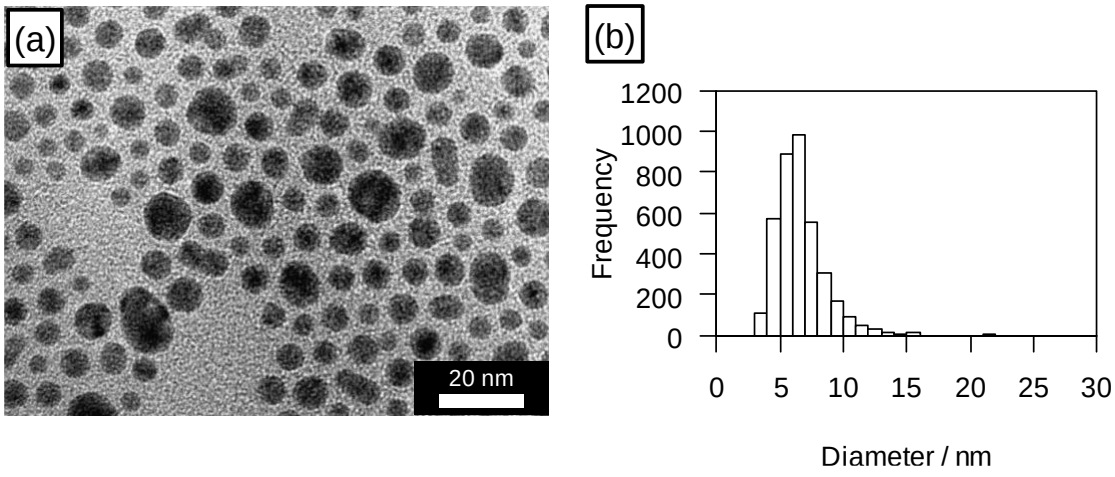

Figure 4-15. (a) TEM image and (b) particle size distribution of silver nanoparticles after the experiment with *n*-octylamine.

TEM image and size distribution of the oleic-acid-capped silver nanoparticles after the experiment with *n*-octylamine are shown in **Figure 4-15**. The mean diameter of the silver nanoparticles was 6.6 ± 1.9 nm. The diameter and size distribution of the silver nanoparticles were larger and wider than those of original silver nanoparticles (**Figure 4-2**). This result can be explained by the following mechanism. *n*-Octylamine, which exists with a sufficient amount in the solution, does not adsorb on the surface of silver nanoparticles in the process of the ligand exchange although some surfaces of silver nanoparticles are likely to be exposed to the solution containing *n*-octylamine by the desorption of oleic acid. Oleic acid desorbed from nanoparticles complexes with *n*-octylamine to form a salt and as a result the amount of oleic acid decreases in the solution. Therefore, some nanoparticles may fuse and coalesce each other. As proof of this assumption, some larger and formless particles were observed in the TEM image (**Figure 4-15 (a)**).

4-2-5 Consideration of Adsorption Strength of Protective Agents Based on Results of Ligand Exchange

The ligand exchange was reversible on the surface of silver nanoparticles in the case of the exchange between oleic acid and octanoic acid. The coexistence of oleic acid and octanoic acid on the silver surface was also observed in some cases. It indicates that two protective agents are at adsorption equilibrium on the surface of silver nanoparticles. In fact, the ligand exchange ratios basically correspond to the ratio of additive octanoic acid and adsorbed oleic acid (**Table 4-1**). On the other hand, oleic acid was not exchanged by excess amounts of *n*-octylamine at all. This result is quite in contrast to the result that more than half of oleic acid on the surface of silver nanoparticles were exchanged in the ligand exchange with 1.5 times octanoic acid (Entry 2). That can be explained by the adsorption strength of *n*-octylamine which is much lower than that of oleic acid in the consideration from the viewpoint of physical adsorption. This finding is different from

other results reported in the chemical synthesis of silver nanoparticles. In the chemical synthetic methods, amine ligands are well-known protective agents for silver nanoparticles with the coexistence of organic acids [34]. However, Chapter 3 indicates that oleic acid showed the best protection performance in the synthesis of silver nanoparticles by the improved VEROS method. On the other hand, oleylamine was not suitable for this synthesis. In the improved VEROS method, protective agents adsorb on the surface of nanoparticles formed by silver vapor in the nonpolar solvent. Therefore, neither ionic precursor nor intermediate exist in this method. In contrast, silver salts and ionized protective agents are used in chemical methods. For instance, Nakamoto and co-workers used amine compounds and silver carboxylate for the synthesis of different size of silver nanoparticles [35,36]. Bunge *et al*. synthesized *n*-octylamine-capped silver nanoparticles from a special organometallic precursor of silver [37]. Hao *et al.* reported the synthesis of silver nanoparticles using silver nitrate and *n*-octadecylamine [38]. Formation mechanism of silver nanoparticles with oleylamine was proposed by Chen *et al*. and therein the ionization of silver was needed in the adsorption process of amine [39]. Driving force for adsorption of protective agents on the metal surface in these reports is not physical adsorption but electrostatic interaction. Therefore, the author's research on the ligand exchange using silver nanoparticles synthesized by the improved VEROS method reflects the physical adsorption strength of protective agents more accurately.

Section 4-3: Experiments

4-3-1 Materials

All chemicals and solvents were obtained commercially and used without further purification. Oleic acid (purity: > 65.0 %) used in the synthesis of silver nanoparticle was obtained from Wako Pure Chemical Industries, Ltd. Octanoic acid was purchased from Tokyo Chemical Industries Co., Ltd. Oleic acid (purity: 99.0 %) and *n*-octylamine used in the ligand exchange were obtained from Nacalai tesque, Inc.

4-3-2 Synthesis of Oleic-Acid-Capped Silver Nanoparticles

Oleic-acid-capped silver nanoparticles were synthesized by the improved VEROS method according to the procedure shown in the previous chapters. **Figure 4-1** shows the schematic illustration of this synthesis. Silver at a granular state was used as a source material for vacuum evaporation. Silver (total amount: 60 g) was evaporated under vacuum conditions. This process was accomplished by evaporating 10 g of silver six times because the amount of silver per batch is limited by the size of the crucible. The pressure in the reaction chamber was kept below 10^{-2} Pa during the evaporation. Oleic acid (200 g) was poured into the cylindrical chamber after stirring for 1 h at 100˚C. The rotation speed of the cylindrical chamber was 8 rpm. The outer wall temperature of the cylindrical chamber was controlled by cooling water at 20˚C. The crucible was heated at 400 W using tungsten filament. This vacuum evaporation was repeatedly continued up to the exhaustion of silver used in this study. In the feed process of silver to the crucible, the inside of the chamber was overflowed with argon as an inert gas.

Oleic-acid-capped silver nanoparticles were isolated from the trap solution. This isolation process was carried out based on the precipitation of nanoparticles by the addition of the excess of methanol, which is a typical poor solvent of hydrophobic nanoparticles. The obtained silver nanoparticles were purple powders and dried *in vacuo*.

The silver nanoparticles were used as the starting material for the following ligand exchanges.

4-3-3 Ligand Exchange

Ligand exchanges were carried out by mixing silver nanoparticle and additive protective agent in the solution. In this process, *n*-heptane was used as a solvent for the additive protective agent not to ionize in the solution as much as possible. The dispersion of silver nanoparticles was prepared by dispersing 50 mg of silver nanoparticles in *n*-heptane (100 mL) at a concentration of 0.50 g L^{-1}. The solution of additive protective agents was prepared by dissolving additive agents in *n*-heptane (10 mL) at specified concentrations. The amount of additive protective agents was varied from 1.5 to 50 times as large as the molar amount of oleic acid adsorbed on the surface of original silver nanoparticles. The additive protective agent solution was added to the silver nanoparticle dispersion and the mixture was stirred at 40˚C for an hour. Next, 30 mL of methanol was added to the mixture (about 5 mL) after the condensation by a rotary evaporator. The flocculated silver nanoparticles were completely precipitated by centrifugation at 14500 rpm for 10 min. After the removal of the supernatant, the same procedure was repeated twice. After this process, silver nanoparticles were isolated from the excess of protective agents. The obtained silver nanoparticles were dried in a vacuum.

Figure 4-3 and 4-10 show the illustration of the ligand exchange and reverse ligand exchange, respectively. Octanoic acid and oleic acid were used as additive protective agents in the ligand exchange and in the reverse ligand exchange, respectively. The effect of the addition amount was investigated with various amounts of octanoic acid. The addition amounts were 6.5 mg, 17 mg, 43 mg, 87 mg, 130 mg, 173 mg, and 217 mg in the mixture. In the case of the reverse ligand exchange, the addition amount of oleic acid was 340 mg. In addition, *n*-octylamine was also used in the ligand exchange and the addition amount was 156 mg.

4-3-4 Characterization

The obtained silver nanoparticles were characterized as follows. The images of silver nanoparticles were taken by a JEM-2100 transmission electron microscope (TEM, JEOL, Japan). The samples for TEM observation were cast on ultrathin amorphous carbon films supported by copper grids COL-C15 (Okenshoji, Japan) and dried fully under vacuum conditions before observation. The particle distribution and mean diameter were quantitatively analyzed from ten of TEM images by LAS Image Analysis, which is a digital image analysis software (Leica, Germany). Thermogravimetric analysis (TGA) was carried out by a ThermoMass Photo (Rigaku, Japan). Heating of the samples was performed in a helium atmosphere at a rate of 10˚C min^{-1}, in the temperature range from 25 to 500˚C. In this range of temperature, organic compounds used here decompose completely but silver remains. The extinction spectra were recorded by a UV-Vis spectrophotometer U-2010 (Hitachi, Japan) at room temperature. The samples for UV-Vis spectra were diluted by cyclohexane at 0.17 g L^{-1}. The diluted samples were left to stand in quartz cell with PTFE cap for several hours until their extinction spectra reached almost constant. Total ion chromatograms (TICs) for determination of protective agents adsorbed on the silver nanoparticles were obtained from a Gas chromatograph mass spectrometer QP2010 Plus and QP2010SE (Shimadzu, Japan). Ultra ALLOY UA5-30M-0.25F (Frontier Laboratories, Japan) column was used. The samples for GC-MS were heated by a PY-3030D pyrolyzer (Frontier Laboratories, Japan) at 300˚C before the injection. The ratios of protective agents on the surface of silver nanoparticles were determined from the TIC peak area, which was normalized by a calibration curve. The calibration curve was prepared from the mixtures of two ligands with several ratios.

Section 4-4: Summary

Ligand exchanges were carried out for understanding of performance of protective agents in the physical synthetic methods of silver nanoparticles. The results indicate that the adsorption strength of *n*-octylamine is quite weaker than that of oleic acid and octanoic acid. This result contradicts some of results reported in the chemical synthesis with the ionic process of protective agents. However, it was consistent with the result of Chapter 3. Namely, the physical adsorption strength of protective agents on the metal surface is a crucial factor for the efficient synthesis of metal nanoparticles in the physical method. Nowadays, there are many physical methods in the synthesis of metal nanoparticles. Although quantitative investigations are further needed, the present results would be useful for extensive research in the physical synthesis of metal nanoparticles and support the selection of suitable protective agents.

References

[1] T. Gao, Q. Li, and T. Wang, *Chem. Mater.* **2005**, *17*, 887-892.

[2] B. K. Kuila, A. Garai, and A. K. Nandi, *Chem. Mater.* **2007**, *19*, 5443-5452.

[3] M. Manheller, S. Karthäuser, R. Waser, K. Blech, and U. Simon, *J. Phys. Chem. C* **2012**, *116*, 20657-20665.

[4] L. K. Khorashad, L. V. Besteiro, Z. Wang, J. Valentine, and A. O. Govorov, *J. Phys. Chem. C* **2016**, *120*, 13215-13226.

[5] I. Papagiannouli, P. Aloukos, D. Rioux, M. Meunier, and S. Couris, *J. Phys. Chem. C* **2015**, *119*, 6861-6872.

[6] Y. Son, J. Lee, Y. Soong, D. Martello, and M. Chyu, *Chem. Mater.* **2010**, *22*, 2226-2232.

[7] K. Mori, Y. Miyauchi, Y. Kuwahara, and H. Yamashita, *Bull. Chem. Soc. Jpn.* **2017**, *90*, 556-564.

[8] X. Zhang, Z. Luo, Y. Wang, and S. Zhang, *Chem. Lett.* **2016**, *45*, 1288-1290.

[9] S. Y. Hwang, C. Zhang, E. Yurchekfrodl, and Z. Peng, *J. Phys. Chem. C* **2014**, *118*, 28739-28745.

[10] Ph. Buffat and J-P. Borel, *Phys. Rev. A* **1976**, *13*, 2287-2298.

[11] J. R. McKenzie, A. C. Cognata, A. N. Davis, J. P. Wikswo, and D. E. Cliffel, *Anal. Chem.* **2015**, *87*, 7857-7864.

[12] A. Martínez-Olmos, J. Fernández-Salmerón, N. Lopez-Ruiz, A. R. Torres, L. F. Capitan-Vallvey, and A. J. Palma, *Anal. Chem.* **2013**, *85*, 11098-11105.

[13] A. M. Joseph, B. Nagendra, E. B. Gowd, and K. P. Surendran, *ACS Omega* **2016**, *1*, 1220-1228.

[14] A. Kosmala, R. Wright, Q. Zhang, and P. Kirby, *Mater. Chem. Phys.* **2011**, *129*, 1075-1080.

[15] S. Magdassi, A. Bassa, Y. Vinetsky, and A. Kamyshny, *Chem. Mater.* **2003**, *15*,

2208-2217.

[16] B. S. Kim, K. Shin, J. B. Pyo, J. Lee, J. G. Son, S. Lee, and J. H. Park, *ACS Appl. Mater. Interfaces* **2016**, *8*, 2582-2590.

[17] L. Song, A. C. Myers, J. J. Adams, and Y. Zhu, *ACS Appl. Mater. Interfaces* **2014**, *6*, 4248-4253.

[18] J. Song, J. Bian, E. Zheng, X. Wang, W. Tian, and T. Miyasaka, *Chem. Lett.* **2015**, *44*, 610-612.

[19] I. D. Scott, Y. S. Jung, A. S. Cavanagh, Y. Yan, A. C. Dillon, S. M. George, and S. Lee, *Nano Lett.* **2011**, *11*, 414-418.

[20] J. Ma, M. Zhan, and K. Wang, *ACS Appl. Mater. Interfaces* **2015**, *7*, 563-576.

[21] E. Smirnov, M. D. Scanlon, D. Momotenko, H. Vrubel, M. A. Méndez, P. Brevet, and H. H. Girault, *ACS Nano* **2014**, *8*, 9471-9481.

[22] B. Ding, S. Shen, L. Wu, X. Qi, H. Ni, and Y. Ge, *Chem. Lett.* **2015**, *44*, 858-860.

[23] S. Yatsuya, K. Mihama, and R. Uyeda, *Jpn. J. Appl. Phys.* **1974**, *13*, 749-750.

[24] S. Yatsuya, Y. Tsukasaki, K. Yamauchi, and K. Mihama, *J. Cryst. Growth* **1984**, *70*, 533-535.

[25] I. Nakatani, T.Furubayashi, T. Takahashi, and H. Hanaoka, *J. Magn. Magn. Mater.* **1987**, *65*, 261-264.

[26] T. Ienaga, Y. Nakahara, and K. Kimura, *Chem. Lett.* **2014**, *43*, 1893-1895.

[27] T. Ienaga, Y. Nakahara, S. Yajima, and K. Kimura, *J. Nanosci. Nanotechnol.* **2018**, *18*, 2547-2554.

[28] M. Chen, W. H. Ding, Y. Kong, and G. W. Diao, *Langmuir* **2008**, *24*, 3471-3478.

[29] F. Dubois, B. Mahler, B. Dubertret, E. Doris, and C. Mioskowski, *J. Am. Chem, Soc.* **2007**, *129*, 482-483.

[30] R. R. Knauf, J. C. Lennox, and J. L. Dempsey, *Chem. Mater.* **2016**, *28*, 4762-4770.

[31] C. Keum, N. Ishii, K. Michioka, P. Wulandari, K. Tamada, M. Furusawa, and H. Fukushima, *J. Nonlinear Optic. Phys. Mat.* **2008**,*17*, 131-142.

[32] C. A. Lane, D. E. Burton and C. C. Crabb, *J. Chem. Educ.* **1984**, *61*, 815.

[33] K. B. Mogensen and K. Kneipp, *J. Phys. Chem. C* **2014**, *118*, 28075-28083.

[34] S. Mourdikoudis and L. M. Liz-Marzań, *Chem. Mater.* **2013**, *25*, 1465-1476.

[35] Y. Kashiwagi, M. Yamamoto, and M. Nakamoto, *J. Colloid Interface Sci.* **2006**, *300*, 169-175.

[36] M. Yamamoto, Y. Kashiwagi, and M. Nakamoto, *Langmuir* **2006**, *22*, 8581-8586.

[37] S. D. Bunge, T. J. Boyle, and T. J. Headley, *Nano lett.* **2003**, *3*, 901-905.

[38] C. Hao, D. Wang, W. Zheng, and Q. Peng, *J. Mater. Res.* **2009**, *24*, 352-356.

[39] M. Chen, Y. Feng, X. Wang, T. Li, J. Zhang, and D. Qian, *Langmuir* **2007**, *23*, 5296-5304.

General Conclusions

Protective agents on the surface of silver nanoparticles synthesized by the improved VEROS method were investigated from the viewpoint of their physical adsorption. Although there are some useful analytical methods such as QCM for the investigation of physical adsorption on the surface of metal nanoparticles, they are still insufficient for the actual evaluation because they cannot reproduce the situation completely. In this thesis, the author adopted the improved VEROS method not only as a production method of metal nanoparticles but also as an investigation method of physical adsorption of protective agents.

In Chapter 1, the synthetic methods of metal nanoparticles were explained and classified. The importance of protective agents in many synthetic processes in the cases of synthesis and application was described. The improved VEROS method is suitable for the investigation of adsorption of protective agents on the surface of metal nanoparticles because the method provides a simple synthetic environment.

In Chapter 2, the effect of adsorption moieties of protective agents on the synthesis of silver nanoparticles in the improved VEROS method was investigated by using the molecules with the same structure of lipophilic group. The adsorption moieties are sorbitol, carboxyl, amino, hydroxyl, and ester groups. Sorbitol and Carboxyl molecules showed the excellent performance for the protection and redispersion of silver nanoparticles. Hydroxyl and Ester molecules were not effective protective agents for the protection of silver nanoparticles as the author expected beforehand. Although the usefulness of amino group was reported in many chemical methods, amino molecule did not effectively protect silver nanoparticles in this study. Furthermore, the concentration effect of protective agents in the trap solution was investigated in the synthesis of silver nanoparticles with sorbitan monoolate. The protective agent concentration in the trap solution rarely affected the primary particle size, but decisively contributed to prevention

of the aggregation between the nanoparticles. Therefore, it can be thought that the surface of silver nanoparticles is stabilized by protective agents after the growth of the nanoparticles.

In Chapter 3, the synthesis of silver nanoparticles by the improved VEROS method was compared with that by the thermal decomposition technique. As a result, there were some differences between the two synthetic methods. In the thermal decomposition technique, it was difficult to eliminate the influence of protective agents on the growing process of metal nanoparticles. Although the adsorption processes of protective agents are completely different between the two synthetic methods, oleic acid on the surface of silver nanopatricles showed almost the same IR spectra. Therefore, it is speculated that the adsorption states of oleic acid in the two synthetic methods are almost the same and that it is determined only by the interaction between oleic acid and silver nanoparticles.

In Chapter 4, the physical adsorption strength of protective agents was compared via ligand exchange of silver nanoparticles synthesized by the improved VEROS method. In these experiments, carboxyl and amino molecules were adopted as ligands for the comparison because they indicate the interesting difference between physical and chemical synthesis methods. The ligand exchange was carried out in a non-polar solvent in order not to ionize the protective agent as much as possible. Although adsorbed oleic acid on the surface of silver nanoparticles was easily changed to octanoic acid by the ligand exchange process, it was not changed to *n*-octylamine. The result indicates that the adsorption strength of *n*-octylamine is quite weaker than that of oleic acid and octanoic acid. Therefore, the result shown in Chapter 3 was supported by this ligand exchange.

In summary, the improved VEROS method was adopted as a synthetic method of silver nanoparticles without ionization. There has been no research for molecular adsorption focusing on this feature of the improved VEROS method as far as the author knows. This method supplies the extremely simple experiment environment for molecular adsorption. Furthermore, these results showed that the improved VEROS method is useful for

selecting protective agents for the protection of metal nanoparticles with physical adsorption.

Future Perspectives

The researches on protective agents in the improved VEROS method have hardly progressed so far. Therefore, the feature on adsorption phenomenon in this method was firstly demonstrated by experiments with the well-known material such as silver. By using the synthesized silver nanoparticles, the superiority of the improved VEROS method in the investigation of physical adsorption was clarified as compared with other synthetic methods. Although this study succeeded in examining the adsorption of protective agents on silver nanoparticles, further research is needed for the application to another metal species.

Effective protective agents for each metal pay much attention to researchers for metal nanoparticles because the selection of protective agents is the most important for synthesis of metal nanoparticles. Although the author tried to synthesize several kinds of metal nanoparticles, systematic experiments about the adsorption performance investigation of protective agents on metals other than silver have not been conducted sufficiently. In addition, studies on the adsorption of protective agents will be further extended by using molecules bearing other adsorptive groups and macromolecules. Naturally, metals other than silver will also be considered in these experiments.

On the other hand, there are still some rooms for research on the trap solution in the improved VEROS method. Researches on the trap solution would bring about some information about the influence of the surrounding environment around protective agents. Polar solvents and ionic liquids at room temperature are attractive materials as a trap solution for these researches because the protective agent is likely to be ionized in these solutions. As for an advantage of the physical method, it is possible to evaluate the adsorption of protective agents on the metal in different environments.

Growth mechanism and size control of metal nanoparticles are also challenging tasks in the improved VEROS method. The determinant factor of the particle size in the improved VEROS method is not clear yet at the present time. For the sake of elucidating the factor, the effect of the rotation speed of the rotary chamber and the deposition rate of row material should be investigated. If the technology for particle size control is established, the relationship between the adsorption of protective agents and the particle size can be discussed.

The author does not think that the improved VEROS method becomes the main stream in the mass production of metal nanoparticles. This is because the merit of this synthetic method cannot be fully utilized when there is no flexibility in the selection of the product. In other words, running costs and initial investment are not suitable for industrial production. However, it is highly useful to explain the results of the adsorption of protective agents obtained by various synthesis methods. In conjunction with this feature, it can be used for the production of many prototypes and investigation for metal nanoparticles.

Even if chemical adsorption is stronger than physical adsorption, physical adsorption cannot be eliminated in all the processes. As long as flocculation and redispersion are used in the handling process for metal nanoparticles, physical adsorption of protective agents is universally important in the synthesis process of metal nanoparticles. The author believes that the improved VEROS method will contribute significant knowledge on physical adsorption of protective agents on the metal surface to researchers for metal nanoparticles in the near future.

List of Publications and International Conferences

Publication

1) "Synthesis and Characterization of Silver Nanoparticles by Vacuum Evaporation on Running Hydrocarbon Solution Containing Nonionic Surfactant in Cylindrical Glass Chamber"
   Takashi Ienaga, Yoshio Nakahara, and Keiichi Kimura
   Chemistry Letters **2014**, *43*, 1893-1895. (Chapter 2)

2) "Effect of Protective Agents on Silver Nanoparticle Preparation by Vacuum Evaporation on Running Hydrocarbon Solution"
   Takashi Ienaga, Yoshio Nakahara, Setsuko Yajima, and Keiichi Kimura
   Journal of Nanoscience and Nanotechnology **2018**, *18*, 2547-2554. (Chapter 2,3)

3) "Comparison of Physical Adsorption Strength of Protective Agents via Ligand Exchange of Silver Nanoparticles Prepared by Vacuum Evaporation on Running Oil Substrate Method"
   Takashi Ienaga, Soichiro Okada, Yoshio Nakahara, Mitsuru Watanabe,
   Toshiyuki Tamai, Setsuko Yajima, and Keiichi Kimura
   The Bulletin of the Chemical Society of Japan **2017**, *90*, 1251-1258. (Chapter 4)

International Conference

1) "Comparison of silver nanoparticles prepared by physical and chemical synthetic methods using the same protective agents"
   Takashi Ienaga, Yoshio Nakahara, and Keiichi Kimura
   International Chemical Congress of Pacific Basin Societies, December 2015,
   Honolulu, USA (Oral, MTLS 150) (Chapter 3)

Acknowledgments

These studies have been conducted under the direction of Professor Setsuko Yajima, Graduate School of Systems Engineering, Wakayama University. It was pleasure to work with his friends in the Analytical Chemistry lab. Particularly the author would like to thank Mr. Soichiro Okada. The author is greatly appreciative of his work and help in the ligand exchange experiments.

The author would like to express his sincere gratitude to his advisor Professor Setsuko Yajima for the continuous support for his Ph.D. study and related research, her patience, attitude, and immense knowledge. Her guidance helped him in all the time of research and writing of this thesis. The author cannot imagine having a better advisor and mentor for his Ph.D. study.

The author is especially grateful to Honorary Professor Keiichi Kimura at Wakayama University. His hard guidance with his indefatigable attitude enabled me to learn not only advanced technical knowledge but also stance of humility toward science. The author is here because of his continuous support even after his retirement.

The author is also thankful to Associate Professor Yoshio Nakahara at Faculty of Systems Engineering, Wakayama University for his kindness and advice on this thesis. His dedication to his time-consuming questions and discussions prove invaluable and his advice from his viewpoint of organic chemistry was eye-opening. The author was fortunate to learn from a teacher like him.

Additionally, the author would like to thank Dr. Shinpei Kado at Faculty of Systems Engineering, Wakayama University for his accurate advice in the rehearsal for conference

presentations.

Moreover, the presence of Professor Hidefumi Sakamoto at Faculty of Systems Engineering, Wakayama University has been highly valuable. The author sincerely appreciates his support.

Besides the advisors, the author wishes to thank Dr. Toshiyuki Tamai and Dr. Mitsuru Watanabe at Morinomiya Center, Osaka Research Institute of Industrial Science and Technology for not only measurements of samples on TEM and GC-MS but also for their insightful comments, encouragement and enlightening questions, which helped him to widen his research from various perspectives.

All of his researches were carried out with irreplaceable support by Kishugiken Kogyo Co. Ltd. The author received hearty supports from everyone in the office. The author is thankful to Senior Managing Director Shinji Kamanaka and General Manager Akito Endo for their extensive arrangements made for him. Specifically, the author is grateful to President and Chief Executive Officer Toshiyuki Kamanaka for his strong support and persevering guidance.

One more thing, the author thanks his MacBook Pro. The author has been with her since his 1st day of his Ph.D. study.

Last but not the least, the author would like to thank his family: his parents and to his brother for supporting him spiritually throughout writing this thesis and his life in general.

Takashi IENAGA

March 2018